PEDRO PAULO DE CARVALHO TEIXEIRA

FROM RHIZOSPHERE TO DETRITUSPHERE: UNRAVELING THE FATE OF ROOT CARBON INPUTS IN THE SOIL

Tese apresentada à Universidade Federal de Viçosa, como parte das exigências do Programa de Pós-Graduação em Solos e Nutrição de Plantas, para obtenção do título de *Doctor Scientiae*.

Orientador: Ivo Ribeiro da Silva
Coorientador: Leonardus Vergütz

VIÇOSA - MINAS GERAIS
2021

Ficha catalográfica elaborada pela Biblioteca Central da Universidade Federal de Viçosa - Campus Viçosa

T
T266f
2021

Teixeira, Pedro Paulo de Carvalho, 1990-
From rhizosphere to detritusphere [recurso eletrônico]: unraveling the fate of root carbon inputs in the soil / Pedro Paulo de Carvalho Teixeira. – Viçosa, MG, 2021.
1 tese eletrônica (110 f.): il. (algumas color.).

Orientador: Ivo Ribeiro da Silva.
Tese (doutorado) - Universidade Federal de Viçosa.
Inclui bibliografia.
DOI: https://doi.org/10.47328/ufvbbt.2021.023
Modo de acesso: World Wide Web.

1. Eucalipto. 2. Isótopos. 3. Solos - Respiração. 4. Micro-organismos do solo. I. Universidade Federal de Viçosa. Departamento de Solos. Programa de Pós-Graduação em Solos e Nutrição de Plantas. II. Título.

CDD 22. ed. 634.973766

Bibliotecário(a) responsável: Renata de Fatima Alves CRB6/2578

PEDRO PAULO DE CARVALHO TEIXEIRA

FROM RHIZOSPHERE TO DETRITUSPHERE: UNRAVELING THE FATE OF ROOT CARBON INPUTS IN THE SOIL

Tese apresentada à Universidade Federal de Viçosa, como parte das exigências do Programa de Pós-Graduação em Solos e Nutrição de Plantas, para obtenção do título de *Doctor Scientiae*.

APROVADA: 14 de maio de 2021.

Assentimento:

Pedro Paulo Carvalho Teixeira

Pedro Paulo de Carvalho Teixeira
Autor

Ivo Ribeiro da Silva
Orientador

Aos meus pais e irmãos.

ACKNOWLEDGMENTS

À Universidade Federal de Viçosa e ao Programa de Pós-graduação em Solos e Nutrição de Plantas, pela oportunidade;

Ao Conselho Nacional de Desenvolvimento Científico (CNPq), pela concessão de bolsas de estudos;

À Coordenação de Aperfeiçoamento de Pessoal de Nível Superior (CAPES), no âmbito do Programa Capes-PrInt, pela bolsa de doutoramento sanduíche;

Ao *Lehrstuhl für Bodenkunde* da *Technische Universität München* pelo excelente ambiente e oportunidade;

Ao Prof. Ivo Ribeiro da Silva, pela orientação e pelo suporte durante o doutorado;

À Alix Vidal e Carsten W. Mueller, por me receberem no grupo de estudo e por todos os ensinamentos e pela orientação durante minhas atividades na *Technische Universität München;*

À Ana Paula Mendes Teixeira, por ser a melhor dupla que pode existir;

A Ivan Francisco de Souza, pela enorme ajuda desde o início do doutorado;

Ao estagiário Danilo Henrique Souza da Silva, cujo esforço e dedicação foram essenciais para realização deste estudo;

Aos meus amigos do Laboratório de Isótopos Estáveis (LIE): João Milagres, Humberto Rosado, Luís Fernando Almeida, Daniela Costa, Bernardo Amorim, Ricardo Fialho, Matheus Barreto, Helen Amorim, Fabrício Gebrim, Rafael Santos, Rafael Teixeira, Rodrigo Nogueira de Sousa, Josias Amaral, Gustavo Mayrink, Aymbiré Fonseca, Raphael Melo, Eduardo Medina, Jônatas Silva; Maria Cardoso, Pedro Renato de Souza e Júlio Nunes;

Aos meus amigos do *Lehrstuhl für Bodenkunde*: Luis Carlos Colocho, Thiago Inagaki, Christopher Just, Julien Guigue, Noelia Garcia Franco, Franziska Bucka, Steffen Schweizer, Isabel Prater, Stefanie Mayer, Kristina Witzgall, Yaser Ostovari, Franziska Fella, Tianyi Wu, Evelin Pihlap, Vincent Buness, Lena Reifschneider e Franziska Steiner;

Aos meus estagiários que me ajudaram durante todo o meu doutorado: Letícia Freitas, Luísa Cotta, Natal Castro, Pedro Batista e Antônio Consentino;

“Why do trees conceal the splendor of their roots?”.

(Pablo Neruda)

ABSTRACT

TEIXEIRA, Pedro Paulo de Carvalho, D.Sc., Universidade Federal de Viçosa, May, 2021. **From rhizosphere to detritusphere: unraveling the fate of root carbon inputs in the soil.** Adviser: Ivo Ribeiro da Silva. Co-adviser: Leonardus Vergütz.

The conversion of root carbon (C) into soil organic matter (SOM) is regarded as the "hidden half" of the terrestrial C cycle. Nevertheless, recent evidence shows that root C inputs exert an important role in SOM formation, although the reasons behind these results are not understood. Roots create two temporally separated hotspots for carbon cycling in the soil: the rhizosphere, which is shaped by living roots C inputs, and the detritusphere, which is formed after root death. The succession between rhizosphere and detritusphere can affect the incorporation of these C inputs in MOS and can be an important mechanism to explain the high efficiency of root C inputs to form SOM. The general objective of this work was to gain knowledge about the processes that control the conversion of rhizodeposition and root litter C into SOM. To this end, we designed two complementary studies that simulate the sequential root C inputs in the soil, from the rhizosphere (Chapter 1) to the rhizosphere-detritusphere transition (chapter 2). We employed isotopic techniques (double labeling of ^{13}C and ^{15}N) to follow the fate of *Eucalyptus* spp. rhizodeposits and root litter in a Rhodic Ferralsol. Our results show that the persistence of rhizodeposit-derived C (rhizo-C) and root litter C is given by distinct mechanisms. More than 70% of recovered rhizo-C present in the soil was retained in the mineral-associated fraction (MAOM), and about 90% of this fraction persisted in the soil after 166 days of incubation. This result attests that rhizodeposits are capable to form persistent SOM through mineral associations. However, we observed that only a minor quantity of rhizo-C was incorporated with organo-metallic complexes and short-range order phases of iron and aluminum. In contrast to rhizo-C, the majority of root litter C remained in particulate fractions and about 10% of decomposed root litter C was incorporated into SOM. Further, we observed that rhizo-C concentrated more closer to roots, but was detected even up to 25 mm away. This result is evidence that rhizo-C can have a wider distribution in the soil volume in comparison to root litter, whose transfer was restricted to the first 4 mm from its surroundings. The root litter inputs tended to favor the fungal community, which is more adapted to process more complex C sources and can directly assimilate C from the litter layer. Furthermore, from the NanoSIMS (Nanoscale Secondary Ion Mass

Spectrometry) results, we provide direct evidence for the incorporation of root litter into microbial structures and the formation of mineral-associated SOM at the detritusphere. Still, we observed that the decomposition of root litter and rhizo-C occurred independently in the rhizosphere-detritusphere transition. This result suggests that different microbial groups are responsible to process each type of root C input. Overall, our holistic approach reveals the intricate dependence between plant, soil, and microorganisms in the formation of SOM, and reinforces the importance of rhizodeposits as a source of C stable SOM formation.

Keywords: Eucalypt. Soil organic matter. Isotopes. NanoSIMS. Legacy effects. Phospholipid fatty acids.

RESUMO

TEIXEIRA, Pedro Paulo de Carvalho, D.Sc., Universidade Federal de Viçosa, maio de 2021. **Da rizosfera à detritosfera: desvendando o destino dos aportes de carbono da raiz no solo.** Orientador: Ivo Ribeiro da Silva. Coorientador: Leonardus Vergütz.

A conversão dos aportes de carbono (C) derivados de raízes em matéria orgânica do solo (MOS) ainda é considerada como a "parte oculta" do ciclo terrestre do C. Todavia, novas evidências demonstram que as raízes desempenham papel importante na formação da MOS, apesar das razões ainda não serem compreendidas. As raízes criam dois "hotspots" para a ciclagem de C no solo; a rizosfera que é formada pelo aporte de C proveniente de raízes vivas, e a detritosfera que é formada após a morte das raízes. A sucessão de tipos distintos de C durante a transição entre rizosfera e detritosfera pode afetar a incorporação desses aportes em MOS, e pode constituir importante mecanismo para explicar a elevada eficiência das raízes na formação de MOS. O objetivo geral deste estudo é elucidar os processos que controlam a conversão das rizodepósitos e do litter de raízes em MOS. Para esse fim, realizaram-se dois experimentos complementares que simularam o aporte sequencial de C derivado das raízes, desde a rizosfera (capítulo 1) até a transição entre rizosfera e detritosfera (capítulo 2). Foram empregadas técnicas isotópicas (dupla marcação com ^{13}C e ^{15}N) que possibilitaram rastrear o destino dos rizodepósitos e do litter de raízes de Eucaliptus spp. em um Latossolo Vermelho. Nossos resultados demonstram que a persistência de C derivado de rizodepósitos (rizo-C) e de litter de raízes são controladas por mecanismos distintos. Mais de 70% do rizo-C recuperado foi encontrado como matéria orgânica associada aos minerais (MAOM) e a cerca de 90% dessa fração permaneceu retida no solo após 166 dias de incubação. Esse resultado é uma evidência direta de que os rizodepósitos são capazes de formar MOS estável a partir de interações com minerais. Todavia, observou-se que apenas pequena quantidade de rizo-C estava associada a complexos organominerais e frações de baixa cristalinidade de ferro e alumínio. Em contraste com rizo-C, a maior parte do C derivado do litter de raízes permaneceu como MOS particulada e cerca de 10% do litter decomposto foi convertido da MOS. Além disso, observou-se que o rizo-C concentrou-se próximo às raízes, apesar ter sido detectado até uma distância de 25 mm. Esse resultado é uma evidência de que o rizo-C pode ter distribuição mais ampla no volume do solo em comparação com C do litter de raízes, cuja transferência ficou

restrita aos primeiros 4 mm. Verificou-se que os aportes de litter de raízes tendem a favorecer a comunidade de fungos, que está mais adaptada para processar fontes de C mais complexas e que podem assimilar diretamente o C da camada de litter. Além disso, a partir dos resultados de NanoSIMS (Espectrometria de Massa de Íons Secundários em Nanoescala), foram apresentadas evidências diretas para a incorporação de litter de raízes em estruturas microbianas e a formação de MOS associada a minerais na detritosfera. Porém, ao contrário de nossas hipóteses, observou-se que a decomposição do litter de raízes e de rizo-C ocorreu de forma independente na transição rizosfera-detritosfera. Este resultado sugere que diferentes grupos microbianos são responsáveis por processar cada tipo de aporte de C proveniente das raízes. Em suma, nossa abordagem holística revela a existência de dependência complexa entre planta, solo e microrganismos para a formação de MOS, e reforça a importância dos rizodepósitos como fonte de formação de MOS estável.

Palavras-chave: Eucalipto. Matéria orgânica do solo. Isótopos. NanoSIMS. Efeito legado. Análise de perfis de ácidos graxos.

SUMMARY

GENERAL INTRODUCTION

In their classical book “Plant Roots: The Hidden Half”, Waisel et al., (1991) drew attention to our enormous lack of knowledge about the processes that roots perform belowground. Since then, our knowledge has advanced quickly and several secrets of the underground world of roots have been literally “dug up”. Nevertheless, the never-ending saga of root research is still going on, and currently, one of the major gaps in this field is related to the role of roots in the terrestrial carbon (C) cycle (ESHEL; BEECKMAN, 2014; JACKSON et al., 2017; POWLSON; XU; BROOKES, 2017). Recent evidence indicates that root C inputs have great importance in soil organic matter (SOM) formation, but the reasons behind these observations are not well understood (JACKSON et al., 2017; RASSE; RUMPEL; DIGNAC, 2005; SOKOL et al., 2018).

Root C inputs can be separated into two types: rhizodeposition, which comprises exudates, mucilage, and slough-off cells that are released in the soil by living roots (JONES; NGUYEN; FINLAY, 2009) and root litter, which represents the input of C from dead roots (RASSE; RUMPEL; DIGNAC, 2005). Rhizodeposits are majorly composed of simple soluble compounds that can be directly processed by microorganisms (HÜTSCH; AUGUSTIN; MERBACH, 2002) and are usually more efficiently converted into microbial byproducts, which is the major precursor for the formation of mineral-associated SOM (MAOM) (COTRUFO et al., 2013; SOKOL et al., 2018). Root litter is formed mainly by structural compounds that need to be depolymerized to be processed by microorganisms (KÖGEL-KNABNER, 2002). The root litter conversion into microbial byproducts is usually less efficient in comparison with other sources of C (COTRUFO et al., 2015; LAVALLEE et al., 2018). Nevertheless, root litter can persist due to a slower decomposition rate given by its inherent chemical recalcitrance (high lignin and low N content) (RASSE; RUMPEL; DIGNAC, 2005).

One aspect that is commonly neglected about rhizodeposits and root litter is that they are temporally separated (KUZYAKOV; BLAGODATSKAYA, 2015). Initially, the growth of living roots releases rhizodeposits into the soil, and after root death, the input of rhizodeposits ceases, but their associated effects persist in the soil for some time (KÖGEL-KNABNER, 2017). Effects that persist in the soil after its source is no more exerting its activity are referred to as legacy effects (WURST; OHGUSHI, 2015), and

its importance for root-derived SOM formation has not yet been investigated (OLIVER et al., 2021).

The main objective of this work is to improve the understanding of processes that control the conversion of rhizodeposition and root litter C into SOM. We predict that the mechanisms of protection of distinct sources of root C will be different, and we expect to detect interactions between these 2 types of root C in the rhizosphere-detritusphere transition (legacy effects). For this purpose, we designed two complementary studies that simulate the sequential root C inputs in the soil, from the rhizosphere (chapter 1) to the rhizosphere-detritusphere transition (chapter 2). We used isotopic approaches (double labeling of ^{13}C and ^{15}N) that allowed the tracking of rhizodeposits and root litter independently to obtain quantitative information about the allocation of root C in the soil.

In chapter 1, we aimed at gaining knowledge about the formation of rhizodeposit-derived C, its spatial distribution, and associated effects in the rhizosphere. To this end, we exposed eucalypt (*Eucalyptus grandis* x *E. urophylla* clone - I144) seedlings to a ^{13}C-CO_2 enriched atmosphere (multiple-pulse labeling) and evaluated the spatial distribution of rhizodeposit derived-C and its conversion into SOM fractions. Further, we evaluated potential alterations in the microbial communities using phospholipid fatty acid analysis (PLFA) and assessed the rhizodeposition impacts in Al and Fe organo-metallic complexes and short-range order phases.

In chapter 2, we investigated the occurrence of legacy effects in the rhizosphere-detritusphere succession. We designed two complementary incubation experiments using isotopic labeling (^{13}C and ^{15}N) to track the fate of root-derived C from rhizodeposits and root litter in the rhizosphere-detritusphere transition. In the first incubation experiment, a former rhizospheric soil containing ^{13}C and ^{15}N labeled rhizodeposits was incubated in the presence of unlabeled root litter to follow the fate of rhizodeposit-derived C. Conversely, in the second experiment we incubated ^{13}C and ^{15}N labeled root litter in a former rhizospheric soil to follow the fate of root litter-derived C. Along with the incubation, we evaluated the soil respiration rates, and after 166 days we sectioned the soil in layers according to the distance to the root litter to obtain information about the spatial distribution of root C inputs in the detritusphere. Additionally, we characterized the impacts of legacy effects on microbial communities (PLFAs) and followed the incorporation of root C in the distinct SOM fractions. We also

evaluated the root litter-soil interface at the microscale using a nano-scale secondary ion mass spectrometry (NanoSIMS).

CHAPTER 1

RHIZODEPOSIT-DERIVED CARBON CONVERSION IN SOIL ORGANIC MATTER FRACTIONS REVEALED BY MULTIPLE PULSE $^{13}CO_2$ LABELING

ABSTRACT

There is growing evidence that rhizodeposits display a major role in the formation of soil organic matter (SOM). Nevertheless, some specific aspects of the conversion of rhizodeposits into soil C pools are still unknown. In this study we investigated (i) the distance from the rhizoplane that can be reached by rhizodeposits; (ii) the fate of rhizodeposit-derived C (rhizo-C) in SOM fractions; and (iii) the extent to which rhizo-C interacts with soil minerals. To address these questions, we followed the rhizo-C by exposing eucalypt (*Eucalyptus* spp.) seedlings to a ^{13}C-CO_2 enriched atmosphere (multiple-pulse labeling) and evaluated the spatial distribution of rhizo-C and its conversion into SOM fractions. Additionally, we quantified and characterized the microbial community using phospholipid fatty acid (PLFA), and studied potential alterations in the C associated with aluminum (Al) and iron (Fe) organo-metallic (OM) complexes and short-range order (SRO) phases. Our results show that rhizo-C formation is not only restricted to small soil volumes closer to the root (0-4 mm) but was detected in more distant regions of the rhizosphere (up to 15-25 mm from the rhizoplane). Furthermore, our work provides direct evidence that 76% of the rhizo-C was retained within the mineral-associated organic matter (MAOM) fraction. However, our results revealed that Al and Fe OM complexes and SRO phases are not affected by rhizodeposition and only a minor quantity of rhizo-C was incorporated into these fractions. These findings show rhizodeposits as major sources of the formation of mineral-associated organic SOM and suggest that Al and Fe OM complexes and SRO phases are minimally involved in the retention of rhizo-C in the soil.

Keywords: ^{13}C pulse labeling. Tropical soils. Spatial distribution. Eucalypt. Phospholipid fatty acids. Short-range order minerals. Organic-metallic complexes.

1. Introduction

Plants have a fundamental role in the terrestrial carbon (C) cycle; they convert atmospheric CO_2 into organic compounds that are the major source for the formation of soil organic matter (SOM). From all C assimilated by plants, between 7 and 11% are released in the soil as rhizodeposits, a general term for root exudates, mucilage, gases, and sloughed-off cells released from living roots (JONES; NGUYEN; FINLAY, 2009; PAUSCH; KUZYAKOV, 2018). The transformation of rhizodeposits into SOM is one of the least understood steps of the terrestrial C cycle (DIJKSTRA; ZHU; CHENG, 2020; PAUSCH; KUZYAKOV, 2018).

After entering the soil, rhizodeposits are promptly processed by microorganisms and about 60% returns to the atmosphere as CO_2 (HAFNER et al., 2012; KUZYAKOV; RAZAVI, 2019; PAUSCH; KUZYAKOV, 2018). The remaining C in the soil is referred to as net rhizodeposition (rhizo-C), and it was historically associated with more labile SOM fractions, e.g., microbial biomass and dissolved organic C (DUNGAIT et al., 2012; MARX et al., 2007, 2010; PAUSCH; KUZYAKOV, 2018). However, there is recent evidence that rhizo-C might persist longer in the soil due to the interaction with minerals or occlusion within aggregates and thus add to the overall soil C stocks (ANGST et al., 2019; BAUMERT et al., 2018; HERTEL, 2018; SOKOL et al., 2018).

Rhizodeposits are transferred in a spatially constrained region of the soil, that extends only about 0.5 up to 4 millimeters from the root surface (HOLZ et al., 2018; KUZYAKOV; RAZAVI, 2019). Nevertheless, these conclusions were drawn from studies that evaluated the spatial distribution of rhizo-C after few days of a single pulse of ^{13}C or ^{14}C (HOLZ et al., 2018; KUZYAKOV; RASKATOV; KAUPENJOHANN, 2003; SAUER; KUZYAKOV; STAHR, 2006; ZU SCHWEINSBERG-MICKAN; JÖRGENSEN; MÜLLER, 2012). Increasing the number of pulses and the interval between the pulses and the evaluation can provide valuable information about the dispersion of rhizo-C from the roots to the surrounding soil (PEIXOTO et al., 2020; QIAO et al., 2014).

Rhizodeposits are one of the main sources of C and energy for soil microorganisms and have an important role in shaping the rhizospheric microbiome (GUNINA et al., 2014; PATERSON et al., 2007). However, studies that associate the spatial distribution of microbial communities in the rhizosphere are scarce (MARSCHNER; MARHAN; KANDELER, 2012). The concentration of rhizo-C in the vicinity of the roots may provide favorable conditions for the microorganisms that are more dependent on the transport of C, such as bacteria (INGWERSEN et al., 2008;

POLL et al., 2006). In contrast, the growth of fungal hyphae can serve as a conduit to the transference of rhizo-C into more distant regions of the rhizosphere and the bulk soil (JOHNSON et al., 2002).

Another aspect that is not well understood is the relation between the mineralogy and the formation of rhizo-C. Aluminum (Al) and iron (Fe) hydroxide phases have a widespread distribution in tropical soils, and recent studies suggest these minerals have a strong affinity for rhizodeposits (JEEWANI et al., 2020; SCHAEFER, FABRIS, KER, 2008). Results from the literature show that rhizodeposits are capable of promoting both the formation and destabilization of metal-bound C associations (JEEWANI et al., 2020; KEILUWEIT et al., 2015; RASMUSSEN; SOUTHARD; HORWATH, 2007). The coupled disruption/formation cycling of metal-bound C driven by rhizodeposits can be an important mechanism to explain the apparent contradictory effects of rhizodeposition in SOM dynamics ((DIJKSTRA; CHENG, 2007; DIJKSTRA; ZHU; CHENG, 2020). The disruption of metal-bound C generated by rhizodeposits (KEILUWEIT et al., 2015) may result in the formation of free reactive surfaces that can be preferential spots for new rhizodeposit-derived SOM formation. Yet, few studies attempted to evaluate the short-term effects of rhizodeposition on the disruption/formation of metal-bound C, especially in soils rich in secondary minerals (COLLIGNON; RANGER; TURPAULT, 2012; KLEBER et al., 2015).

In this study, we tackled the mechanisms driving the conversion of rhizodeposits into SOM by determining (i) the distance from the rhizoplane at which rhizodeposits can reach; (ii) the distribution of rhizo-C in SOM fractions; (iii) the extent to which rhizo-C interacts with minerals. Using a multiple pulse ^{13}C labeling approach, we tracked the rhizo-C of eucalypt (*Eucalyptus* spp.) along a root-to-soil gradient and its allocation into SOM fractions. We further investigated the potential impacts of rhizodeposition on microbial community structure, organo-metallic (OM) complexes, and short-range order (SRO) phases of iron (Fe) and aluminum (Al). We predict that: (a) rhizo-C accumulates at the first millimeters from the root, (ii) rhizodeposition promotes the release of the C protected by Al and Fe OM complexes and SRO phases (iii) and rhizo-C is predominantly incorporated into Al and Fe OM complexes and SRO phases.

2. Material and Methods

2.1 Soil characteristics

The soil was sampled from the superficial layer (0-20 cm) of a eucalypt plantation in São Sebastião da Vargem Alegre – Brazil (21°01'37" S 42°34'12" W) and is classified as a Rhodic Ferralsol (IUSS Working Group WRB, 2014) (Table A1). Before the eucalypt implantation, the site was a cultivated pasture of C_4 tropical grass (*Urochloa decumbens*). The general biogeochemical soil characteristics are available in Table A1. Within the clay fraction, kaolinite and gibbsite were the predominant minerals, and goethite was also present, but in lower amounts compared to the other minerals (data not shown). The fresh sampled soil was sieved through a 2.0 mm sieve, homogenized, and coarse plant residues were manually removed. A nutrient solution was applied to soil to provide nutrients before the mesocosm assembly, according to specific requirements of plant cultivation in pot experiments (adapted from Novais et al., 1991 - Table A2).

2.2 Experimental setup

The soil was packed inside root isolator cylinders (heigh 2.5 cm, diameter 4.7 cm) at the density of 1.13 g cm^{-3} (adapted from Shahzad et al., 2015). The cylinders were capped at one extremity with a nylon mesh membrane of 5 µm pore size (Tegape, Curitiba, Brazil) and sealed at the other extremity. We further prepared 16 mesocosms (2.5 l plastic pots) filled with the same soil and inserted four of the above-described root isolators in each mesocosm. The root-isolators cylinders were placed horizontally with the sealed extremity of the cylinder leaning against the walls of the pots at 7 cm from the soil surface (Figure A1). We set two treatments: *with rhizodeposition*, which had an actively growing eucalypt seedling (*Eucalyptus grandis* x *E. urophylla* clone - I144), and *control*, which was left unplanted (Figure 1). The soil had a water holding capacity (WHC) of 0.33 g g^{-1} soil and the mesocosms were daily irrigated with deionized water to maintain the moisture above 80% of the soil field capacity. The experiment was conducted in a greenhouse in a randomized block design with 4 replicates.

2.3 ^{13}C labeling and reference unlabeled treatments

Half of the mesocosms were artificially labeled with ^{13}C (four mesocosms with plants and four mesocosms without plants) using a multiple-pulse labeling approach

(adapted from Machado et al., 2011) (Figure 1). The ^{13}C labeling campaign started 15 days after planting and consisted of 10 labeling events (Figure 2). In each labeling event, the mesocosms were placed randomly inside a labeling glass chamber (448 cm^3) for 10 h and submitted to a ^{13}C-CO_2 enriched atmosphere (Figure A2). We applied the first four labeling events once per week, with one pulse per day. The remaining labeling events were applied twice a week with two pulses per labeling event (one pulse in the morning and another in the afternoon, each one lasting 5 h). The ^{13}C-CO_2 enriched atmosphere was generated by injecting 20 mL of a 1M H_2SO_4 solution through a septum into a petri-dish located inside the chamber containing 1 g of $Na_2{}^{13}CO_3$ (99 atom%). In total, 1.85 g of ^{13}C was added during the labeling campaign, which is equivalent to 0.46 g of ^{13}C per plant. During each labeling procedure, we monitored the temperature and the concentration of ^{12}C-CO_2 and ^{13}C-CO_2 inside the chamber with a cavity ring-down spectrometer (CRDS, Picarro, Sunnyvale, United States of America) (Table A3). For the unlabeled treatments, the $Na_2{}^{13}CO_3$ was substituted for a non-isotopically enriched Na_2CO_3 analog (Figure 1).

2.4 Sampling

The seedlings were sampled 66 days after planting, and the dry biomass of each compartment (leaves, twigs, and roots) was weighed (Table A4). We observed an abundant growth of roots in the vicinity of root-isolator mesh in all the planted mesocosms, thus creating the desired rhizospheric soil (Figure A3). We collected one of the root-isolator (out of four) per mesocosms and sliced it into four layers: 0-4, 4-8, 8-15, and 15-25 mm (distance to root). The sectioning of the layers was done with an adapted holding device pushing the soil layer out of the cylinder and, progressively cutting the layers manually with a razor. Approximately 3 g of each layer of soil was freeze-dried for phospholipid fatty acid (PLFA) analysis and the remaining soil was air-dried and sieved at 2 mm. The three remaining cylinders were separated and used in the experiment described in Introduction of this thesis.

Figure 1 — Simplified representation of the experimental design and the soil slicing. For simplification purposes, only two (not four) root-isolators are represented in each mesocosm.

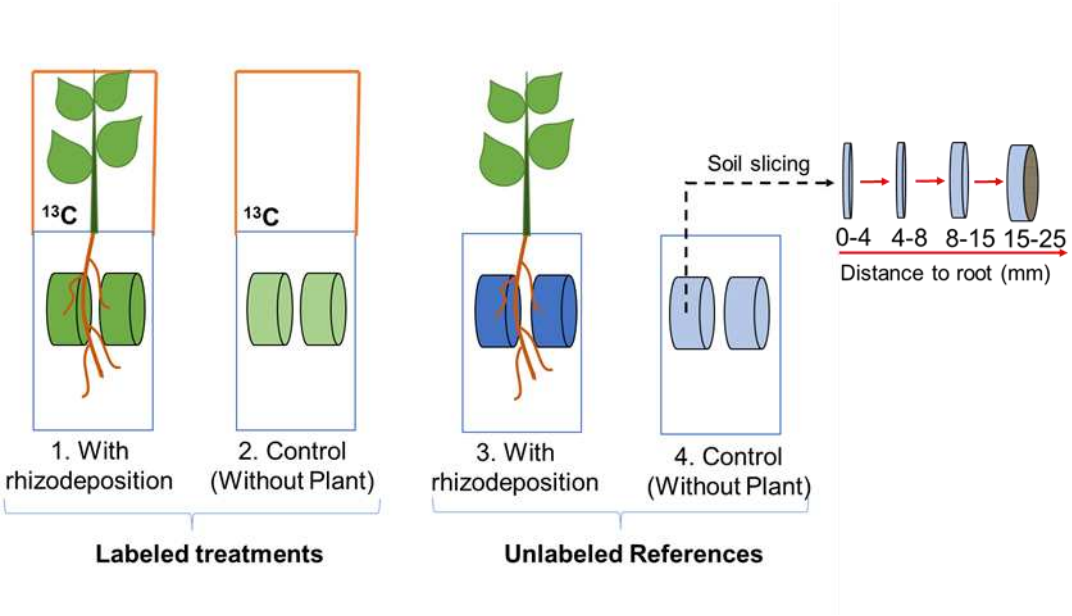

Source: Author.

Figure 2 — Timeline of the experiment presenting the timing of labeling events.

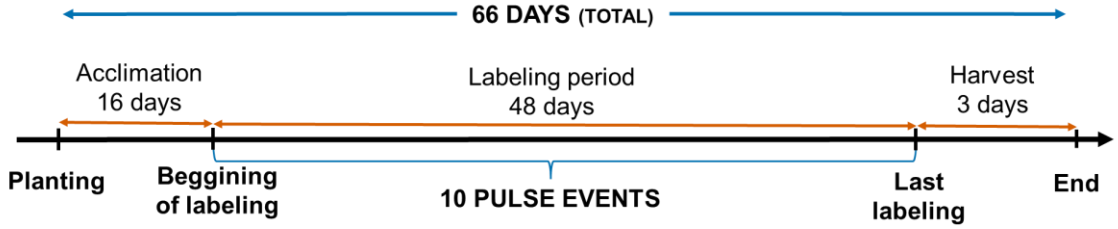

Source: Author.

2.5 SOM fractionation

The distribution of rhizo-C in the different SOM pools was quantified in soil samples from the 0-4 mm layer, using a combined density and particle size fractionation adapted from Mueller and Koegel-Knabner, (2009). Briefly, 3 g of air-dried soil was left overnight in 40 mL of sodium polytungstate (SPT) solution (density of 1.8 g cm^{-3}). The supernatant free organic material (fPOM) was further collected with a vacuum pump. The remaining material was ultrasonicated with an energy of 463 J mL^{-1}, centrifugated at 2744*g* for 30 min and the supernatant, i.e., the organic material occluded within the aggregates (oPOM) was collected with a vacuum pump (CAROLINO DE SÁ et al., 1999). The fPOM and oPOM fractions were rinsed with deionized water in a pressure filtration system (0.22 µm pore nylon filter – Berrytec,

Grünwald, Germany) until the electrical conductivity was below 2 µS cm^{-1} (ANGST et al., 2016). The remaining mineral fraction was washed with deionized water until the electrical conductivity was below 50 µS cm^{-1} (ANGST et al., 2016). To avoid the loss of mineral particles, the water used to wash the mineral fraction was collected and rinsed in a pressure filtration system in the same manner as the fPOM and oPOM fractions. After the removal of salts, the mineral material retained in the filter was combined with the remaining mineral fraction and wet sieved through a 63 µm mesh sieve to obtain the fractions smaller than 63 µm (mineral-associated organic matter - MAOM) and greater than 63 µm (sand-sized organic matter - SSOM). The mean recovery rate of the SOM fractionation for C and N was 92% and 89%, respectively. All fractions were transferred to an oven at 40°C to reduce the volume of water and further freeze-dried.

2.6 Sequential extraction of Al and Fe hydroxide phases

We explored the effects of rhizodeposition on the Al and Fe hydroxides phases using a method adapted from Heckman et al., (2018). We extracted the organo-metallic complexes (OM) with sodium pyrophosphate and short-range order (SRO) phases with hydroxylamine using 1.0 g of the MAOM fraction from the 0-4 mm layer. Both extracts were shaken for 16 h (at 300 RPM) in the dark and centrifugated (2744 *g*) for 1 h. The supernatants were filtered through 0.2 µm polyethersulfone syringe filters (Phenomenex Ltd, Aschaffenburg, Germany). The residual soil was oven-dried at 40°C, ground, homogenized and subsampled before the next extraction. Concentrations of Fe, Al in filtered extracts were determined using an inductively coupled plasma-optic emission spectrometer (ICP-OES) (Vista-Pro CCD simultaneous, Varian, Darmstadt, Germany). Carbon contents were obtained by the difference of the residual soil after and before each extraction (solid-phase approach - HECKMAN et al., 2018). Also, the molar ratio of the extracted C and Fe was calculated to provide an insight into the structure of extracted organo-mineral association (COWARD; THOMPSON; PLANTE, 2017; WAGAI et al., 2013).

2.7 Phospholipid fatty acid analysis

The shifts in the structure of the soil microbial community caused by rhizodeposition were assessed by phospholipid fatty acid analysis (PLFA). We employed the methodology described by Frostegård et al. (1991) with adaptations of Kramer et al. (2013). The total lipid extraction was carried out by treating 2 g of freeze-dried soil with Bligh & Dyer solution (methanol, chloroform, and citrate pH 4, 2:1:0.8, v/v/v). The lipids were separated by solid-phase extraction on silica gel columns (0.5 g SiOH, Bond Elut, Agilent) in neutral, acidic, and polar fractions. The neutral and acidic fractions were discarded and the polar fraction was converted into fatty acid methyl esters (FAMEs) by alkaline methanolysis. The extracts were then dissolved in isooctane and determined in a Trace 1300 gas chromatograph (Thermofisher Scientific, Waltham, USA) equipped with a ZB-5HT column (60m, 0.25 I.D., 0.25µm film thickness; Phenomenex, Aschaffenburg, Germany) and flame ionization detector. The FAMEs identification was based on their retention time in comparison to a fungal and bacterial fatty acid methyl ester standard (37-Component FAME Mix and Bacterial Acid Methyl Esters Mix; Supelco, Bellefonte, USA). The PLFA were quantified relative to an internal standard (non-adecanoic acid methyl ester – 19:0) and normalized according to the mean of results for a standard soil that was extracted along with the samples (BAUMERT et al., 2018). The PLFAs were classified as bacterial biomarker (i15:0, a15:0, i16:0, i17:0, cy17:0, cy19:0, 15:0, 16:1n7, and 17:0) and fungal biomarkers (18:2n6). The total microbial PLFA content, which can be used as an indicator for the changes in microbial biomass (FROSTEGÅRD; TUNLID; BÅÅTH, 2011), was calculated as the sum of previously mentioned biomarkers in addition to the following: 14:0, 16:0, 18:1n9, 18:1n9t, 18:0, and 20:0.

2.8 Elemental and stable isotope analysis

The soil samples (bulk and fractions) were analyzed for total organic carbon content (C), total nitrogen content (N) and $\delta^{13}C$ of all layers using an isotopic ratio mass spectrometer (IRMS delta V Advantage, Thermo Fisher, Dreieich, Germany) coupled to an Elemental Analyzer (Euro EA, Eurovector, Milan, Italy).

2.9 Isotopic calculations

To gain information about the distribution of rhizo-C in the SOM fractions, we expressed the $\delta^{13}C$ as a percentage of the total ^{13}C recovered (adapted from Hafner

et al., 2012). These calculations were only possible for the treatment with rhizodeposition. For the control, as was expected, there were no significant differences between the $\delta^{13}C$ values of the corresponding unlabeled treatment (data not shown). For all samples, the $\delta^{13}C$ (‰) values were converted to the isotopic ratio (R_{sample}) according to equation 1:

$$R_{sample} = \left(\frac{\delta^{13}C}{1000} \times R_{PBD}\right) + R_{PDB} \quad (1)$$

Where R_{sample} is the carbon isotopic ratio of the sample, $\delta^{13}C$ (‰) is the isotopic signature from the sample obtained from isotope ratio mass spectrometer, and R_{PDB} is the isotopic ratio in the Pee Dee Belemnite standard (0.011237).

The percentage of ^{13}C relative to total C atoms ($^{13}C_{atom\%}$) was calculated following equation 2:

$$^{13}C_{atom\ \%} = \left(\frac{R_{sample}}{R_{sample}+1}\right) \quad (2)$$

From equation 2, we calculated the average atomic mass of C (g mol^{-1}) using equation 3:

$$C_{average\ mass} = (^{13}C_{mass\ number} \times {}^{13}C_{atom\ \%}) + (^{12}C_{mass\ number} \times (1 - {}^{13}C_{atom\ \%})) \quad (3)$$

Where $C_{average\ mass}$ is the C average atomic mass in the sample, $^{13}C_{mass\ number}$ is the mass number of ^{13}C which is considered as 13.0034 u, $^{12}C_{mass\ number}$ is the mass number of ^{12}C which is considered as 12 u, and $^{13}C_{atom\%}$ is the percentage of ^{13}C relative to total C atoms.

The enrichment of ^{13}C in each soil layer or SOM fraction ($^{13}C_{atom\%\ excess}$) resulting from the pulse labeling was calculated according to equation 4:

$$^{13}C_{atom\ \%\ excess} = {}^{13}C_{atom\ \%}\ \text{of sample} - {}^{13}C_{atom\ \%}\ \text{of unlabeled reference} \quad (4)$$

Where $^{13}C_{atom\%\ excess}$ is the enrichment of ^{13}C, $^{13}C_{atom\%}$ is the percentage of ^{13}C relative to total C atoms in the samples and the unlabeled treatments. The unlabeled treatments comprised the unlabeled mesocosms (with and without plants) which received pulses of non-isotopic enriched $NaCO_3$ analog (Table A5).

The amount of ^{13}C in excess that was incorporated in each soil layer or SOM fraction (rhizo-C) was calculated according to equation 5:

$$\text{Rhizo-C} = {}^{13}C_{atom\ \%\ excess} \times C_{content} \times C_{average\ mass} \times {}^{13}C_{mass\ number} \times 1000 \quad (5)$$

Where rhizo-C is the amount of ^{13}C in excess in a given SOM fraction (µg of ^{13}C g^{-1} of soil), $^{13}C_{atom\%excess}$ is the enrichment of ^{13}C (taken from equation 4), $C_{content}$ is the content of C (mg g^{-1} of soil), $C_{average\ mass}$ is C average atomic mass taken from equation 3 (g mol^{-1}), $^{13}C_{mass\ number}$ is the molar number of ^{13}C (13.0034 g mol^{-1}). The relative distribution of rhizo-C in the SOM fractions of the same experimental unit was calculated by the ratio between the rhizo-C in a given fraction and the sum of rhizo-C in all SOM. This approach allowed us to quantify potential losses of ^{13}C.

2.10 Statistical analysis

We assessed the impacts of rhizodeposition using non-paired t-tests (With Rhizodeposition vs. Control). Homogeneity of variance was checked by Levene's test and the Shapiro-Wilk test was performed to test the normal distribution of the data. We used two-way repeated-measures ANOVA followed by a Tukey's HSD *post hoc* test to evaluate differences in the $\delta^{13}C$ values of the residual soil after each step of the Al and Fe hydroxide phases sequential extraction (rhizodeposition and extractions as factors). This was done due to the dependence structure of the data, where the same sample was successively submitted to chemical extractions. All statistical analysis was conducted in R v. 3.6.0 (R CORE TEAM, 2021) with the packages *agricolae* (DE MENDIBURU, 2020) and *car* (FOX; WEISBERG, 2019). The probability level used to determine significance was $P < 0.05$.

3. Results

3.1 Soil carbon and nitrogen contents and $\delta^{13}C$ values

Rhizodeposition did not affect soil C content in any distance from the root, with a mean C content of 32.97 ±0.19 mg g^{-1} (mean of all distances) (Table 1). The N content was only affected by rhizodeposition in the 0-4 mm layer, with a 6% decrease ($p< 0.05$) as compared to the control (2.14 ±0.03 *vs.* 2.29 ±0.03 mg g^{-1}, respectively) (Table 1). Rhizodeposition also increased the C/N ratio by 4% and 3% at distances 0-4 and 15-25 mm, respectively (Table 1). The $\delta^{13}C$ values were significantly higher with rhizodeposition at all distances from the rhizoplane (Figure 3). The layer closer to the root (0-4 mm) exhibited the highest $\delta^{13}C$ values, with a mean of -20.40‰ ±1.1, which decreased along with the distancing to the rhizoplane. The $\delta^{13}C$ values of the control remained unaltered along with the distance, with an average value of 22.81‰ ±0.3 (Figure 3), regardless of the layer considered.

3.2 Soil OM fractionation

Regardless of the treatment, the MAOM fraction presented the highest C and N contents, gathering 80% and 90% of the total soil C and N, respectively (Table 2). With rhizodeposition, the C content within the oPOM fraction was twofold higher ($p < 0.05$), while it was 20% lower within the SSOM fraction ($p < 0.05$) compared with the control. Rhizodeposition tended to decrease the C in the MAOM fraction by 2% (25.03 ±0.04 *vs.* 25.58 ±0.14 mg g^{-1}), although it was not significant at 5% ($P < 0.10$). The N content in SOM fractions followed the same pattern as the C content. The presence of rhizodeposition significantly increased the $\delta^{13}C$ values in MAOM from -22.44‰ to -19.99‰ ($P < 0.05$) and in oPOM from -28.14‰ to -27.84‰ ($P < 0.05$) (Table 2). There was no significant effect of rhizodeposition in the $\delta^{13}C$ values of the fPOM and SSOM fractions (Table 2).

3.3 Sequential extraction of Al and Fe hydroxide phases

The rhizodeposition did not affect the amount of Fe, Al, and C bound to the OM complexes and SRO phases of the MAOM fraction (Table 3). Over 44% of total MAOM C was co-extracted with the OM complexes, whereas 18% of the total MAOM C was extracted with the SRO phases. The recovery rate of OM complexes and SRO phases extractions for Fe were respectively 20% and 1%, and the recovery rate of Al OM complexes and SRO phases were 11% and 17% respectively. The molar ratio of C-Fe was not affected by rhizodeposition and was on average 2.2 and 11.5 for the OM complexes and SRO extractions, respectively (Table A6).

The extractions of Fe and Al hydroxide phases affected the $\delta^{13}C$ values of the residual soil (the soil remaining after the extractions) of each treatment differently. The extraction of OM complexes changed the $\delta^{13}C$ values from -20.0 ±0.46‰ to -22.4 ±0.01‰ for the treatment with rhizodeposition ($P < 0.05$), but did not affect the $\delta^{13}C$ values of the control. Conversely, the extraction of SRO phases decreased $\delta^{13}C$ values from -22.2 ±0.08‰ to -23.1 ±0.12‰ for the control, but it did not affect the $\delta^{13}C$ values of the treatment with rhizodeposition ($P < 0.05$) (Figure 4). In all extractions, rhizodeposition treatment exhibit higher $\delta^{13}C$ values than the control (Figure 4).

3.4 PLFA and microbial communities

The rhizodeposition modified the abundance and the characteristics of the microbial community at 0-4 mm but not at 15-25 mm layer (Table 4). In the 0-4 mm

layer, rhizodeposition increased significantly the total microbial PLFAs by 53% (P< 0.05), the bacterial biomarkers in 101% (P< 0.05), the fungi biomarker in 61% (P< 0.05) and the GP:GN ratio in 102% (P< 0.05). In the 15-25 mm layer, there was no difference between the treatment with rhizodeposition and the control in any of the parameters evaluated (Table 4).

Table 1 — Total organic carbon (C) and total nitrogen (N) contents, and C/N ratios of the treatments with rhizodeposition and control along with the distances from the rhizoplane (mm).

	Treatment	Distance to rhizoplane			
		0-4 mm	4-8 mm	8-15 mm	15-25 mm
C (mg g^{-1})	With rhizodeposition	32.2 ±0.45 **a**	34.1 ±0.73 **a**	33.0 ±0.20 **a**	32.5 ±0.38 **a**
	Control	33.1 ±0.43 **a**	33.3 ±0.40 **a**	33.0 ±0.33 **a**	31.9 ±0.76 **a**
N (mg g^{-1})	With rhizodeposition	2.14 ±0.03 **a**	2.25 ±0.02 **a**	2.20 ±0.02 **a**	2.16 ±0.02 **a**
	Control	2.29 ±0.03 **b**	2.28 ±0.03 **a**	2.24 ±0.01 a	2.19 ±0.03 **a**
C/N	With rhizodeposition	15.1 ±0.07 **a**	15.2 ±0.02 **a**	15.0 ±0.10 **a**	15.0 ±0.10 **a**
	Control	14.5 ±0.07 **b**	14.6 ±0.03 **a**	14.7 ±0.13 **a**	14.6 ±0.12 **b**

Different letters indicate significant differences between the treatments with rhizodeposition and control. Means (n = 4) are compared between treatments by t-test at 0.05 of significance.
Source: Author.

3.5 Relative distribution of rhizo-C in SOM fractions

We detected that 76.2% ±3 of rhizo-C was contained in the MAOM fraction (Figure 5 and Table A7). The other fractions retained much less rhizo-C, with oPOM and fPOM accounting for only 1.4% ±3 and 2.8% ±1, respectively. The amount of rhizo-C in SSOM was neglectable (Figure 5). It has to be noted that 20% of the rhizo-C of the unfractionated soil was not recovered after the fractionation procedure (Figure 5). Additionally, we observed that only 6.4% of the rhizo-C was associated with OM complexes while 12.5% was associated with SRO phases (Figure 5). Unexpectedly, 57.8% of rhizo-C was not associated with organo-metallic (OM) complexes or Short-range order (SRO) phases and was not extracted with Al and Fe hydroxide sequential extraction (Figure 5).

Table 2 — Organic carbon (C) and total nitrogen (N) contents, C/N ratios, and $\delta^{13}C$ of SOM fractions for the treatments with rhizodeposition and control for the 0-4 mm layer.

	Treatment	SOM fraction			
		fPOM	oPOM	SSOM	MAOM
C (mg g^{-1})	With rhizodeposition	2.55 ±0.62 **a**	4.75 ±0.69 **a**	0.70 ±0.03 **b**	25.03 ±0.04 **a**
	Control	1.80 ±0.51 **a**	2.43 ±0.61 **b**	0.88 ±0.05 **a**	25.58 ±0.14 **a**
N (mg g^{-1})	With rhizodeposition	0.08 ±0.01 **a**	0.20 ±0.03 **a**	0.04 ±0.01 **a**	1.78 ±0.01 **a**
	Control	0.07 ±0.02 **a**	0.10 ±0.02 **b**	0.05 ±0.01 **b**	1.83 ±0.02 **b**
C/N	With rhizodeposition	30.3 ±4.5 **a**	23.4 ±0.5 **a**	20.2 ±0.8 **a**	13.6 ±0.1 **a**
	Control	26.1 ±0.1 **a**	24.4 ±0.4 **a**	19.6 ±07 **a**	14.4 ±0.1 **a**
$\delta^{13}C$ (‰)	With rhizodeposition	-28.2 ±0.3 **a**	-27.8 ±0.1 **a**	-24.6 ±0.1 **a**	-19.9 ±0.5 **a**
	Control	-28.7 ±0.1 **a**	-28.1 ±0.1 **b**	-24.3 ±0.1 **a**	-22.4 ±0.1 **b**

Different letters indicate significant differences between the treatments with rhizodeposition and control. Means (n = 4) are compared between treatments by t-test at 0.05 of significance.
Source: Author.

Table 3 — Iron (Fe), Aluminum (Al), and Carbon (C) bound in organo-metallic (OM) complexes (Pyrophosphate) and short-range-order (SRO) phases of Al and Fe (Hydroxylamine) from the mineral associated fraction (MAOM) of the treatment with rhizodeposition and control at 0-4 mm layer.

	Treatment	Before extraction	OM complexes	SRO phases
Fe (mg g^{-1})	With rhizodeposition	156.16± 0.95	29.85 ±1.00 **a**	2.35 ±0.13 **a**
	Control		33.46 ±2.79 **a**	2.15 ±0.12 **a**
Al (mg g^{-1})	With rhizodeposition	200.35± 1.46	21.48 ±0.44 **a**	34.09 ±1.20 **a**
	Control		23.40 ±1.28 **a**	34.03 ±1.57 **a**
C (mg g^{-1})	With rhizodeposition	33.26± 0.20 **a**	14.20 ±0.63 **a**	5.84 ±0.73 **a**
	Control	33.30± 0.13 **a**	14.91 ±0.47 **a**	5.24 ±1.01 **a**

Different letters indicate significant differences between the treatments with rhizodeposition. Means ± SE (n = 4) are compared between treatments by t-test at 0.05 of significance.
Source: Author.

Table 4 — Total Phospholipid fatty acid (PLFA), bacterial and fungi biomarkers, fungal: bacterial ratio, and gram-positive: gram-negative ratio for the treatment with rhizodeposition and control for the distances from the root of 0-4 mm and 15-25 mm.

	Treatment	Distance to root	
		0-4 mm	15-25 mm
Total PLFA (µmol g^{-1} C)	With rhizodeposition	1.90 ±0.35 **a**	1.74 ±0.28 **a**
	Control	1.26 ±0.44 **b**	2.02 ±0.61 **a**
Bacteria (µmol g^{-1} C)	With rhizodeposition	0.67 ±0.11 **a**	0.62 ±0.13 **a**
	Control	0.33 ±0.22 **b**	0.89 ±0.35 **a**
Fungi (µmol g^{-1} C)	With rhizodeposition	0.13 ±0.01 **a**	0.12 ±0.02 **a**
	Control	0.08 ±0.02 **b**	0.10 ±0.02 **a**
Fungal:Bacteria ratio	With rhizodeposition	0.20 ±0.04 **a**	0.18 ±0.02 **a**
	Control	0.26 ±0.08 **a**	0.12 ±0.05 **a**
GP:GN	With rhizodeposition	6.45 ±0.35 **a**	8.70 ±0.28 **a**
	Control	3.18 ±0.28 **b**	10.29 ±0.61 **a**

Different letters indicate significant differences between the treatments with rhizodeposition. Means ± SE (n = 3) are compared between treatments by t-test at 0.05 of significance.
Source: Author.

Figure 3 — Soil $\delta^{13}C$ values for the treatment with rhizodeposition and control as a function of the distance from the rhizoplane. Different letters indicate significant differences between the treatments with rhizodeposition and control. Means ± SE (n = 4) from all treatments is compared by t-test at 0.05 of significance.

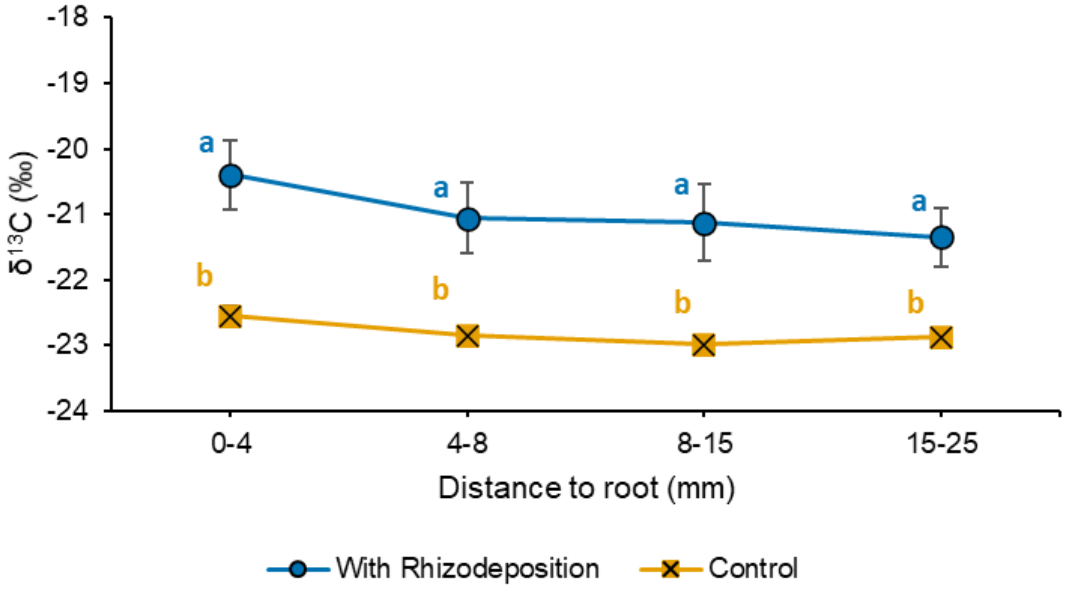

Source: Author.

Figure 4 — $\delta^{13}C$ values in the mineral associated fraction (MAOM) of the sequential extraction of Al and Fe from OM (organo-metallic) complexes and short-range order (SRO) phases for the treatment with rhizodeposition and control in the 0-4 mm layer. Lowercase letters indicate significant differences between the treatments with rhizodeposition and the control. Uppercase letters indicate significant differences between the extractions. Means ± SE (n = 4) from all treatments is compared by repeated-measures ANOVA followed by Tukey's HSD test at 0.05 of significance.

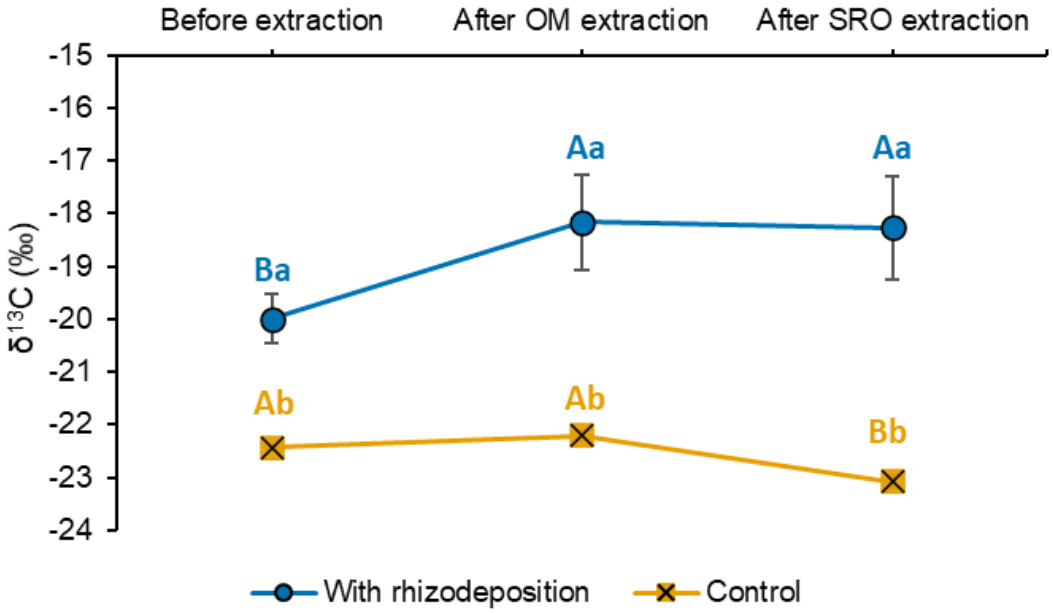

Source: Author.

Figure 5 — Relative distribution of rhizosphere-derived C (rhizo-C) in the SOM fractions and organo-metallic (OM) complexes and short-range order (SRO) phases. Means (n = 4) of the relative distribution were calculated in relation to bulk soil (unfractionated). A detailed version of this graph is provided in Table A7.

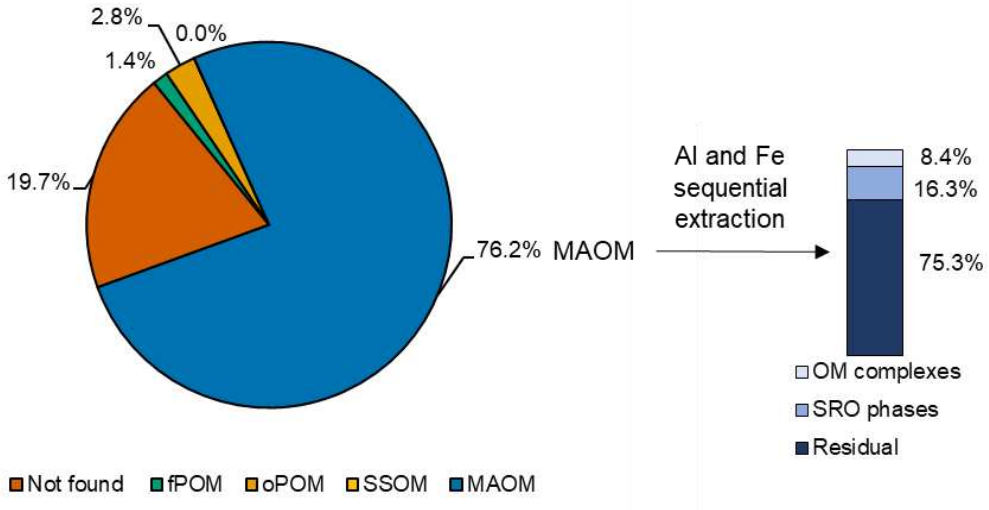

Source: Author.

4. Discussion

4.1 Effects of rhizodeposition on soil C and N contents

Overall, rhizodeposition did not have a significant short-term effect (66 days) in soil C content and only affected N content in the layer closer to the rhizoplane (0-4 mm, Table 1). This limited impact of rhizodeposition on the C budget reflects the low concentration of rhizodeposition in comparison with other soil C pools (KUZYAKOV; DOMANSKI, 2000). Further, we observed that root presence reduced the N content and increased the C/N ratio at the 0-4 mm layer (Table 1). Rhizodeposition exhibit an important role in N acquisition and can increase N availability for the plants through the destabilization of mineral-associated N-bearing minerals and the stimulation of microbial activity (JILLING et al., 2018; KEILUWEIT et al., 2015; KUZYAKOV, 2010; VALADARES et al., 2020).

4.2 Rhizo-C accumulated closer to the roots

Our results showed that the ^{13}C enrichment was inversely proportional to the distance to the rhizoplane, and the greatest $\delta^{13}C$ values were found in the layer closer to the root (0-4 mm) (Figure 3). This is supported by the current knowledge claiming that rhizodeposits have a small dispersal potential in the rhizosphere (KUZYAKOV; RAZAVI, 2019), due to their rapid processing by microorganisms and to their high affinity with the mineral matrix (KAISER; GUGGENBERGER, 2003; KUZYAKOV; RASKATOV; KAUPENJOHANN, 2003). Yet, we also demonstrate the transfer of rhizo-C up to 25 mm away from the roots (Figure 3). Together with environmental conditions, the duration of the root influence on the soil is the main factor controlling the extent of the rhizosphere. In this context, the higher dispersion of rhizo-C found in our study can be attributed to the higher number of pulses and the higher incubation duration (10 pulses of ^{13}C-CO_2 over 66 days). Studies tracking the diffusion of rhizo-C commonly uses a single pulse of ^{13}C and trace the distribution of the rhizodeposits in the soil after only some days (KUZYAKOV; RASKATOV; KAUPENJOHANN, 2003; SAUER; KUZYAKOV; STAHR, 2006; ZU SCHWEINSBERG-MICKAN; JÖRGENSEN; MÜLLER, 2012). The limited-time interval between the pulse and the evaluation can restrict the dispersal of rhizodeposits in the soil, and studies that used the multiple pulse approach to study the spatial distribution of rhizo-C also observed a wider distribution of rhizo-C (PEIXOTO et al., 2020; QIAO et al., 2014).

4.3 From rhizodeposits to mineral-associated OM

More than three-fourths of rhizo-C were recovered in the MAOM fraction (Figure 5). We thus demonstrate that rhizodeposits are key precursors for the formation of mineral-associated SOM, as previously observed by Sokol et al., (2018). Rhizodeposits can form MAOM through 2 distinct pathways: the *in-vivo* microbial turnover pathway, in which the substrates are submitted to microbial processing before its association with the mineral matrix, and the direct sorption pathway, in which the interaction of the plant compounds with the soil matrix occurs directly (LIANG; SCHIMEL; JASTROW, 2017; SOKOL; SANDERMAN; BRADFORD, 2018). Based on several works that demonstrate the high amount of microbial byproducts in SOM composition, we assume that *in-vivo* microbial pathway prevails in the rhizosphere (KLEBER; SOLLINS; SUTTON, 2007; KOPITTKE et al., 2018, 2020; SOKOL; SANDERMAN; BRADFORD, 2018). The enhanced availability of C in the rhizosphere creates a hotspot that allows microorganisms to grow and turn over rapidly (KUZYAKOV; BLAGODATSKAYA, 2015; LIANG; SCHIMEL; JASTROW, 2017) and the microbial residues resulting from successive microbial life-cycles interacts with the mineral matrix, becoming less susceptible to be subsequently mineralized (DUNGAIT et al., 2012; KÖGEL-KNABNER et al., 2008).

Our results also show that rhizodeposition almost doubled the amount of C associated with the oPOM fraction (Table 2). The occlusion of SOM inside aggregates represents an important mechanism of protection against decomposition (DUNGAIT et al., 2012). Rhizodeposition-induced aggregation is mainly associated with the formation of macroaggregates and is mostly controlled by root growth and fungal hyphae (BAUMERT et al., 2018; JEEWANI et al., 2020; OADES; WATERS, 1991). An enhanced fungal activity is supported by the PLFAs results, which show a 61% increase in the fungal biomarker due to rhizodeposition (Table 4). We propose that the fungal hyphae serve as a nucleus for the formation of oPOM via encrustation with mineral particles (DUNGAIT et al., 2012; OADES; WATERS, 1991). However, this effect was not followed by a proportional increase in ^{13}C enrichment, since oPOM $\delta^{13}C$ values were only slightly changed from -28.14 ±0.08‰ to -27.84 ±0.08‰ (Table 2). Thus, we would expect that fungal structures would reflect more the high ^{13}C enrichment of the rhizodeposits. One possibility is that those organisms were also feeding on native SOM and not exclusively on rhizodeposits. Vidal et al., (2018) observed that bacterial cells in the rhizosphere were less enriched in ^{13}C than the roots

themselves, and concluded that this was a dilution effect caused by the consumption of “native” SOM.

4.4 Rhizodeposition alters the microbial community structure

Our results showed that rhizodeposition increased the living microbial biomass (estimated by total PLFA) and the biomarkers of both fungal and bacterial communities in 0-4 mm layer, but not at 15-25 mm (Table 4). These results reflect the distribution pattern of rhizo-C, which was maximum closer to roots and decreased along with the distancing to the rhizoplane (Figure 3). Soil microorganisms are mostly limited by C, and the input of easily decomposable organic substrates removes this limitation and boosts microbial activity (KUZYAKOV; BLAGODATSKAYA, 2015; SCHIMEL; WEINTRAUB, 2003). However, since we observed a significant presence of rhizo-C at the distance 15-25 mm, it was expected an enhanced microbial activity at this distance. Notwithstanding, our results suggest that the amount of rhizo-C that was dispersed through the 15-25 mm layer was not enough to increase the microbial activity or change the microbial community structure composition. In this context, our results indicate that rhizodeposition impacts in microbial activity are spatially constrained to a small region in the soil closer to the roots (KUZYAKOV; BLAGODATSKAYA, 2015).

We observed that the rhizodeposits stimulated more the bacterial than the fungal community (Table 4). The bacterial community is highly competitive for low mass water-soluble compounds such as root exudates (GUNINA et al., 2014). In contrast, the fungal community has more advantage in the decomposition of more complex substrates, which are present in smaller amounts in the rhizodeposits (sloughed-off cells, mucilage, etc.) (GUNINA et al., 2014; HÜTSCH; AUGUSTIN; MERBACH, 2002; JONES; NGUYEN; FINLAY, 2009). Additionally, we observed an unexpected increase in the GP: GN ratio due to rhizodeposition (Table 4). Rhizodeposits are regarded as an easy-decomposable source of C, which is normally associated with gram-negative bacterial groups (GARCIA-PAUSAS; PATERSON, 2011; GUNINA et al., 2014; PATERSON et al., 2007; PEIXOTO et al., 2020). The dominance of gram-positive bacteria is more common in soils that are more restricted in C due to its capacity to process more complex C compounds (FANIN et al., 2019). In our study, the increase in GP:GN ratio may be related to the N fertilization that was done at the beginning of the experiment. In long-term experiments, the high N inputs

can promote a negative impact in gram-negative bacterial communities and increase the GP:GN ratio (WANG et al., 2018).

4.5 In short term, rhizodeposits do not promote the release of mineral bound carbon

About 60% of the original MAOM-C was coextracted with Al and Fe OM complexes and SRO phases (Table 3), which highlights the importance of these fractions for SOM retention in tropical soils (KLEBER et al., 2005; SOUZA et al., 2018). Contrary to our hypothesis, rhizodeposition did not promote the release of the mineral-bound C associated with these fractions (Table 3). The intensity of metal-bound C mobilization is dependent on the amount/composition of the rhizodeposits and the reactivity of minerals in the soil (LI et al., 2021).

Recent evidence demonstrated that simple compounds commonly found in root exudates can promote the destabilization of OM complexes and SRO phases in the short term (KEILUWEIT et al., 2015; LI et al., 2021). Nevertheless, these short-term results are restricted only to experiments that used pure reactants as a proxy for rhizodeposits. Since most of these experiments use high exudation rates (> 15 µmol C cm^{-2} root surface d^{-1}) and only one type of substance (KEILUWEIT et al., 2015; LI et al., 2021), it is logical to assume that the intensity of this effect will be higher than the ones promoted by the real roots, especially in the short-term.

Another factor that affects the intensity of the metal-bound C disruption is mineral reactivity (LI et al., 2021). The soil used in our study was predominantly composed of kaolinite and gibbsite (data not shown). These mineral species are considered to be more resistant to disruption in comparison with poorly crystalline minerals such as ferrihydrite (LI et al., 2021). In this context, the smaller vulnerability of our soil may have prevented the destabilization of metal-bound C by rhizodeposition (LI et al., 2021). Moreover, literature shows a significant number of studies reporting the influence of roots in the formation and disruption of mineral-organic associations over pedogenic time scales (GARCIA ARREDONDO et al., 2019; KORCHAGIN et al., 2019; MIKUTTA et al., 2009), but only one study detected this effect in short-term (COLLIGNON; RANGER; TURPAULT, 2012). In this context, we propose that in the short-term and with natural rhizodeposit concentrations, rhizodeposition does not disrupt mineral-organic associations.

Recent studies provide evidence that Fe hydroxide phases strong affinity for rhizo-C (JEEWANI et al., 2020, 2021). In contrast, our results show that only 6.4% and

12.5% of the rhizo-C was associated with Al and Fe OM complexes and SRO phases, respectively (Figure 5). The remaining majority of rhizo-C in the MAOM was not coextracted with these fractions, even though these fractions accounted for about 60% of MAOM-C. Those results contradict our third hypothesis, that rhizo-C would be predominantly incorporated into the Al and Fe OM complexes and SRO phases and suggests that other mechanisms would be more important for the retention of rhizo-C in soil.

Mineral-associated C is not a homogeneous pool and its persistence in the soil is affected by the crystallinity of the minerals (HALL; BERHE; THOMPSON, 2018; HECKMAN et al., 2013). Poorly-crystalline phases (such as OM complexes and SRO phases) are more associated with fast cycling SOM due to its higher reactivity and smaller resistance to disruption (HALL; BERHE; THOMPSON, 2018; KAISER et al., 2016; KEILUWEIT et al., 2015). Our results show that SRO phases retained almost two-fold more rhizo-C than OM complexes (Figure 5), despite accounting for only 15% of total soil C. This result differs from Jeewani et al., (2020), which observed higher incorporation of rhizo-C in the OM complexes of an Alfisol amended with goethite.

Despite these results, 75.3% of rhizo-C was not coextracted with Al and Fe OM complexes and SRO phases (Figure 5). This finding suggests that poorly-crystalline phases, such as OM complexes and SRO phases, are minorly involved with the retention of rhizo-C and other mechanisms must be more important. One possibility may be the interaction of rhizo-C with more crystalline minerals, such as kaolinite and gibbsite, which have a widespread occurrence in Ferrasols (SCHAEFER, FABRIS, KER, 2008). The retention of C in more crystalline phases is taken as less effective due to the smaller surface area and a smaller reactivity in comparison with OM complexes and SRO phases (MIKUTTA et al., 2006). Nevertheless, it has been shown that these fractions can display an important role in the protection of SOM, especially in soils with a little amount of poorly crystalline phases like the Ferralsol used in this study (KHOMO et al., 2017; MIKUTTA et al., 2006). However, the assessment of the rhizo-C retention in crystalline phases was beyond the scope of this study and was not quantified. Our results are in agreement with the understanding that OM complexes and SRO phases are capable to retain rhizo-C, as had been demonstrated by Jeewani et al., (2020). However, our results suggest that these minerals are not the main mechanism responsible for rhizo-C persistence in soils.

5. Conclusions

We provide direct evidence that rhizodeposit-derived C (rhizo-C) predominantly supplies the MAOM fraction. This finding is in agreement with the emerging view that simple organic compounds such as rhizodeposits are preserved in the soil through mineral associations. Furthermore, rhizo-C tended to accumulate in the direct vicinity of the roots where they stimulate both bacterial and fungal communities. The amount of rhizo-C decrease along with the distancing of the root, but was still detectable up to 25 mm of distance. Our results reveal that Al and Fe OM complexes and SRO phases were not affected by rhizodeposition in the short term and only a minor quantity of rhizo-C was incorporated with these fractions.

6. References

ANGST, G.; KÖGEL-KNABNER, I.; KIRFEL, K.; HERTEL, D.; MUELLER, C. W. Spatial distribution and chemical composition of soil organic matter fractions in rhizosphere and non-rhizosphere soil under European beech (Fagus sylvatica L.). **Geoderma**, [S. l.], v. 264, n. May, p. 179–187, 2016.

ANGST, G.; MESSINGER, J.; GREINER, M.; HÄUSLER, W.; HERTEL, D.; KIRFEL, K.; KÖGEL-KNABNER, I.; LEUSCHNER, C.; RETHEMEYER, J.; MUELLER, C. W. Soil organic carbon stocks in topsoil and subsoil controlled by parent material, carbon input in the rhizosphere, and microbial-derived compounds. **Soil Biology and Biochemistry**, [S. l.], v. 122, n. July, p. 19–30, 2018.

ANGST, G.; MUELLER, K. E.; EISSENSTAT, D. M.; TRUMBORE, S.; FREEMAN, K. H.; HOBBIE, S. E.; CHOROVER, J.; OLEKSYN, J.; REICH, P. B.; MUELLER, C. W. Soil organic carbon stability in forests: Distinct effects of tree species identity and traits. **Global Change Biology**, [S. l.], v. 25, n. 4, p. 1529–1546, 2019.

BAUMERT, V. L.; VASILYEVA, N. A.; VLADIMIROV, A. A.; MEIER, I. C.; KÖGEL-KNABNER, I.; MUELLER, C. W. Root exudates induce soil macroaggregation facilitated by fungi in subsoil. **Frontiers in Environmental Science**, [S. l.], v. 6, n. NOV, 2018.

CAROLINO DE SÁ, M. A.; LIMA, J. M.; SILVA, M. L. N.; DIAS JUNIOR, M. S. Índice De Desagregação Do Solo Baseado Em Energia Ultra-Sônica. **Revista Brasileira de Ciência do Solo**, Viçosa-MG, v. 23, n. 3, p. 525–531, 1999.

CHENG, W.; PARTON, W. J.; GONZALEZ-MELER, M. A.; PHILLIPS, R.; ASAO, S.; MCNICKLE, G. G.; BRZOSTEK, E.; JASTROW, J. D. Synthesis and modeling perspectives of rhizosphere priming**. New Phytologist**, [S. l.], v. 201, n. 1, p. 31–44, 2014.

COLLIGNON, C.; RANGER, J.; TURPAULT, M. P. Seasonal dynamics of Al- and Fe-bearing secondary minerals in an acid forest soil: Influence of Norway spruce roots (Picea abies (L.) Karst.). **European Journal of Soil Science**, [S. l.], v. 63, n. 5, p. 592–602, 2012.

DE MENDIBURU, F. **agricolae**: Statistical Procedures for Agricultural Research. 2020.

DIJKSTRA, F. A.; CHENG, W. Interactions between soil and tree roots accelerate long-term soil carbon decomposition. **Ecology Letters**, [S. l.], v. 10, n. 11, p. 1046–1053, 2007.

DUNGAIT, J. A. J.; HOPKINS, D. W.; GREGORY, A. S.; WHITMORE, A. P. Soil organic matter turnover is governed by accessibility not recalcitrance**. Global Change Biology**, [S. l.], v. 18, n. 6, p. 1781–1796, 2012.

FANIN, N.; KARDOL, P.; FARRELL, M.; NILSSON, M. C.; GUNDALE, M. J.; WARDLE, D. A. The ratio of Gram-positive to Gram-negative bacterial PLFA markers

as an indicator of carbon availability in organic soils. **Soil Biology and Biochemistry**, [S. l.], v. 128, n. June 2018, p. 111–114, 2019.

FOX, J.; WEISBERG, S. **An R Companion to Applied Regression**. Sage. Thousand Oaks, USA.

FROSTEGÅRD, Å.; TUNLID, A.; BÅÅTH, E. Microbial biomass measured as total lipid phosphate in soils of different organic content. **Journal of Microbiological Methods**, [S. l.], v. 14, n. 3, p. 151–163, 1991.

FROSTEGÅRD, Å.; TUNLID, A.; BÅÅTH, E. Use and misuse of PLFA measurements in soils. **Soil Biology and Biochemistry**, [S. l.], v. 43, n. 8, p. 1621–1625, 2011.

GARCIA-PAUSAS, J.; PATERSON, E. Microbial community abundance and structure are determinants of soil organic matter mineralisation in the presence of labile carbon. **Soil Biology and Biochemistry**, [S. l.], v. 43, n. 8, p. 1705–1713, 2011.

GARCIA ARREDONDO, M.; LAWRENCE, C. R.; SCHULZ, M. S.; TFAILY, M. M.; KUKKADAPU, R.; JONES, M. E.; BOYE, K.; KEILUWEIT, M. Root-driven weathering impacts on mineral-organic associations in deep soils over pedogenic time scales. **Geochimica et Cosmochimica** Acta, [S. l.], v. 263, p. 68–84, 2019.

GUNINA, A.; DIPPOLD, M. A.; GLASER, B.; KUZYAKOV, Y. Fate of low molecular weight organic substances in an arable soil: From microbial uptake to utilisation and stabilisation. **Soil Biology and Biochemistry**, [S. l.], A, v. 77, p. 304–313, 2014.

HAFNER, S.; UNTEREGELSBACHER, S.; SEEBER, E.; BECKER, L.; XU, X.; LI, X.; GUGGENBERGER, G.; MIEHE, G.; KUZYAKOV, Y. Effect of grazing on carbon stocks and assimilate partitioning in a Tibetan montane pasture revealed by $^{13}CO_2$ pulse labeling. **Global Change Biology**, [S. l.], v. 18, n. 2, p. 528–538, 2012.

HALL, S. J.; BERHE, A. A.; THOMPSON, A. Order from disorder: do soil organic matter composition and turnover co-vary with iron phase crystallinity? **Biogeochemistry**, [S. l.], v. 140, n. 1, p. 93–110, 2018.

HECKMAN, K.; GRANDY, A. S.; GAO, X.; KEILUWEIT, M.; WICKINGS, K.; CARPENTER, K.; CHOROVER, J.; RASMUSSEN, C. Sorptive fractionation of organic matter and formation of organo-hydroxy-aluminum complexes during litter biodegradation in the presence of gibbsite. **Geochimica et Cosmochimica Acta**, [S. l.], v. 121, p. 667–683, 2013.

HECKMAN, K.; LAWRENCE, C. R.; HARDEN, J. W. A sequential selective dissolution method to quantify storage and stability of organic carbon associated with Al and Fe hydroxide phases. **Geoderma**, [S. l.], v. 312, n. September 2017, p. 24–35, 2018.

HOLZ, M.; ZAREBANADKOUKI, M.; KUZYAKOV, Y.; PAUSCH, J.; CARMINATI, A. Root hairs increase rhizosphere extension and carbon input to soil. **Annals of Botany**, [S. l.], v. 121, n. 1, p. 61–69, 2018.

HÜTSCH, B. W.; AUGUSTIN, J.; MERBACH, W. Plant rhizodeposition - An important source for carbon turnover in soils. **Journal of Plant Nutrition and Soil Science**, [S. l.], v. 165, n. 4, p. 397–407, 2002.

INGWERSEN, J.; POLL, C.; STRECK, T.; KANDELER, E. Micro-scale modelling of carbon turnover driven by microbial succession at a biogeochemical interface. **Soil Biology and Biochemistry**, [S. l.], v. 40, n. 4, p. 864–878, 2008
.
IUSS WORKING GROUP WRB. **World Reference Base for Soil Resources 2014, Uptade 2015.** International soil classification system for naming soils and creating legends for soil maps**.** World Soil Resources Reports No. 106. FAO, Rome, 2015.

JEEWANI, P. H.; GUNINA, A.; TAO, L.; ZHU, Z.; KUZYAKOV, Y.; VAN ZWIETEN, L.; GUGGENBERGER, G.; SHEN, C.; YU, G.; SINGH, B. P.; PAN, S.; LUO, Y.; XU, J. Rusty sink of rhizodeposits and associated keystone microbiomes. **Soil Biology and Biochemistry**, [S. l.], v. 147, n. May, p. 107840, 2020.

JEEWANI, P. H.; LING, L.; FU, Y.; VAN ZWIETEN, L.; ZHU, Z.; GE, T.; GUGGENBERGER, G.; LUO, Y.; XU, J. The stoichiometric C-Fe ratio regulates glucose mineralization and stabilization via microbial processes. **Geoderma**, [S. l.], v. 383, n. November 2020, p. 114769, 2021.
.
JILLING, A.; KEILUWEIT, M.; CONTOSTA, A. R.; FREY, S.; SCHIMEL, J.; SCHNECKER, J.; SMITH, R. G.; TIEMANN, L.; GRANDY, A. S. Minerals in the rhizosphere: overlooked mediators of soil nitrogen availability to plants and microbes. **Biogeochemistry**, [S. l.], v. 139, n. 2, p. 103–122, 2018.

JOHNSON, D.; LEAKE, J. R.; OSTLE, N.; INESON, P.; READ, D. J. In situ $^{13}CO_2$ pulse-labelling of upland grassland demonstrates a rapid pathway of carbon flux from arbuscular mycorrhizal mycelia to the soil. **New Phytologist**, [S. l.], v. 153, n. 2, p. 327–334, 2002.

JONES, D. L.; NGUYEN, C.; FINLAY, R. D. Carbon flow in the rhizosphere: Carbon trading at the soil-root interface. **Plant and Soil**, [S. l.], v. 321, n. 1–2, p. 5–33, 2009.

KAISER, K.; GUGGENBERGER, Georg. Mineral surfaces and soil organic matter. **European Journal of Soil Science**, [S. l.], v. 54, n. 2, p. 219–236, 2003.

KAISER, M.; ZEDERER, D. P.; ELLERBROCK, R. H.; SOMMER, M.; LUDWIG, B. Effects of mineral characteristics on content, composition, and stability of organic matter fractions separated from seven forest topsoils of different pedogenesis. **Geoderma**, [S. l.], v. 263, p. 1–7, 2016.

KEILUWEIT, M.; BOUGOURE, J. J.; NICO, P. S.; PETT-RIDGE, J.; WEBER, P. K.; KLEBER, M.. Mineral protection of soil carbon counteracted by root exudates**.** **Nature Climate Change**, [S. l.], v. 5, n. 6, p. 588–595, 2015.

KHOMO, L.; TRUMBORE, S.; BERN, C. R.; CHADWICK, O. A. Timescales of carbon turnover in soils with mixed crystalline mineralogies. **Soil**, [S. l.], v. 3, n. 1, p. 17–30, 2017.

KINDLER, R.; MILTNER, A.; RICHNOW, H. H.; KÄSTNER, M. Fate of gram-negative bacterial biomass in soil - Mineralization and contribution to SOM. **Soil Biology and Biochemistry**, [S. l.], v. 38, n. 9, p. 2860–2870, 2006.

KLEBER, M.; MIKUTTA, R.; TORN, M. S.; JAHN, R. Poorly crystalline mineral phases protect organic matter in acid subsoil horizons. **European Journal of Soil Science**, [S. l.], v. 56, n. 6, p. 717–725, 2005.

KLEBER, M.; SOLLINS, P.; SUTTON, R. A conceptual model of organo-mineral interactions in soils: Self-assembly of organic molecular fragments into zonal structures on mineral surfaces. **Biogeochemistry**, [S. l.], v. 85, n. 1, p. 9–24, 2007.

KLEBER, M.; EUSTERHUES, K.; KEILUWEIT, M.; MIKUTTA, C.; MIKUTTA, R.; NICO, P. S. Mineral-Organic Associations: Formation, Properties, and Relevance in Soil Environments. **Advances in Agronomy**, [S. l.], v. 130, p. 1–140, 2015.

KÖGEL-KNABNER, I.; GUGGENBERGER, G.; KLEBER, M.; KANDELER, E.; KALBITZ, K.; SCHEU, S.; EUSTERHUES, K.; LEINWEBER, P. Organo-mineral associations in temperate soils: Integrating biology, mineralogy, and organic matter chemistry**. Journal of Plant Nutrition and Soil Science**, [S. l.], v. 171, n. 1, p. 61–82, 2008.

KOPITTKE, P. M.; DALAL, R. C.; HOESCHEN, C.; LI, C.; MENZIES, N. W.; MUELLER, C. W. Soil organic matter is stabilized by organo-mineral associations through two key processes: The role of the carbon to nitrogen ratio. **Geoderma**, [S. l.], v. 357, p. 113974, 2020.

KOPITTKE, P. M; HERNANDEZ-SORIANO, M. C.; DALAL, R. C.; FINN, D.; MENZIES, N. W.; HOESCHEN, C.; MUELLER, C. W. Nitrogen-rich microbial products provide new organo-mineral associations for the stabilization of soil organic matter. **Global Change Biology.** [S. l.], n. July 2017, p. 1762–1770, 2018.

KORCHAGIN, J.; BORTOLUZZI, E. C.; MOTERLE, D. F.; PETRY, C.; CANER, L. Evidences of soil geochemistry and mineralogy changes caused by eucalyptus rhizosphere. **Catena**, [S. l.], v. 175, p. 132–143, 2019.

KRAMER, S.; MARHAN, S.; HASLWIMMER, H.; RUESS, L.; KANDELER, E. Temporal variation in surface and subsoil abundance and function of the soil microbial community in an arable soil. **Soil Biology and Biochemistry**, [S. l.], v. 61, p. 76–85, 2013.

KUZYAKOV, Y.; RASKATOV, A.; KAUPENJOHANN, M. Turnover and distribution of root exudates of Zea mays. **Plant and Soil**, [S. l.], v. 254, n. 2, p. 317–327, 2003.

KUZYAKOV, Y. Priming effects: Interactions between living and dead organic matter. **Soil Biology and Biochemistry**, [S. l.], v. 42, n. 9, p. 1363–1371, 2010.

KUZYAKOV, Y.; BLAGODATSKAYA, E. Microbial hotspots and hot moments in soil: Concept & review. **Soil Biology and Biochemistry**, [S. l.], v. 83, n. February, p. 184–199, 2015.

KUZYAKOV, Y.; DOMANSKI, G. Carbon input by plants into the soil. Review. **Journal of Plant Nutrition and Soil Science**, [S. l.], v. 163, n. 4, p. 421–431, 2000.

KUZYAKOV, Y.; RAZAVI, B. S. Rhizosphere size and shape: Temporal dynamics and spatial stationarity. **Soil Biology and Biochemistry**, [S. l.], v. 135, n. December 2018, p. 343–360, 2019.

LIANG, C.; SCHIMEL, J. P.; JASTROW, J. D. The importance of anabolism in microbial control over soil carbon storage. **Nature Microbiology**, [S. l.], v. 2, n. 8, 2017.

MACHADO, D. N.; NOVAIS, R. F.; SILVA, I. R.; LOUREIRO, M. E.; MILAGRES, J. J.; SOARES, E. M. B. S. Enriquecimento e alocação de ^{13}C em plantas de eucalipto. **Revista Brasileira de Ciência do Solo**, Viçosa-MG, v. 35, p. 857–866, 2011.

MARSCHNER, P.; MARHAN, S.; KANDELER, E.. Microscale distribution and function of soil microorganisms in the interface between rhizosphere and detritusphere**. Soil Biology and Biochemistry,** [S. l.], v. 49, p. 174–183, 2012.

MARX, M.; BUEGGER, F.; GATTINGER, A.; ZSOLNAY, Á.; MUNCH, J. C. Determination of the fate of ^{13}C labelled maize and wheat exudates in an agricultural soil during a short-term incubation. **European Journal of Soil Science**, [S. l.], v. 58, n. 5, p. 1175–1185, 2007.

MARX, M.; BUEGGER, F.; GATTINGER, A.; ZSOLNAY, Á.; MUNCH, J. C. Determination of the fate of regularly applied ^{13}C-labeled-artificial-exudates c in two agricultural soils. **Journal of Plant Nutrition and Soil Science**, [S. l.], v. 173, n. 1, p. 80–87, 2010.

MIKUTTA, R.; KLEBER, M.; TORN, M. S.; JAHN, R. Stabilization of soil organic matter: Association with minerals or chemical recalcitrance? **Biogeochemistry**, [S. l.], v. 77, n. 1, p. 25–56, 2006.

MIKUTTA, R.; SCHAUMANN, G. E.; GILDEMEISTER, D.; BONNEVILLE, S.; KRAMER, M. G.; CHOROVER, J.; CHADWICK, O. A.; GUGGENBERGER, G.. Biogeochemistry of mineral-organic associations across a long-term mineralogical soil gradient (0.3-4100 kyr), Hawaiian Islands. **Geochimica et Cosmochimica Acta**, [S. l.], v. 73, n. 7, p. 2034–2060, 2009.

MUELLER, C. W.; KOEGEL-KNABNER, I. Soil organic carbon stocks distribution, and composition affected by historic land use changes on adjacent sites. **Biology and Fertility of Soils**, [S. l.], v. 45, p. 347–359, 2009.

NOVAIS, R. F.; NEVES, J. C. L.; BARROS, N. F. Ensaio em ambiente controlado. In: OLIVEIRA, A. J. de; GARRIDO, W. E.; ARAUJO, J. D. de; LOURENÇO, S. (Coord.).

(org.). **Métodos de pesquisa em fertilidade do solo**. 1. ed. Brasília: Embrapa, 1991. p. 189–209.

NUCCIO, E. E.; STARR, E.; KARAOZ, U.; BRODIE, E. L.; ZHOU, J.; TRINGE, S. G.; MALMSTROM, R. R.; WOYKE, T.; BANFIELD, J. F.; FIRESTONE, M. K. PETT-RIDGE, J. Niche differentiation is spatially and temporally regulated in the rhizosphere. **The ISME Journal**, [S. l.], v. 14, n. 4, p. 999–1014, 2020.

OADES, J. M.; WATERS, A. G. Aggregate hierarchy in soils. **Australian Journal of Soil Research**, [S. l.], v. 29, n. 6, p. 815–825, 1991.

PATERSON, E.; GEBBING, T.; ABEL, C.; SIM, A.; TELFER, G. Rhizodeposition shapes rhizosphere microbial community structure in organic soil. **The New Phytologist**, [S. l.], v. 173, n. 3, p. 600–10, 2007.

PAUSCH, J.; KUZYAKOV, Y. Carbon input by roots into the soil: Quantification of rhizodeposition from root to ecosystem scale. **Global Change Biology**, [S. l.], v. 24, n. 1, p. 1–12, 2018.

PEIXOTO, L.; ELSGAARD, L.; RASMUSSEN, J.; KUZYAKOV, Y.; BANFIELD, C. C.; DIPPOLD, M. A.; OLESEN, J. E. Decreased rhizodeposition, but increased microbial carbon stabilization with soil depth down to 3.6 m. **Soil Biology and Biochemistry**, [S. l.], v. 150, n. June, 2020.

POLL, C.; INGWERSEN, J.; STEMMER, M.; GERZABEK, M. H.; KANDELER, E. Mechanisms of solute transport affect small-scale abundance and function of soil microorganisms in the detritusphere. **European Journal of Soil Science**, [S. l.], v. 57, n. 4, p. 583–595, 2006.

QIAO, Y.; MIAO, S.; LI, N.; HAN, X.; ZHANG, B. Spatial distribution of rhizodeposit carbon of maize (Zea mays L.) in soil aggregates assessed by multiple pulse ^{13}C labeling in the field. **Plant and Soil**, [S. l.], v. 375, n. 1–2, p. 317–329, 2014.

R CORE TEAM. R: A language and environment for statistical computing. v. 3.6.0., Vienna: R Foundation for Statistical Computing, 2021.

RASMUSSEN, C.; SOUTHARD, R. J.; HORWATH, W. R. Soil Mineralogy Affects Conifer Forest Soil Carbon Source Utilization and Microbial Priming. **Soil Science Society of America Journal**, [S. l.], v. 71, n. 4, p. 1141, 2007.

RUIZ, H. A. Incremento da exatidão da análise granulométrica do solo por meio da coleta da suspensão (Silte + Argila). **Revista Brasileira de Ciência do Solo**, Viçosa-MG, v. 29, n. 2, p. 297–300, 2005.

SAUER, D.; KUZYAKOV, Y.; STAHR, K. Spatial distribution of root exudates of five plant species as assessed by ^{14}C labeling. **Journal of Plant Nutrition and Soil Science**, [S. l.], v. 169, n. 3, p. 360–362, 2006.

SCHAEFER, C. E. G. R.; FABRIS, J. D.; KER, J. C. Minerals in the clay fraction of Brazilian Latosols (Oxisols): a review. **Clay Minerals**, [S. l.], v. 43, p. 137–154, 2008.

SCHIMEL, J. P.; WEINTRAUB, M. N. The implications of exoenzyme activity on microbial carbon and nitrogen limitation in soil: A theoretical model. **Soil Biology and Biochemistry**, [S. l.], v. 35, n. 4, p. 549–563, 2003.

SHAHZAD, T.; CHENU, C.; GENET, P.; BAROT, S.; PERVEEN, N.; MOUGIN, C.; FONTAINE, S. Contribution of exudates, arbuscular mycorrhizal fungi and litter depositions to the rhizosphere priming effect induced by grassland species. **Soil Biology and Biochemistry**, [S. l.], v. 80, p. 146–155, 2015.

SOKOL, N. W.; KUEBBING, S. E.; KARLSEN-AYALA, E.; BRADFORD, M. A. Evidence for the primacy of living root inputs, not root or shoot litter, in forming soil organic carbon. **New Phytologist**, [S. l.], p. 233–246, 2018.

SOKOL, N. W.; SANDERMAN, J.; BRADFORD, M. A. Pathways of mineral-associated soil organic matter formation: integrating the role of plant carbon source, chemistry, and point-of-entry. **Global Change Biology**, [S. l.], n. August, p. 1–13, 2018.

SOUZA, I. F.; ALMEIDA, L. F. J.; JESUS, G. L.; PETT-RIDGE, J.; NICO, P. S.; KLEBER, M.; SILVA, I. R. Carbon Sink Strength of Subsurface Horizons in Brazilian Oxisols. **Soil Science Society of America Journal**, [S. l.], v. 82, n. 1, p. 76–86, 2018.

TEDESCO, M. J.; GIANELLO, C.; BISSANI, C. A.; BOHNEN, H.; VOLKWEISS, S. J. **Análise de solo, plantas e outros materiais**. Porto Alegre. 2nd ed. 1995. 174 p.

VIDAL, A.; HIRTE, J.; BENDER, S. F.; MAYER, J.; GATTINGER, A.; HÖSCHEN, C.; SCHÄDLER, S.; IQBAL, T. M.; MUELLER, C. W. Linking 3D Soil Structure and Plant-Microbe-Soil Carbon Transfer in the Rhizosphere. **Frontiers in Environmental Science**, [S. l.], v. 6, n. February, p. 1–14, 2018.

WAGAI, R.; MAYER, L. M.; KITAYAMA, K.; SHIRATO, Y. Association of organic matter with iron and aluminum across a range of soils determined via selective dissolution techniques coupled with dissolved nitrogen analysis. **Biogeochemistry**, [S. l.], v. 112, n. 1–3, p. 95–109, 2013.

WANG, C.; LU, X.; MORI, T.; MAO, Q.; ZHOU, K.; ZHOU, G.; NIE, Y.; MO, J. Responses of soil microbial community to continuous experimental nitrogen additions for 13 years in a nitrogen-rich tropical forest. **Soil Biology and Biochemistry**, [S. l.], v. 121, n. March, p. 103–112, 2018.

WANG, Q.; WANG, Y.; WANG, S.; HE, T.; LIU, L. Fresh carbon and nitrogen inputs alter organic carbon mineralization and microbial community in forest deep soil layers. **Soil Biology and Biochemistry**, [S. l.], v. 72, p. 145–151, 2014.

ZU SCHWEINSBERG-MICKAN, M. S.; JÖRGENSEN, R. G.; MÜLLER, T. Rhizodeposition: Its contribution to microbial growth and carbon and nitrogen turnover within the rhizosphere. **Journal of Plant Nutrition and Soil Science**, [S. l.], v. 175, n. 5, p. 750–760, 2012.

YEOMANS, J. C.; BREMNER, J. M. A rapid and precise method for routine determination of organic carbon in soil. **Communications in Soil Science and Plant Analysis**, [S. l.], v. 19, n. May 2013, p. 1467–1476, 1988.

CHAPTER 2

ROOT LEGACY EFFECTS: THE FATE OF ROOT CARBON INPUTS AT RHIZOSPHERE-DETRITUSPHERE SUCCESSION

ABSTRACT

The reasons for the enhanced efficiency of conversion of root carbon (C) inputs into soil organic matter (SOM) are one of the great gaps in the terrestrial C cycle. One possible mechanism to explain this phenomenon is the occurrence of legacy effects. Legacy effects are triggered after root death when the former rhizospheric soil stops receiving labile rhizodeposits, and there is a shift to more recalcitrant C inputs that are derived from root litter. The transition between rhizospheric to detrituspheric soil represents a "*hot moment*" of biogeochemical C processing in the soil that remains poorly understood. In this study, we examined the impacts of legacy effects on the processing of rhizodeposit-derived C (rhizo-C) and in the incorporation of root litter into SOM. We designed two complementary incubation experiments using isotopic labeling (^{13}C and ^{15}N) to track the fate of root-derived C from rhizodeposits and root litter individually. In the first experiment, a former rhizospheric soil (clayey Rhodic Ferrasol) containing ^{13}C and ^{15}N labeled rhizodeposits from *Eucalyptus spp.* was incubated in the presence of unlabeled root litter, to follow the fate of rhizodeposit-derived C. Analogously, in the second experiment we incubated ^{13}C and ^{15}N labeled root litter in a former *Eucalyptus* spp. rhizospheric soil, to follow the fate of root litter-derived C. Along with the incubation, we periodically evaluated the soil respiration and the ^{13}C enrichment of CO_2. After 166 days, we sliced the soil cylinders in layers according to the distance to root litter (0-4, 4-8, 8-15, and 15-25 mm) to gain knowledge of the spatial distribution of root C inputs. We performed a density/size fractionation to obtain elemental and isotopic information of specific soil C fractions and evaluated the impacts of legacy effects in microbial communities by PLFA analysis. Further, we investigated the incorporation of root litter C in SOM at the microscale using NanoSIMS (Nanoscale secondary ion mass spectrometry). Our results show that neither rhizo-C nor root litter fate was affected by legacy effects. This finding suggests that each of these types of C is processed independently in the rhizosphere-detritusphere transition. We detected that the majority of rhizo-C persisted in the soil through the 166-days incubation and was mostly found in the MAOM fraction. This result attests

that rhizo-C forms stable SOM through mineral associations. In contrast, we observed that root litter conversion in SOM was restricted up to 4 mm on its surroundings, and only about 10% of the decomposed root litter was incorporated in SOM. Further, our NanoSIMS imaging provides direct evidence for the incorporation of root litter into mineral-associated SOM mediated by microorganisms at the soil-litter interface.

Keywords: Eucalypt. Soil organic matter. Isotopes. NanoSIMS. Priming effect

1. Introduction

Current evidence indicates that root carbon (C) inputs are more efficiently converted into soil organic matter (SOM) than aboveground inputs but the reasons for these observations are still not understood (JACKSON et al., 2017; KÖGEL-KNABNER, 2017; LAVALLEE et al., 2018; RASSE; RUMPEL; DIGNAC, 2005; SOKOL et al., 2018). One important feature that differentiates root C inputs is related to the rhizospheric effects.

Root activity strongly affects the surrounding soil, and this effect produces a region in the soil with distinct biological, chemical, and physical properties that are known as rhizosphere (HINSINGER et al., 2009). One of the most important alterations in the rhizosphere is the release of organic compounds by roots, which are known as rhizodeposits (JONES; NGUYEN; FINLAY, 2009; KUZYAKOV; DOMANSKI, 2000). Rhizodeposits are mostly constituted by soluble, easily decomposable root exudates, besides other more recalcitrant materials, such as sloughed-off cells and mucilage (HÜTSCH; AUGUSTIN; MERBACH, 2002; JONES; NGUYEN; FINLAY, 2009). The enhanced availability of C driven by rhizodeposition boosts the activity of microorganisms and creates a hotspot for both formation and destabilization of SOM (DIJKSTRA; ZHU; CHENG, 2020; KUZYAKOV; BLAGODATSKAYA, 2015). Rhizodeposition can proportionate a positive impact on SOM formation by being efficiently converted into microbial byproducts, which are the main precursors for mineral-associated SOM formation (COTRUFO et al., 2013; LIANG; SCHIMEL; JASTROW, 2017). In contrast, rhizodeposition is also associated with the occurrence of priming effects, which frequently results in the destabilization of SOM (CHENG et al., 2014; HUO; LUO; CHENG, 2017; KEILUWEIT et al., 2015; KUZYAKOV; CHENG, 2001). Results from the literature show that negative impacts of rhizodeposition prevail and the amount of SOM that is formed does not compensate for what is lost (DIJKSTRA; CHENG, 2007; HENNERON et al., 2020).

Another important root-derived source of C input is the root litter, which is formed within the soil after root death. Similar to rhizodeposition, the decomposition of root litter generates a region in the soil with distinct properties that are named as detritusphere (KUZYAKOV; BLAGODATSKAYA, 2015; POLL et al., 2006). Root litter is mainly formed by structural compounds that need to be depolymerized by extracellular enzymes before microbial processing (KÖGEL-KNABNER, 2017; RASSE; RUMPEL; DIGNAC, 2005). In this context, root litter is more commonly

associated with particulate organic matter (POM), but it is also are capable to form MAOM as it is processed by microorganisms (COTRUFO et al., 2015). Due to its poor biochemical quality (high content lignin and low N), the efficiency of conversion of root litter in MAOM is usually lower than aboveground (BIRD; TORN, 2006; LAVALLEE et al., 2018). Moreover, root litter C inputs also can originate positive priming effects, which increases the mineralization rate of SOM (SHAHBAZ et al., 2017). Thus, the enhanced efficiency of conversion of root C inputs cannot be explained by either root litter or rhizodeposits alone.

The majority of the studies that followed the fate of root C inputs into SOM investigated rhizodeposits and root litter independently, and possible interactions between these two C sources are unknown. One possible interaction can be related to the occurrence of legacy effects, which can be defined as long-term effects that persist in the soil after its source is no more exerting its activity (WURST; OHGUSHI, 2015). After root senescence, rhizodeposition ceases, but the alterations induced by living roots persist in the soil for some time, influencing the conversion of root litter into SOM. This effect has not yet been investigated and can be important to explain the elevated efficiency of root-derived C conversion into SOM (OLIVER et al., 2021).

During the initial stage of rhizosphere-detritusphere transition, we have an enhanced availability of labile C in the soil that is derived not only from rhizodeposition but also from the root litter itself (COTRUFO et al., 2015). In this stage, the microbial community competes for these two sources of labile C until they are depleted or incorporated in non-accessible SOM fractions (DUNGAIT et al., 2012). The input of additional labile C from root litter can affect the extension on which the remaining rhizodeposit-derived C (rhizo-C) is processed by microorganisms. We predict that root litter presence will decrease the amount of rhizo-C processed by microorganisms, favoring its retention in the soil.

In the later stages of rhizosphere-detritusphere transition, the bioavailability of labile C diminishes, and the decomposition of more recalcitrant forms of C prevails (COTRUFO et al., 2015). The higher microbial activity provided by former labile C inputs can accelerate the decomposition rates of root litter (HICKS PRIES et al., 2018; KUZYAKOV; HILL; JONES, 2007; WANG et al., 2014) and modify the efficiency of conversion of root litter into SOM (SOKOL; SANDERMAN; BRADFORD, 2018). Sokol and Bradford, (2019) found that the efficiency of conversion of soluble C inputs into MAOM was higher in areas of enhanced microbial density, such as the rhizosphere.

We predict that the same effect will be observed for root litter, and the efficiency of root litter incorporation into SOM will be greater in the root-affected soil.

This study evaluated the impact of root legacy effects on the processing of rhizo-C and the incorporation of root litter into SOM. We designed two complementary incubation experiments using isotopic labeling (^{13}C and ^{15}N) to track the fate of root-derived C from rhizodeposits and root litter individually. Our hypothesis is that: (i) the presence of root litter will reduce the microbial processing of rhizo-C, favoring its retention in the soil; and (ii) the efficiency of root litter C conversion into SOM will be higher in the rhizospheric soil due to enhanced microbial activity.

2. Material and Methods

We designed two complementary incubation experiments that enabled the tracking of rhizodeposit and root litter-derived C by isotopic methods. Both experiments had the same treatments, and the only difference was the labeling that was present in rhizo-C for the first experiment and in root litter-derived C in the second experiment.

2.1 Experimental setup and soil cores

The soil cores and root litter used in this study were obtained from previous research (Chapter 1) and consisted of aluminum cylinders (height 2.5 cm, diameter 4.7 cm) filled with a Rhodic Ferralsol (IUSS Working Group WRB, 2014 - Table B1) that were incubated in the presence of active growing eucalypt roots (*Eucalyptus grandis* x *E. urophylla* clone - I144) (Figure B1). These soil cores were covered in one of their sides by a nylon membrane, that allowed the input of rhizodeposition-derived compounds into the cores. Pots without plants were also included to serve as a reference. The cultivation of the plants was done in a greenhouse, and the pots were periodically taken to the labeling chamber. The ^{13}C labeling was performed with a multiple-pulse labeling approach adapted from (MACHADO; NOVAIS; LOUREIRO, 2011), and it is described in detail in chapter 1. The ^{15}N labeling was done by the application of 50 mg de ^{15}N as ammonium sulfate (98%-atom) in the surface of the mesocosm, divided into 4 applications (25, 32, 40, and 46 days after planting). Besides the labeled treatments, unlabeled experimental units were also included to be used as a reference. All treatments had 4 replicates (Figure 1). After 66 days, the eucalypt plants were harvested and the root was carefully separated from the soil, washed with

deionized water, and freeze-dried. The membrane that covered the cores was removed and they were stored at 5°C.

2.2 Incubation of soil cores

The incubation experiment consisted of two complementary experiments that were formed by the combination of root litter and soil cores after the cultivation and labeling of the plants (Chapter 1). Each experiment was formed by the same 4 treatments: (i) Rhizospheric - With root litter; (ii) Rhizospheric - Without root litter; (iii) Non-rhizospheric - With root litter; (iv) Non-rhizospheric - Without root litter. Those materials were combined in a way that allowed the individual tracking of rhizodeposit-derived C for the first experiment and the tracking of root litter-derived C for the second experiment (Figure 1). Experiment 1 (tracking of rhizodeposit-derived C), was formed from soil cores from the labeled treatment with and without plants and the unlabeled root litter. Analogously, experiment 2 (tracking of root litter-derived C) was formed from soil cores from the unlabeled treatments with and without plants and the labeled root litter (Figure 1)

The soil cores were placed in air-tight jars (0.6 L) and root litter was added to the top of the soil cylinders at the rate of 0.0707 g cylinder^{-1} (0.58 mg C g^{-1} soil). The root litter added to experiment 1 was not labeled and had an isotopic enrichment within the natural abundance range (1.007% and 0.368% for ^{13}C and ^{15}N, respectively expressed as Atom%). The root litter added to experiment 2 was double-labeled and had an isotopic enrichment of 2.868% and 10.611% for ^{13}C and ^{15}N, respectively. We did not mix the root litter with the soil to gain information about the spatial distribution of root litter-derived C and N. The jars were kept in the dark at 25°C for 166 days, and the water content was maintained above 80% of the soil water holding capacity.

2.3 Soil respiration assessments

The CO_2 evolved from the soil cores were assessed at 0.5, 1, 2, 3, 7, 11, 14, 18, 21, 25, 28, 32, 39, 46, 56, 63, 70, 77, 84, 91, 98, 105, 119, 133, 147 and 161 days after the beginning of incubation (27 times in total). Between each assessment, the vials were kept closed and measurement intervals changed along with the incubation (Table B2). After each sampling, the jars were vented to prevent anaerobiosis. The incubation was done at 25°C and the jars remained closed until the next assessment (ALMEIDA et al., 2018). The atmosphere of the incubation jars was sampled with a 60

mL syringe and analyzed for C-CO_2 concentration and δ^{13}C-CO_2 in a cavity ring-down spectrometer (CRDS, Picarro, Sunnyvale, United States of America).

2.4 Soil core slicing

After 166 days, the remaining root litter was carefully collected from the top of the soil cores. Further, the soil cores were sliced into four layers: 0-4, 4-8, 8-15, and 15-25 mm (distance from the top of the core). The slicing was done with an adapted holding device that pushes the soil layer out of the cylinder, and the cuts of the layers were done manually with a razor (Figure B2) Between each slice, the device was cleaned to avoid cross-contamination. Approximately 3 g of each layer of soil was freeze-dried for phospholipid fatty acid (PLFA) analysis and the remaining soil was air-dried and sieved at 2 mm.

2.5 SOM fractionation

The changes in SOM pools were assessed in the 0-4 mm layer using a combined density and particle size fractionation adapted from Angst et al. (2016). Briefly, we used sodium polytungstate (SPT) solution (density of 1.8 g cm^{-3}) to separate the free organic material (fPOM) and the organic material occluded within the aggregates (oPOM) (after sonication). Then, we wet sieved the remaining material through a 63 µm mesh sieve to obtain the fractions smaller than 63 µm (mineral-associated organic matter - MAOM) and greater than 63 µm (sand-sized organic matter - SSOM). All fractions were further freeze-dried and ground before elemental measurement.

2.6 Elemental and stable isotope analyses

The root and soil samples (bulk and fractions) were analyzed for total organic carbon (C) content, total nitrogen content (N) and abundance of ^{13}C (Atm%) using an isotopic ratio mass spectrometer (IRMS delta V Advantage, Thermo Fisher, Dreieich, Germany) coupled to an Elemental Analyzer (Euro EA, Eurovector, Milan, Italy).

2.7 Phospholipid Fatty Acid Analysis

The structure of the soil microbial community was assessed by phospholipid fatty acid (PLFA) analysis. We used the methodology described by Frostegård et al. (1991) and modified by Baumert et al., (2018). Briefly, soil lipids were extracted from 2

g of freeze-dried soil with Bligh & Dyer solution (methanol, chloroform, and citrate pH 4, 2:1:0.8, v/v/v) and then separated on silica gel columns (0.5 g SiOH, Bond Elut, Agilent). The polar fraction was collected and submitted to alkaline methanolysis, and the resultant fatty acid methyl esters (FAMEs) were measured in a Trace 1300 gas chromatograph with flames ionization detector (GC-FID, Thermofisher Scientific, Waltham, USA) equipped with a ZB-5HT column (60m, 0.25 I.D., 0.25µm film thickness; Phenomenex, Aschaffenburg, Germany). The PLFA were quantified relative to an internal standard (non-adecanoic acid methyl ester – 19:0) and normalized according to the mean of results for a standard soil that was extracted along with the samples (BAUMERT et al., 2018). PLFAs were classified as bacterial biomarkers (i15:0, a15:0, i16:0, i17:0, cy17:0, cy19:0, 15:0, 16:1n7, and 17:0) and fungal biomarkers (18:2n6), and the fungal-to-bacterial ratio (F:B ratio) was calculated. The total microbial PLFA content, which can be used as an indicator for changes in microbial biomass (FROSTEGÅRD; TUNLID; BÅÅTH, 2011), was calculated by the sum of bacterial and fungal biomarkers plus unspecified microbial PLFAs (14:0, 16:0, 18:1n9, 18:1n9t, 18:0, and 20:0).

2.8 Solid-state CPMAS ^{13}C NMR spectroscopy

We evaluated the changes in root litter chemical composition using a solid-state cross-polarization magic angle spinning (CPMAS) ^{13}C nuclear magnetic resonance (NMR) spectroscopy (KÖGEL-KNABNER, 1997). Measurements were done with Bruker DSX 200 NMR spectrometer (resonance frequency: 50.323 MHz, Bruker Corp. Rheinstetten, Germany). The samples were rotated at the magic angle (54.78°) with a spinning speed of 6.8 kHz and recycle delay time of 700 ms. The NRM spectra were integrated using four major chemical shift regions: alkyl-C (10-45 ppm), O/N-alkyl C (45-110 ppm), aryl C (110-160 ppm), and carboxyl/amide/carbonyl C (160-220 ppm). Then, the molecular mixing model was applied to the spectra to obtain information about the relative contribution of different biomolecules (carbohydrates, proteins, etc.) (NELSON; BALDOCK, 2005). We also calculated the alkyl C to O/N-alkyl C ratio as a proxy for root litter decomposition (BONANOMI et al., 2013).

Figure 1 — Simplified representation of the experimental design and treatments of experiments 1 and 2.

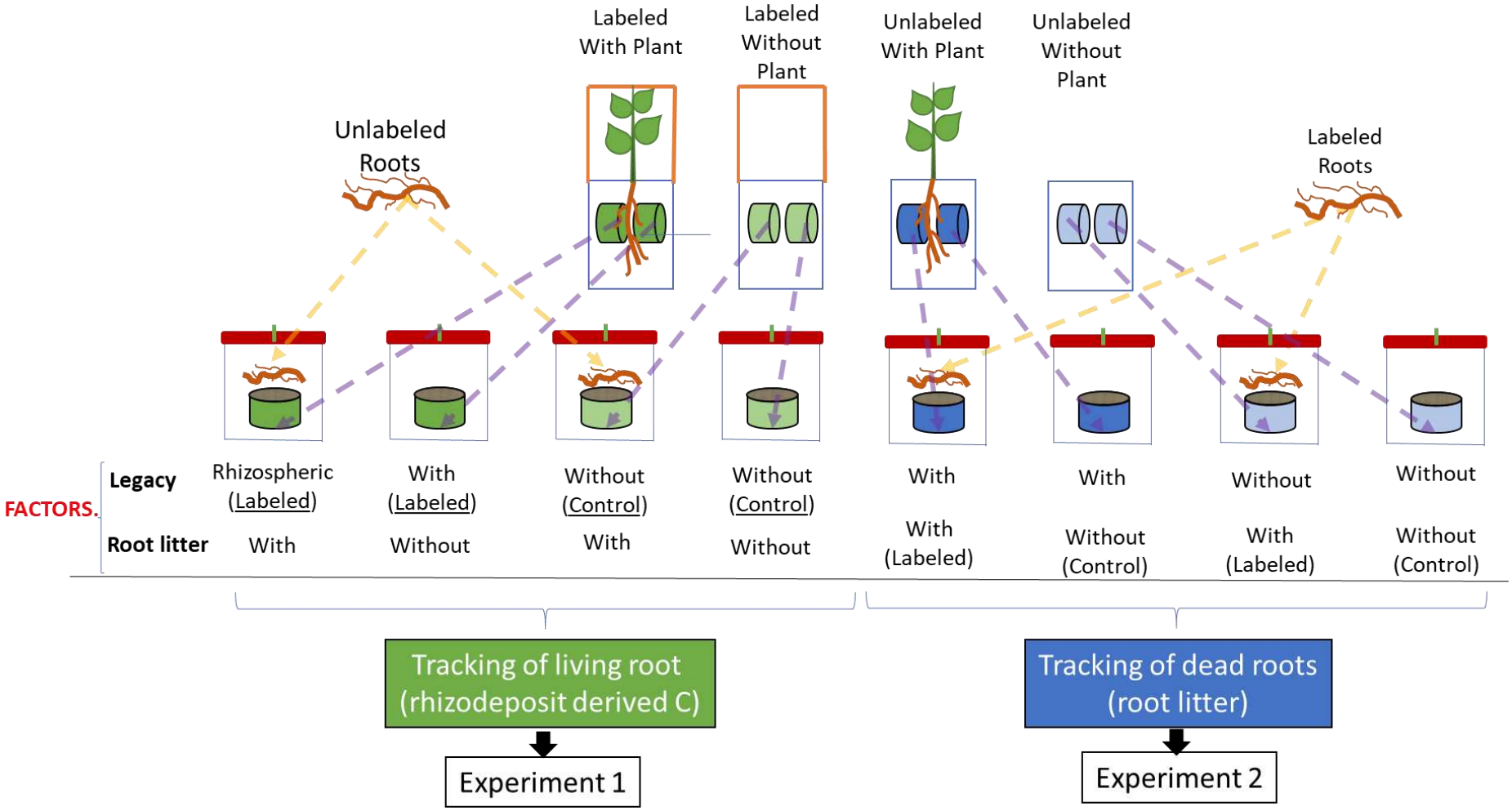

Source: Author.

2.9 Imaging with Scanning Electron Microscope (SEM) and Nanoscale secondary ion mass spectrometry (NanoSIMS)

Small fragments of root and root-adhered soil were collected in the top of the soil cores and dispersed in 1-2 mL of ultrapure water (Sigma-Aldrich, ACS reagent for ultra-trace analysis). The suspension was gently shaken, and an aliquot of 90 µL was collected with a micropipette and placed onto a silica wafer. The suspension was dried under a laminar-flow hood and subsequently were sputter-coated with gold (Au). The NanoSIMS analysis was performed with a Cameca NanoSIMS 50L of the Chair of Soil Science (TU München) (Cameca, Gennevilliers, France). A Cs^+ primary ion probe with an impact energy of 16 eV, was used to obtain secondary ion images of $^{12}C^-$, $^{13}C^-$, $^{16}O^-$, $^{14}N^-$ and $^{15}N^-$. The data gathered from NanoSIMS were processed using ImageJ software and converted into mosaics by using OpenMIMS and MosaicJ plugins (VIDAL et al., 2018).

2.10 Isotopic calculations

2.10.1 Rhizo-C - experiment 1

The calculation of rhizo-C present in soil and gas samples was calculated as described by Hafner et al., (2012). First, the $\delta^{13}C$ (‰) values were converted to the isotopic ratio (R_{sample}) according to equation 1:

$$R_{sample} = \left(\frac{\delta^{13}C}{1000} \times R_{PBD}\right) + R_{PDB} \quad (1)$$

Where R_{sample} is the carbon isotopic ratio of the sample, $\delta^{13}C$ (‰) is the isotopic signature from the sample obtained from isotope ratio mass spectrometer, and R_{PDB} is the isotopic ratio in the Pee Dee Belemnite standard (0.011237).

The percentage of ^{13}C relative to total C atoms (^{13}Catom%) was calculated following equation 2:

$$^{13}C_{atom\ \%} = \left(\frac{R_{sample}}{R_{sample} + 1}\right) \quad (2)$$

From equation 2, we calculated the average atomic mass of C (g mol^{-1}) using equation 3:

$$C_{average\ mass} = (^{13}C_{mass\ number} \times {}^{13}C_{atom\ \%}) + (^{12}C_{mass\ number} \times (1 - {}^{13}C_{atom\ \%})) \quad (3)$$

Where $C_{average\ mass}$ is the C average atomic mass in the sample, $^{13}C_{mass\ number}$ is the mass number of ^{13}C which is considered as 13.0034 u, $^{12}C_{mass\ number}$ is the mass number of ^{12}C which is considered as 12 u, and $^{13}C_{atom\%}$ is the percentage of ^{13}C relative to total C atoms.

The enrichment of ^{13}C in each soil or gas sample ($^{13}C_{atom\%\ excess}$) was calculated according to equation 4.

$$^{13}C_{atom\ \%\ excess} = {}^{13}C_{atom\ \%}\ \text{of sample} - {}^{13}C_{atom\ \%}\ \text{control} \quad (4)$$

Where $^{13}C_{atom\%}$ excess is the enrichment of ^{13}C, $^{13}C_{atom\%}$ is the percentage of ^{13}C relative to total C atoms in the soil and gas samples. The control treatments comprised of the non-rhizospheric treatments with and without root litter from experiment 1.

The amount of ^{13}C in excess that was incorporated in each soil layer or SOM fraction (rhizo-C, µg of ^{13}C in excess) was calculated according to equation 5.

$$\text{Rhizo-C} = {}^{13}C_{atom\ \%\ excess} \times C_{content} \times C_{average\ mass} \times {}^{13}C_{mass\ number} \times 1000 \quad (5)$$

2.10.2 Root-litter derived C - experiment 2

The root litter C and N contribution ($f_{root\ litter}$) to each soil layer and SOM fraction was calculated using a two-source mixing model (STEWART et al., 2009):

$$f_{root\ litter} = \frac{Atom\%_{sample} - Atom\%_{control}}{Atom\%_{root} - Atom\%_{control}} \quad (6)$$

Where: $Atom\%_{sample}$ is the isotopic enrichment of ^{13}C or ^{15}N in each soil layer and SOM fraction; $Atom\%_{control}$ is isotopic enrichment of ^{13}C or ^{15}N the corresponding layers and SOM fractions for treatment without labeled root litter; $Atom\%_{root}$ is the isotopic enrichment of ^{13}C or ^{15}N of the added root litter, which is 2.868% and 10.611%, respectively. The amount of root litter-derived C or N formed in layer and each fraction of SOM was calculated by the multiplication of contribution factor ($f_{root\ litter}$) by its total C or N content.

2.10.3 Partitioning of soil respiration - experiment 2

The partitioning of CO_2 derived from the root litter and "native" SOM was done using the same approach used for soil root litter contribution. The partitioning of CO_2 derived from the root litter and "native" SOM was done using the same approach used for soil root litter contribution (Equation 6).

The cumulative priming effect (PE, in %) according to the equation:

$$PE = \left(\frac{\left(f_{SOM} \times C{\cdot}CO_{2\,sample}\right) - C{\cdot}CO_{2\,control}}{C{\cdot}CO_{2\,control}} \right) \times 100 \quad (7)$$

Where f_{SOM} is the contribution of "native" SOM; $C\text{-}CO_{2sample}$ is the cumulative amount of $C\text{-}CO_2$ produced from soil that received the labeled root litter at a given interval (mg g^{-1} of soil); $C\text{-}CO_{2control}$ is the cumulative amount of $C\text{-}CO_2$ produced in the corresponding control.

2.11 Statistical analyses

We ran two sets of statistical analyses. In the first set, we employed one-way ANOVAs followed by a Tukey's HSD *post hoc* test to evaluate changes in soil C, N, isotopic measurements, PLFAs, and differences between the isotopic enrichment before and after the incubation. In the second set, we used t-tests to compare the differences between legacy or root litter treatments in the gas samplings and the chemical composition of the non-decomposed root litter. In both sets, homogeneity of variance was checked by Levene's test and the Shapiro-Wilk test was performed to test the normal distribution of the data (t-tests) and the residues (ANOVA). When the data failed to attend statistical assumptions and no transformation was possible, we opted to use an equivalent non-parametric test. All statistical analysis was conducted in R v. 3.6.0 (R CORE TEAM, 2021) with the package *agricolae* and the probability level used to determine significance was $P < 0.05$.

3. Results

3.1 Experiment 1 – Tracking of rhizo-C

3.1.1 Remaining root litter mineralization and chemical composition

Overall, no difference between rhizospheric and non-rhizospheric treatments was observed for C and N contents, C/N ratio, and isotopic measurements of the remaining root litter. However, we observed that root litter decomposition tended to decrease its C/N ratio from 29 to 21 ±0.9 in comparison with the initial root litter (Table 1). At the end of incubation, the root litter had higher ^{15}N enrichment (0.368% to 0.796 ±0.186%) in comparison with the initial root litter, as the ^{13}C enrichment remained constant (Table 1).

The chemical composition of the root litter at the end of incubation was modified in comparison to the initial root litter, but it was not affected by the rhizosphere treatments (Table 1). In comparison to the initial root litter, the carbohydrate proportion of both treatments decreased from 54.5% to 44.6 ±1.5%. Meanwhile, the proportions of lignin, protein, and lipids had slightly increased. Along with root litter decomposition, the Alkyl-C/O-N-alkyl-C ratio decreased from 3.12 in initial root litter up to 2.12 ±0.108 (mean of rhizospheric and non-rhizospheric treatments) (Table 1).

3.1.2 Rhizo-C mineralization

Overall, the mineralization rate of rhizo-C was not affected by the presence of root litter, and its dynamics showed two distinct phases (Figure 2 - A and B). In phase 1 (first 46 days), the rhizo-C respiration rate followed an exponential decay behavior, with higher rates at the beginning of the incubation and their gradual decline up to 46 days (Figure 2 - A). Within the first 46 days of the incubation, 54% and 65% of the total respired rhizo-C were mineralized for the treatments with root and without root litter, respectively. Phase 2 started after 46 days of the beginning of incubation, with a slight increase in rhizo-C mineralization rates compared to phase 1. After this, the mineralization rates gradually declined up to the end of the experiment (Figure 2 - A). Along with all the incubation, the mineralization rates of rhizo-C tended to be higher in the treatment with root litter (Figure 2 - A). Nevertheless, we did not detect significant differences between the root litter treatments, except for the sampling done 2 days after the start of incubation. At 2 days after the beginning of the experiment, the mineralization rate in the presence of root litter was 80% higher compared to the treatment without root litter (0.71 ±0.26 *vs.* 0.39 ±0.25 μg ^{13}C-CO_2 g^{-1} C day^{-1}, respectively, $P< 0.05$) (Figure 2 - A). The cumulative amount of rhizo-C evolved through the incubation followed the same trends observed for the mineralization rates, and was not affected by the presence of root litter in any of the sampling events (Figure 2). After 161 days of incubation, the treatment with roots tended to have higher values of rhizo-C with 0.44 ±0.10 ^{13}C-CO_2 g^{-1} C against 0.35 ±0.07 ^{13}C-CO_2 g^{-1} C for the treatment without root (Figure 2 - B).

Table 1 — Carbon (C) and nitrogen (N) contents, C/N ratio, ^{13}C and ^{15}N enrichment (Atom%), and chemical composition (NMR-MMM) in the initial root litter and remaining root litter after 166 days for incubation of experiment 1.

Measurements		Initial Root litter	After 166 days of Incubation	
			Rhizospheric	Non-Rhizospheric
C (mg g^{-1})		438.098	411.7 ±3.4 **a**[1]	414.6 ±2.8 **a**
N (mg g^{-1})		14.046	19.52 ±0.76 **a**	19.45 ±0.61 **a**
C/N		29	21 ±1.0 **a**	21 ±0.8 **a**
^{13}C (atom%)		1.077	1.007 ±0.0 **a**	1.006 ±0.0 **a**
^{15}N (atom%)		0.368	0.782 ±0.11 **a**	0.811 ±0.09 **a**
Chemical composition[2] (%)	Carbohydrate	54.5	46.80 ±0.2 **a**	42.80 ±2.1 **a**
	Lignin	26.3	28.07 ±0.8 **a**	29.21 ±1.4 **a**
	Protein	18.9	20.99 ±0.2 **a**	23.11 ±0.9 **a**
	Lipid	0.4	4.62 ±0.6 **a**	4.66 ±0.5 **a**
Alkyl-C/O-N-alkyl-C[3]		3.12	2.26 ±0.12 **a**	1.97 ±0.09 **a**

[1] Differents letters indicate significant differences between rhizospheric and non-rhizospheric treatments. Means (n = 4) are compared between treatments by t-test at 0.05 of significance.
[2] The chemical composition of root litter was obtained by ^{13}C solid-state nuclear magnetic resonance (NMR) spectroscopy and molecular mixing model (NELSON; BALDOCK, 2005).
[3] Calculated by the ratio between the areas of the regions 70-75 and 52-57 regions obtained by ^{13}C solid-state spectroscopy as proposed by Bonanomi *et al.*, (2013).

3.1.3 SOM fractionation

The C and N associated with the SOM fractions were neither affected by legacy or root litter treatments (Table B3). In all treatments, the majority of C and N was observed in the MAOM fraction, which contained 77% and 88% of the total C and N contents, respectively (Table B3). The MAOM fraction of rhizospheric treatment presented higher $\delta^{13}C$ in comparison with non-rhizospheric treatments regardless of the presence of root litter (-20.77‰ vs. -22.80‰, respectively - Table 2). For the other fractions, we did not observe any difference between the treatments for ^{13}C enrichment (Table 2).

Table 2 — $\delta^{13}C$ (‰) and ^{15}N (Atom%) of SOM fractions for legacy (rhizospheric vs. non-rhizospheric) and root litter (with and without) treatments for the 0-4 mm layer of experiment 1.

Fractions	$\delta^{13}C$ (‰)			
	Rhizospheric		Non-rhizospheric	
	With root	Without root	With root	Without root
fPOM	-27.67 ±0.16 **a**	-27.79 ±0.25 **a**	-28.18 ±0.14 **a**	-28.24 ±0.10 **a**
oPOM	-27.82 ±0.14 **a**	-27.66 ±0.09 **a**	-27.76 ±0.10 **a**	27.92 ±0.22 **a**
SSOM	25.64 ±0.11 **a**	-25.28 ±0.09 **a**	-25.30 ±0.11 **a**	-25.32 ±0.04 **a**
MAOM	-20.70 ±0.50 **a**	-20.83 ±0.41 **a**	-22.84 ±0.03 **b**	-22.75 ±0.03 **b**
	^{15}N (Atom%)			
fPOM	0.44 ±0.05 **a**	0.42 ±0.01 **a**	0.40 ±0.05 **a**	0.39 ±0.01 **a**
oPOM	0.40 ±0.01 **a**	0.39 ±0.00 **a**	0.38 ±0.00 **a**	0.38 ±0.01 **a**
SSOM	0.39 ±0.01 **a**	0.38 ±0.01 **a**	0.39 ±0.01 **a**	0.40 ±0.00 **a**
MAOM	0.42 ±0.01 **a**	0.42 ±0.01 **a**	0.39 ±0.01 **a**	0.40 ±0.01 **a**

Different letters indicate significant differences between the legacy and root litter treatments within the same SOM fraction. Means ± SE (n = 4) from all treatments is compared within depths by the Kruskal-Wallis test followed by pairwise Mann–Whitney U-tests at 0.05 of significance.
Source: Author.

3.1.4 Soil carbon and nitrogen, $\delta^{13}C$ and ^{15}N atom%

Soil C and N contents were neither affected by the legacy or root litter treatments (mean of all layers 32.16 ±0.68 mg g^{-1} and 2.14 ±0.04 mg g^{-1}, respectively - Figure B4 - A). At the end of the incubation, the soil $\delta^{13}C$ values were -21.09 ±0.59‰ and -21.62 ±0.39‰ (average of all layers) for the treatment with root and without root litter respectively, and were significantly higher than the non-rhizospheric treatments (mean of all layers-23.32 ±0.08‰, $P< 0.05$). For the rhizospheric treatment, higher values of $\delta^{13}C$ were observed in the 0-4 mm layer with a tendency of decrease along with the distancing from the root litter, while the $\delta^{13}C$ values of non-rhizospheric remained unchanged along with the layers (Figure 4 - A). For ^{15}N enrichment, no difference between the treatments was observed in any of the layers, which had an overall mean of 0.48 ±0.08 (^{15}N Atom, Figure 4 - C).

Figure 2 — Rhizodeposit-derived (rhizo-C) respiration rate (µg of ^{13}C-CO_2 g^{-1} of g C) throughout the incubation (A); Cumulative rhizo-C (µg of ^{13}C-CO_2 g^{-1} of C) mineralized throughout the incubation (B). Asterisks denote differences between rhizospheric and non-rhizospheric treatments compared by t-test at 0.05 of significance. Means ± SE (n = 4) are presented and each sampling time was compared independently.

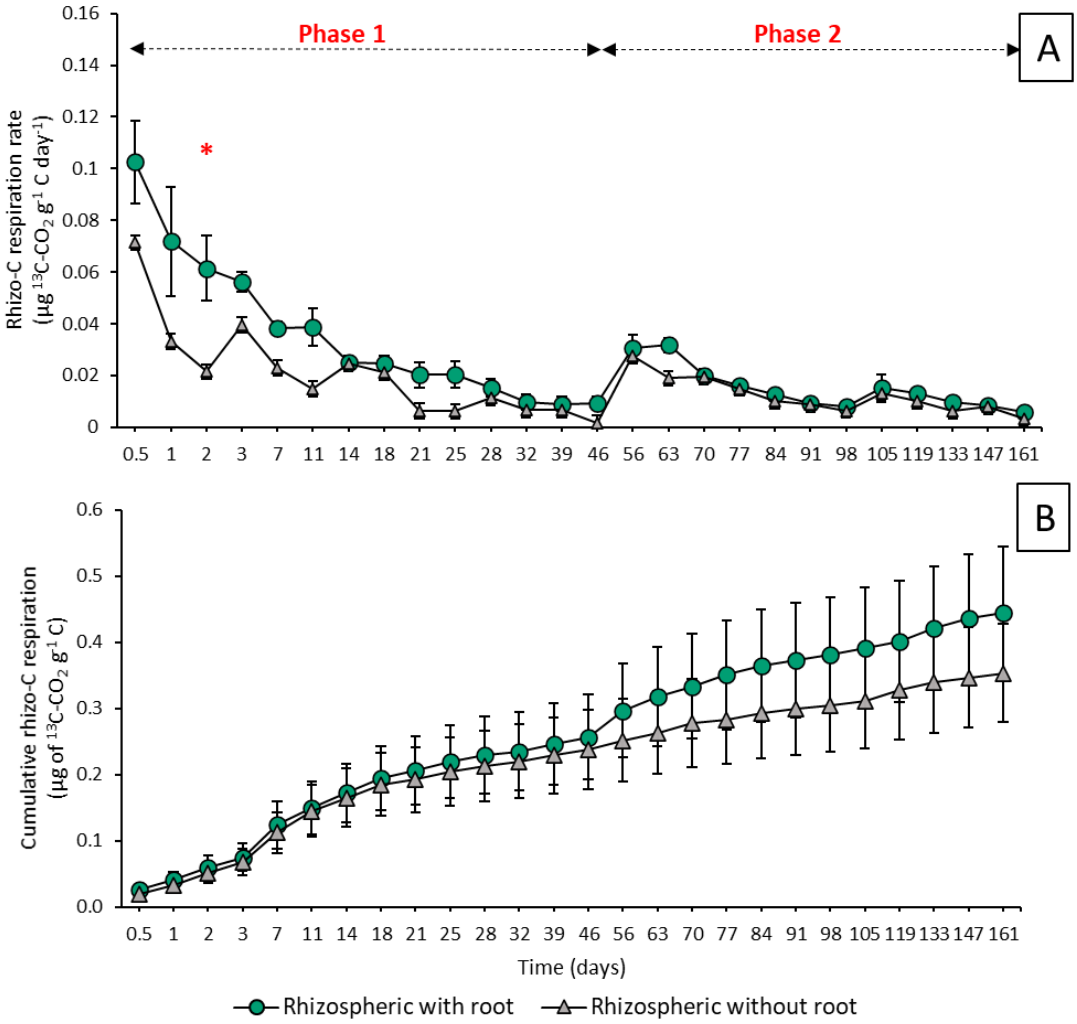

Source: Author.

3.1.5 Comparison of rhizo-C before and after the incubation

In this previous research (Chapter 1), the cultivation of labeled plants increased the $\delta^{13}C$ values of the 0-4 mm of the cylinder from -22.55‰ ±0.06 to -20.40% ±0.53 and the amount of rhizo-C from 8.11 ±1.35 to 43.22 ±10.16 µg^{-1} of ^{13}C $cylinder^{-1}$ (Figure 3) After 166 days of incubation, soil $\delta^{13}C$ values at 0-4 mm layer were not statistically different from the initial $\delta^{13}C$ values (before the incubation), regardless of the presence of root litter. The $\delta^{13}C$ values of the treatment without root litter tended to be smaller (-21.15‰) in comparison to the treatment with root (-20.64‰) and were not statistically

different from the soil original ^{13}C abundance of soil (Figure 3). The same behavior was observed for other layers (data not shown).

Likewise, $\delta^{13}C$ values of the MAOM fraction after and before the incubation were not distinct, independently of the root litter treatment (Figure 3). The MAOM $\delta^{13}C$ values of treatments with root and without root were -20.83‰ ±0.25 and -20.70 ‰±0.16, respectively (Figure 3). Following the same trends observed for $\delta^{13}C$ values, the amount of rhizo-C before and after the incubation was not statistically different regardless of the presence of root litter. Before the incubation, the amount of rhizo-C was 43.22 ±10.16 µg ^{13}C cylinder^{-1}. After the incubation, the amount was 40.61 ±12.77 and 36.32 ±6.46 µg ^{13}C cylinder^{-1} for the treatments with and without root litter, respectively (Figure 3). Using the amount of rhizo-C before the incubation as reference (43.22 µg ^{13}C cylinder^{-1}), it is possible to say that about 93% and 84% of the rhizo-C that was in the soil after the incubation was still present after 166 days.

3.2 Experiment 2 – Tracking of root litter derived C

3.2.1 Remaining root litter mineralization and chemical composition

In the same way as experiment 1, the legacy treatments (rhizospheric vs. non-rhizospheric) did not affect the C and N contents, C/N ratio, and isotopic measurements of non-decomposed root litter. We observed a reduction in the C/N ratio of the root litter from 31 to 21 ±0.7 after 166 days of incubation. The isotopic measurements (^{13}C and ^{15}N Atom%) followed the inverse pattern that was observed for bulk C and N measurements. While the ^{13}C enrichment tended to increase along with the root litter decomposition (2.686% to 2.865 ±0.314%, expressed as ^{13}C Atom%), the bulk C content decreased from 437.51 to 390.1 ±6.925 mg g^{-1} (Table 1). The opposite was observed for ^{15}N enrichment, which tended to decrease along with the decomposition from 10.611% to 8.235% ±0.314 (^{15}N Atom%) while the total N content increased from 14.838 to 18.845 ±0.565 mg g^{-1}. In the same manner as experiment 1, the chemical composition of root litter was not impacted by legacy effect treatments (rhizospheric vs. non-rhizospheric). Nevertheless, we observed that decomposition tended to modify the root litter chemical composition in relation to the initial amendment. Carbohydrate proportion decreased from 55% in initial root litter to 47.85 ±0.9% while the proportions of lignin, protein, and lipids had increased. The Alkyl-C/O-N-alkyl-C decreased from 3.22 in the initial root litter to 2.37 ±0.08 at the end of incubation.

Figure 3 — Comparison of $\delta^{13}C$ values (‰) of soil (A), MAOM (B), and rhizodeposit derived C (rhizo-C, µg of ^{13}C $cylinder^{-1}$) (C) before and after the incubation of 166 days. Treatments are compared by one-way ANOVA followed by Tukey's HSD test at 0.05 of significance. Means ± SE (n = 4) are presented.

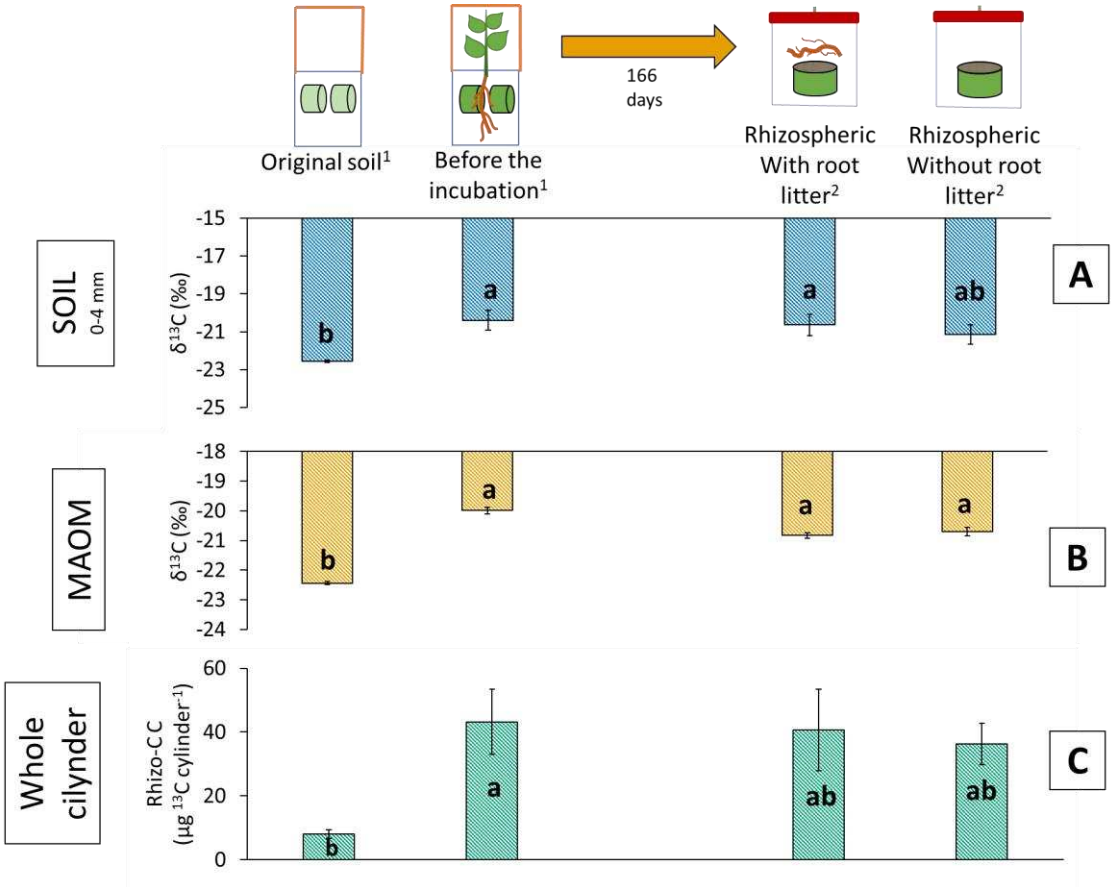

[1]The results were obtained from previous research described in chapter 1 of this thesis which planted and unplanted treatments were artificially enriched in ^{13}C (multiple pulses of ^{13}C-CO_2).
[2]Results taken from rhizospheric with and without root litter treatments of experiment 1 (tracking of rhizodeposits).
Source: Author.

Figure 4 — Soil $\delta^{13}C$ values (‰) for the legacy (rhizospheric and non-rhizospheric soil) and root litter treatments as a function of the distance to the detritusphere for experiments 1 (A) and 2 (B); Soil ^{15}N enrichment (Atom% for the legacy and root litter treatments as a function of the distance to the detritusphere for experiments 1 (C) and 2 (D). Means ± SE (n = 4) from all treatments is compared within depths by the Kruskal-Wallis test followed by pairwise Mann–Whitney U-tests. Asterisks denote differences at 0.05 of significance and lowercase letters indicate significant differences between the treatments at the same depth.

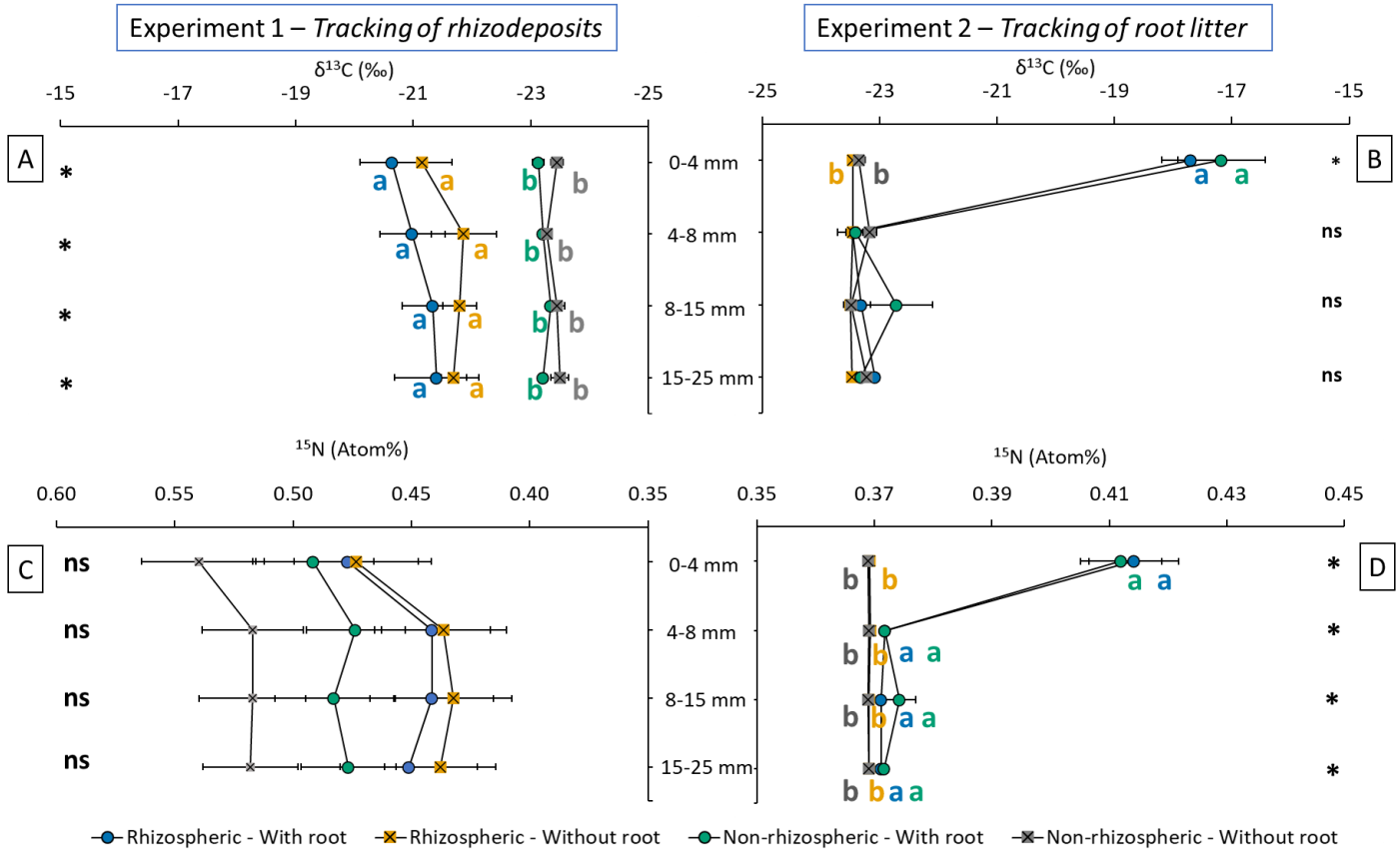

Source: Author.

3.2.2 Root litter mineralization dynamics and priming effects

Overall, legacy treatments (rhizospheric vs. non-rhizospheric) affected neither root litter nor SOM mineralization rates (Figure 6 – A and C). Yet, the respiration rates of rhizospheric treatment tended to be higher in comparison with the non-rhizospheric for both root litter and SOM, although it was not significant at most of the sampling times (Figure B5). For root litter, the rhizospheric treatment had only significantly higher mineralization rates at 2 days after the start of incubation (0.0615 *vs.* 0.0215 mg C-CO_2 g^{-1} C day^{-1}). For "native" SOM, the rhizospheric treatment had higher mineralization rates at specific samplings events of 2, 3, 21, and 46 days after the beginning of the incubation.

Similar to what was observed for rhizo-C mineralization, the C-CO_2 respiration rates of both root-litter and SOM had 2 distinct phases (Figure 6 - A). In the first phase (first 46 days), both root-litter and "native" SOM mineralization followed an exponential decay behavior, with higher mineralization rates in the first days of the experiment and a subsequent decline up to 46 days (Figure 6 – A and C). In the second phase, we observed a peak of both root litter and "native" SOM mineralization. Nevertheless, the increase in the mineralization rates of root litter was smaller in comparison with the "native" SOM mineralization and gradually decreased up to the end of the experiment. The "native" SOM mineralization had a different behavior in this phase, as the mineralization rates maintained constant through the rest of the incubation experiment, regardless of the legacy treatment. The average mineralization rate of SOM-derived at phase 2 was almost 80% higher than the average mineralization rate of phase 1 (0.166 ±0.03 vs. 0.093 ±0.04 mg C-CO_2 g^{-1} C day^{-1}, respectively) (Figure 6 – C).

The effect of legacy treatments in the cumulative amount of root-derived and SOM-derived C-CO_2 mineralized was dependent on the phase of the incubation. In phase 1 (first 46 days), the amount of root-derived SOM and SOM-derived C-CO_2 evolved in rhizospheric soil was superior in comparison to non-rhizospheric soil for several sampling times (Figure 6 - B and D). On the other hand, at phase 2 (46 days onward), no significant difference was detected between the legacy treatments for the amount of root-derived SOM mineralized (Figure 6 - B and D). Along with all incubation, the root litter-derived C-CO_2 evolved was 15%, and 16% of the amount evolved from SOM-derived C-CO_2, for the rhizospheric and non-rhizospheric treatment (Figure B5). At the end of the incubation, the rhizospheric treatment with roots tended to have

higher values of cumulative root litter-derived C with 0.44 ±0.10 against 0.35 ±0.07 mg C-CO_2 g^{-1} C for the treatment without root (Figure 6 - B).

The legacy treatments did not affect the cumulative priming effect in any of the sampling events (Figure 5). In both legacy treatments, the priming effect tended to be negative and was highly variable along with the incubation. For the rhizospheric treatment, the priming effect was on average -6 ±5% and remained negative through all incubation periods. The priming effect of non-rhizospheric treatment fluctuated between positive and negative values without a specific trend and was on average -3 ±23% through all the incubation.

Figure 5 — Cumulative priming effect (%) over 161 days of incubation. Asterisks denote differences between rhizospheric and non-rhizospheric treatments compared by t-test at 0.05 of significance. Means ± SE (n = 4) are presented and each sampling time was compared independently.

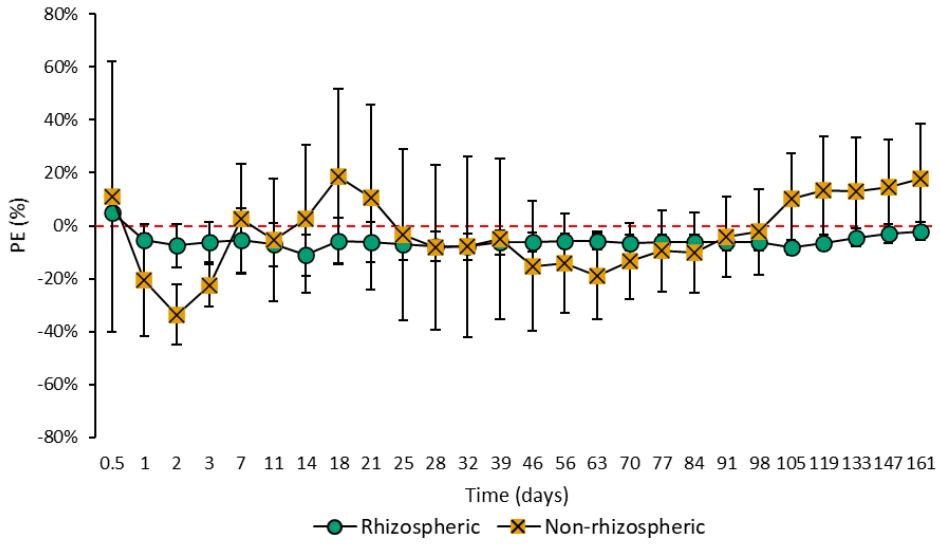

Source: Author.

3.2.3 Soil carbon and nitrogen, $\delta^{13}C$ and ^{15}N atom%

Similar to experiment 1, soil C and N contents were not affected by legacy or root litter treatments (mean of all layers 32.20 ±0.74 mg g^{-1} and 2.25 ±0.04 mg g^{-1}, respectively - Figure B4 - B and D). Root litter amendment only affected significantly the soil $\delta^{13}C$ values in the first layer (0-4 mm). In this layer, the $\delta^{13}C$ values of treatments with root litter were significantly higher than the treatments without root litter, with a mean of -17.43 ±0.04‰ and -17.17 ±0.74‰ for rhizospheric and non-rhizospheric treatments, respectively (Figure 4 - B). For the remaining layers, no difference between the treatments was observed. In contrast, the root litter inputs

enhanced the ^{15}N enrichment in all layers (Figure 4 - D). The ^{15}N enrichment (atom%) was higher at 0-4 mm layer (0.413%) and sensibly decrease for more distant layers (0.372% - D) (Figure 4).

Table 3 — Carbon (C) and nitrogen (N) contents, C/N ratio, ^{13}C and ^{15}N enrichment (Atom%), and chemical composition (NMR-MMM) in the initial root litter and remaining root litter after 166 days for incubation of experiment 2.

		Initial Root litter	After 166 days of Incubation	
			Rhizospheric	Non-Rhizospheric
C (mg g^{-1})		437.513	397.87 ±2.20 **a**	382.33 ±11.65 **a**
N (mg g^{-1})		14.838	18.17 ±0.59 **a**	19.52 ±0.54 **a**
C/N		31	22 ±0.7 **a**	20 ±0.6 **a**
^{13}C (atom%)		2.868	2.881 ±0.034 **a**	2.849 ±0.082 **a**
^{15}N (atom%)		10.611	8.596 ±0.397 **a**	7.874 ±0.231 **a**
Chemical composition[1] (%)	Carbohydrate	55.0	47.97 ±0.9 **a**	47.72 ±0.8 **a**
	Lignin	24.3	26.22 ±0.4 **a**	26.43 ±0.5 **a**
	Protein	17.9	21.97 ±0.4 **a**	21.66 ±0.4 **a**
	Lipid	2.8	3.83 ±0.4 **a**	4.17 ±0.6 **a**
Alkyl-C/O-N-alkyl-C[3]		3.22	2.38 ±0.11 **a**	2.36 ±0.06 **a**

[1] Differents letters indicate significant differences between rhizospheric and non-rhizospheric treatments. Means (n = 4) are compared between treatments by t-test at 0.05 of significance.
[2] The Chemical composition of root litter was obtained by ^{13}C solid-state nuclear magnetic resonance (NMR) spectroscopy and molecular mixing model (NELSON; BALDOCK, 2005).
[3] Calculated by the ratio between the areas of the regions 70-75 and 52-57 regions obtained by ^{13}C solid-state spectroscopy as proposed by Bonanomi *et al.*, (2013).
Source: Author.

3.2.4 SOM fractions

Similar to experiment 1, the C and N associated with the SOM fractions were neither affected by legacy or root litter treatments (Table B4) and the MAOM fraction contained the majority of soil C and N (79% and 89%, respectively). Regardless of the legacy treatment, the input root litter enhanced the $\delta^{13}C$ values of all SOM fractions, except for the SSOM fraction (Table 4). The same behavior was observed for ^{15}N enrichment. The higher increases of $\delta^{13}C$ values were observed for fPOM and oPOM, where the input of labeled litter enhanced the $\delta^{13}C$ values from -28.69‰ to -13.77‰ and from -28.25‰ to-21.51‰, respectively (mean of legacy treatments) (Table 4). For the MAOM fraction, the labeled root litter increased the $\delta^{13}C$ values from -22.88‰ to -

19.10‰ (mean of legacy treatments) and the ^{15}N enrichment (Atom%) from 0.37% to 0.40% (Table 4).

Table 4 — $\delta^{13}C$ (‰) and ^{15}N (Atom%) of SOM fractions for legacy (rhizospheric vs. non-rhizospheric) and root litter (with and without) treatments for the 0-4 mm layer of experiment 2.

Layers	$\delta^{13}C$ (‰)			
	Rhizospheric		Non-rhizospheric	
	With root	Without root	With root	Without root
fPOM	-10.37 ±10.13 **a**	-28.69 ±0.36 **b**	-17.17 ±5.05 **a**	-28.85 ±0.34 **b**
oPOM	-18.50 ±2.78 **a**	-28.26 ±0.09 **b**	-24.51 ±1.50 **a**	-28.24 ±0.08 **b**
SSOM	-20.55 ±2.71 **a**	-27.11 ±2.20 **a**	-23.95 ±0.38 **a**	-24.78 ±0.08 **a**
MAOM	-19.41 ±1.01 **a**	-22.91 ±0.08 **b**	-18.79 ±0.57 **a**	-22.86 ±0.04 **b**
	^{15}N Atom%			
fPOM	0.50 ±0.06 **a**	0.37 ±0.00 **b**	0.49 ±0.07 **a**	0.37 ±0.00 **b**
oPOM	0.43 ±0.01 **a**	0.37 ±0.00 **b**	0.40 ±0.01 **a**	0.37 ±0.00 **b**
SSOM	0.38 ±0.00 **a**	0.37 ±0.00 **a**	0.37 ±0.01 **a**	0.37 ±0.00 **a**
MAOM	0.40 ±0.00 **a**	0.37 ±0.00 **b**	0.40 ±0.00 **a**	0.37 ±0.00 **b**

Different letters indicate significant differences between the legacy and root litter treatments. Means ± SE (n = 4) from all treatments is compared within depths by the Kruskal-Wallis test followed by pairwise Mann–Whitney U-tests at 0.05 of significance. Source: Author.

3.2.5 Root litter C and N fate in rhizospheric and non-rhizospheric soil

The transformation of root litter C into SOM fractions was neither affected by rhizospheric nor non-rhizospheric treatments (Figure 8). After 166 days of incubation, 28.2% and 31.7% of the added root litter C was decomposed for rhizospheric and non-rhizospheric treatments, respectively. The incorporation of root litter into SOM was limited to the layer closer to the root litter (0-4 mm) in both treatments. The conversion efficiency of root litter calculated based on the amount of added C was 2.72% for rhizospheric and 3.01% for non-rhizospheric treatments. Likewise, the distribution of root litter C into SOM fractions was not influenced by legacy treatments and the MAOM fraction retained the majority of root litter derived C (1.2 to 1.6% of added C), followed by oPOM (0.3 to 0.5% of added C) and fPOM (0.3 to 0.4% of added C). SSOM fraction retained a negligible amount of root litter-derived C (smaller than 0.1%). The conversion efficiency of root litter into SOM calculated based on decomposed C was 9.68% and 9.59% for rhizospheric and non-rhizospheric (Figure 8). In this approach, 4.51% and 4.94% of decomposed root litter were converted into the MAOM fraction for rhizospheric and non-rhizospheric, respectively.

Figure 6 — Root litter-derived respiration rate (mg C-CO_2 g^{-1} C day^{-1}) (A); Cumulative root litter-derived respiration (mg C-CO_2 g^{-1} C) along with the incubation experiment (B); SOM -derived respiration rate (mg C-CO_2 g^{-1} C day^{-1}) (C); Cumulative SOM-derived C-CO_2 respiration (mg C-CO_2 g^{-1} C) along with the incubation experiment (D). Asterisks denote differences between rhizospheric and non-rhizospheric treatments compared by t-test at 0.05 of significance. Means ± SE (n = 4) are presented and each sampling time was compared independently.

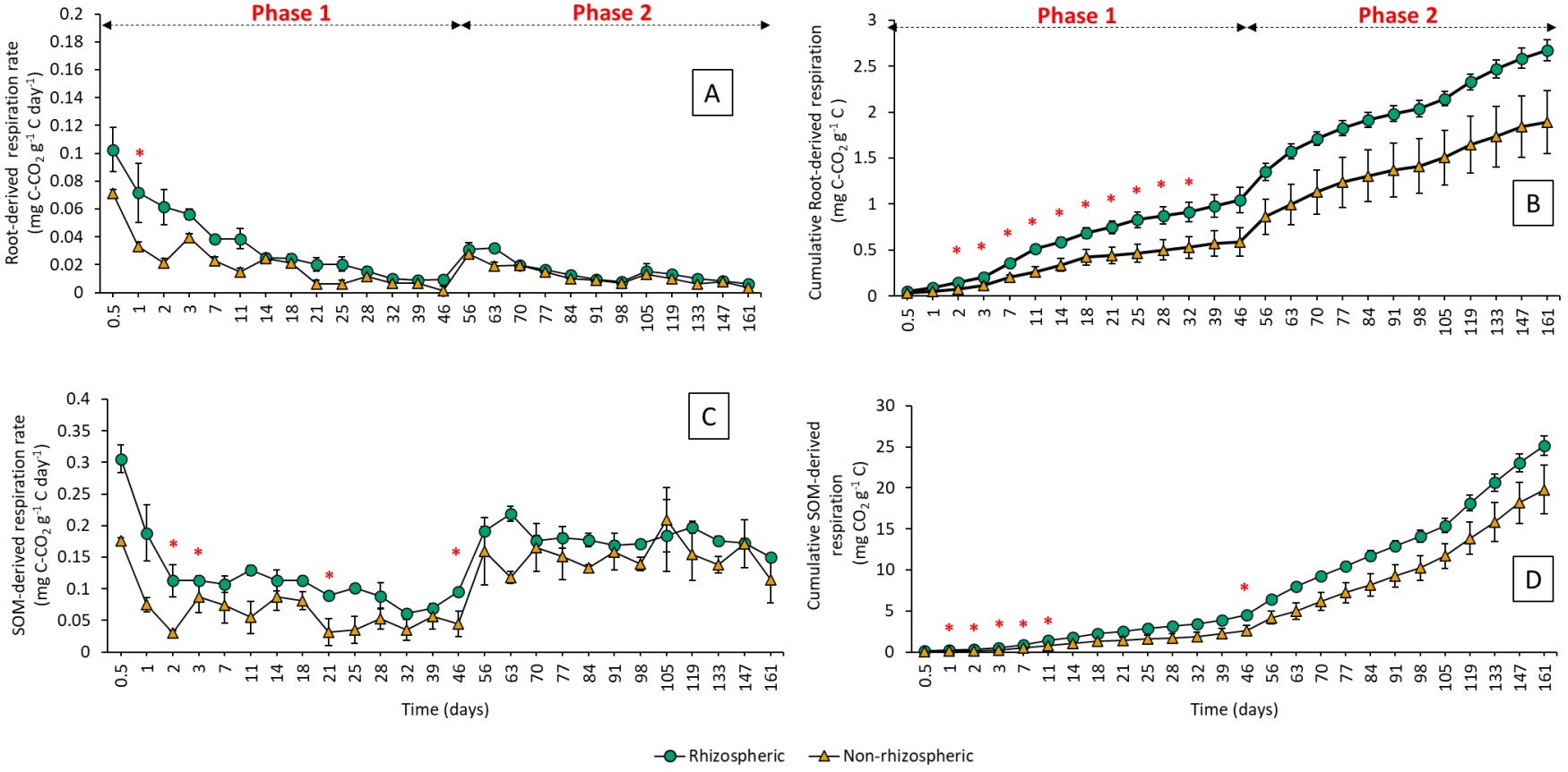

Source: Author.

Similar to the root litter C fate, the legacy treatments did not affect the transformation of root litter-derived N into SOM fractions (Figure 9). The amount N retained in the remaining root litter was similar to the amount of N that was added at the beginning of the incubation, which suggests the occurrence of immobilization of the soil N into root litter. Contrary to the root litter C fate, we observed significant incorporation of root litter-derived N into the 4-25 layer, which contained 2.1% and 3.3% of the root litter derived for rhizospheric and non-rhizospheric treatments. The distribution of root litter N into SOM fractions was not influenced by legacy treatments and the MAOM fraction retained the majority of root litter derived N (4.1 to 4.6% of added C). The transfer of root litter N into other fractions was smaller (<0.5% of added N) and the overall recovery of the added ^{15}N was 86 ±4%.

3.2.6 Root litter decomposition at the microscale

The isotopic and elemental composition of the interface between soil and root litter were analyzed with a scanning electron microscope (SEM) and NanoSIMS. We were able to identify various microorganisms that were growing attached to the surface of root litter (Figure 10) and soil aggregates (Figure 11). Five types of structures were identified in the images: soil mineral particles, filamentous microorganisms, bacteria, root litter, and amorphous organic materials. The ^{13}C and ^{15}N enrichment were highly variable in the structures identified in both images, and we even identified the presence of root litter structures that was not enriched in ^{13}C or ^{15}N (Figure 11). Moreover, we observed that the microorganisms' structures were less enriched in ^{13}C and ^{15}N in relation to root litter. In Figure 11, we detected the presence of amorphous organic material from microbial origin coating the surface of mineral particles.

3.3 PLFA and microbial communities

In both experiments, neither legacy nor root litter treatments affected the total PLFAs, bacterial, and fungi biomarkers (Table B6 and Table B7). Nevertheless, at experiment 1, we observed that the presence of root litter enhanced the F:B ratio from 0.080 ±0.001 to 0.085 ±0.01 ($P< 0.05$) and decreased the GP:GN ratio only for non-rhizospheric soil (8.53 ±0.59 to 6.84 ±0.49, $P< 0.05$) (Table B7). These effects in the microbial community composition (F:B and GP:GN ratio) were not significant for experiment 2 (Table B7).

Since both experiments had the same treatments and showed the same trends in most of the results, we decided to group the data of both experiments. When both experiments were analyzed together, we observed that legacy and root litter treatments affected significantly the abundance and composition of soil microbial communities. The presence of root litter enhanced the abundance of fungi biomarker in 9% (from 0.076 ±0.01 µmol g^{-1} C to 0.083 ±0.01 µmol g^{-1} C, respectively - $P< 0.05$), while the rhizospheric soil exhibited a 12% higher abundance of total PLFA biomarkers in relation to non-rhizospheric soil (from 2.28 ±0.15 µmol g^{-1} C to 2.03 ±0.17 µmol g^{-1} C, respectively - $P< 0.05$) (Figure 7). The GP:GN ratio followed the same trend that was observed when experiment 1 was analyzed individually, which is that the presence of root litter decreased the GP:GN ratio only for non-rhizospheric treatment (8.18 ±0.53 to 6.96 ±0.49, $P< 0.05$) (Figure 7 and Table B7). Nevertheless, when both experiments were analyzed together no significant effect was detected for bacterial biomarker and F:B ratio (Table B7).

Table 5 — Efficiency of root litter-derived C (carbon) conversion in SOM fractions (%) for rhizospheric and non-rhizospheric soil for the 0-4 mm layer of experiment 2 based on the amount of added C and the amount of C that was decomposed along the 166 days of incubation.

Fractions	The efficiency of root litter-derived C conversion in SOM (%)			
	Based on the added C		Based on the decomposed C	
	Rhizospheric	Non-rhizospheric	Rhizospheric	Non-rhizospheric
fPOM	0.44% ±0.22 **a**	0.35% ±0.15 **a**	1.53% ±0.80 **a**	1.08% ± 0.46 **a**
oPOM	0.49% ±0.22 **a**	0.26% ±0.12 **a**	1.70% ±0.69 **a**	0.79% ± 0.36 **a**
SSOM	0.06% ±0.03 **a**	0.01% ±0.00 **a**	0.21% ±0.10 **a**	0.02% ± 0.01 **a**
MAOM	1.24% ±0.33 **a**	1.57% ±0.23 **a**	4.51% ±1.19 **a**	4.94% ± 0.67 **a**
Bulk soil	2.72% ±0.34 **a**	3.06% ±0.41 **a**	9.68% ±1.15 **a**	9.59% ± 1.12 **a**

Different letters indicate significant differences between the legacy and root litter treatments. Means ± SE (n = 4) from all treatments is compared within depths by Kruskal-Wallis test followed by a pairwise Mann–Whitney U-tests at 0.05 of significance.
Source: Author.

Figure 7 — A. Main effect of root litter input treatments for fungal Phospholipid fatty acid (PLFA); B. Main effect of legacy effect (Rhizospheric and Non-rhizospheric soil) treatments for total PLFA; C. Gram-positive: gram-negative ratio (GP:GN) for legacy effect and root litter treatments. Experiments 1 and 2 are compared by two-way ANOVA followed by Tukey's HSD test at 0.05 of significance, and means ± SE (n = 8) are presented.

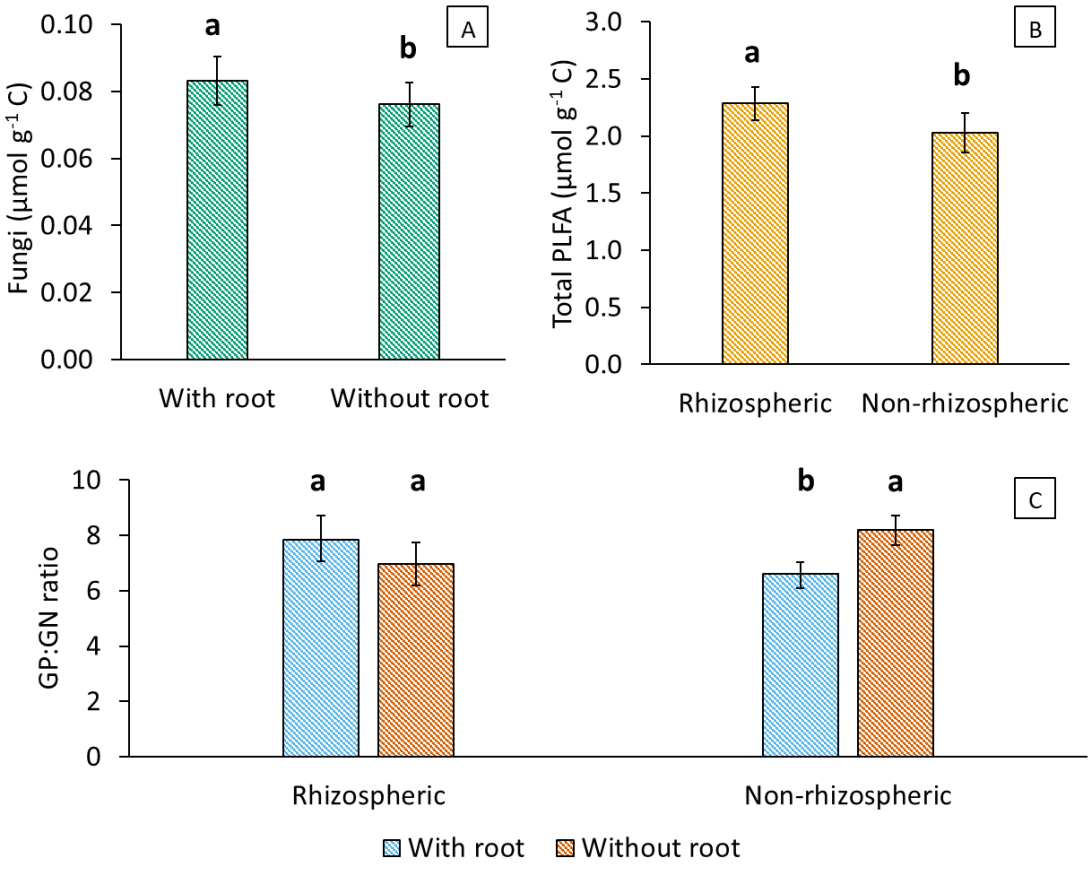

Source: Author.

Figure 8 — Root litter carbon (C) fate for legacy treatments (rhizospheric *vs.* non-rhizospheric). Differences between legacy treatments are compared independently for each C or N pool by a t-test at 0.05 of significance. Means ± SE (n = 4) are presented.

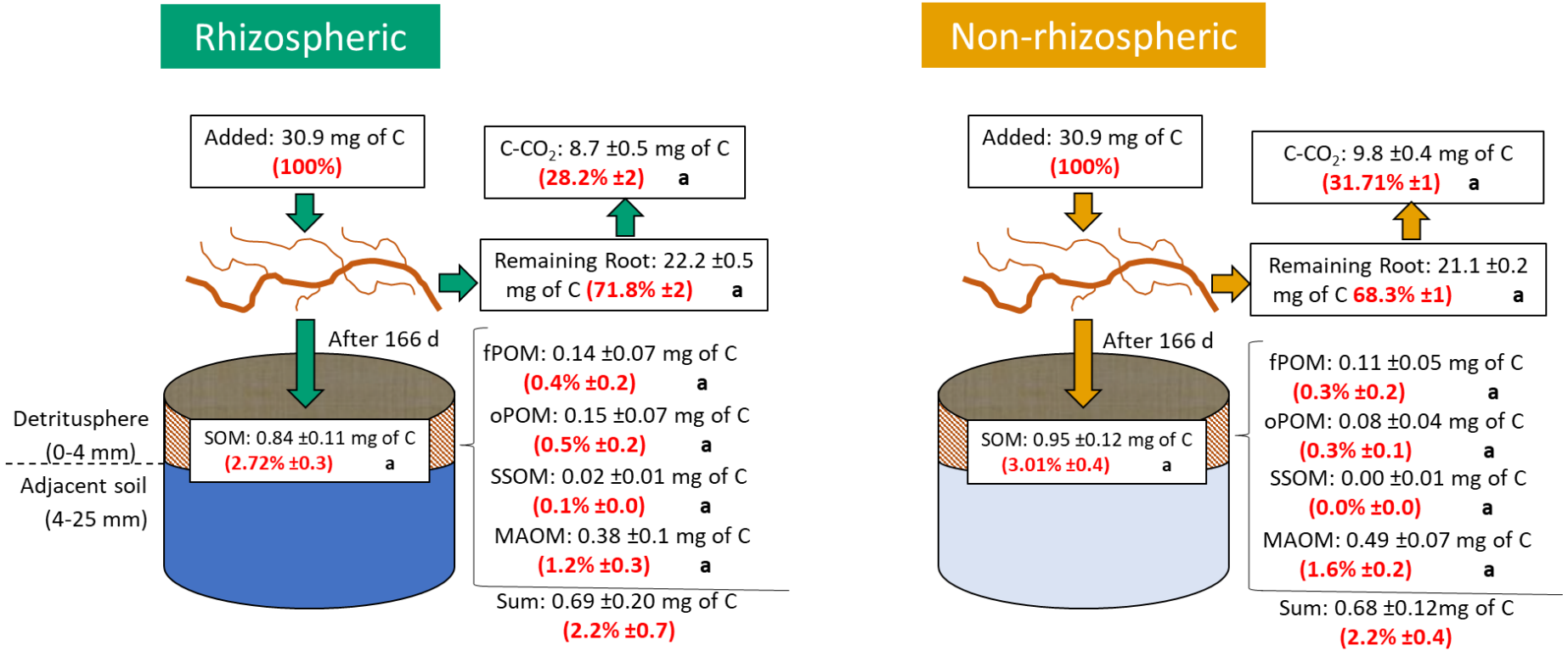

Source: Author.

Figure 9 — Root litter nitrogen (N) fate for legacy treatments (rhizospheric *vs.* non-rhizospheric). Differences between legacy treatments are compared independently for each C or N pool by a t-test at 0.05 of significance. Means ± SE (n = 4) are presented.

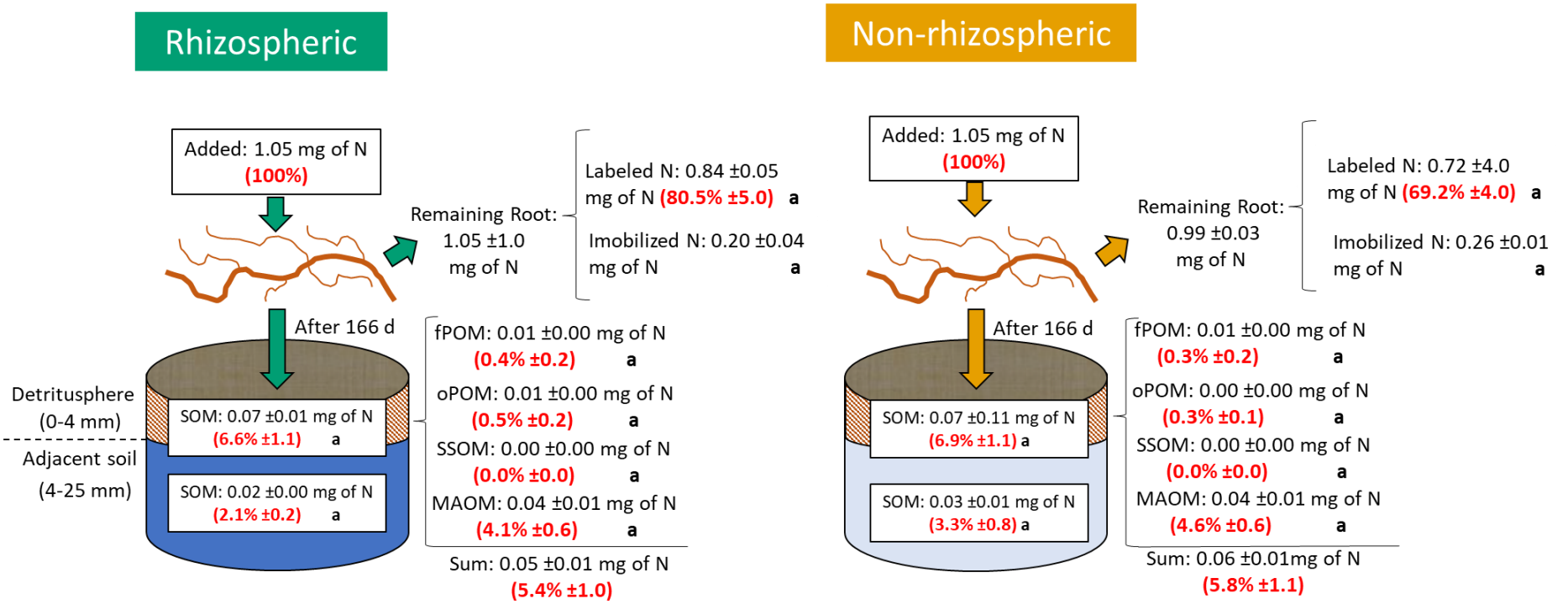

Source: Author.

Figure 10 — Scanning electron microscope (SEM) image of a decomposed root litter fragment at the end of incubation (A); NanoSIMS maps of ^{16}O (red)$^-$ and $^{12}C^-$ (green), representing mineral and organic components, respectively (B); NanoSIMS image of $^{13}C^-/^{12}C^-$ (expressed as Atom% ×1000) (C); NanoSIMS image of $^{15}N^-/^{14}N^-$ (expressed as Atom% ×1000) (D).

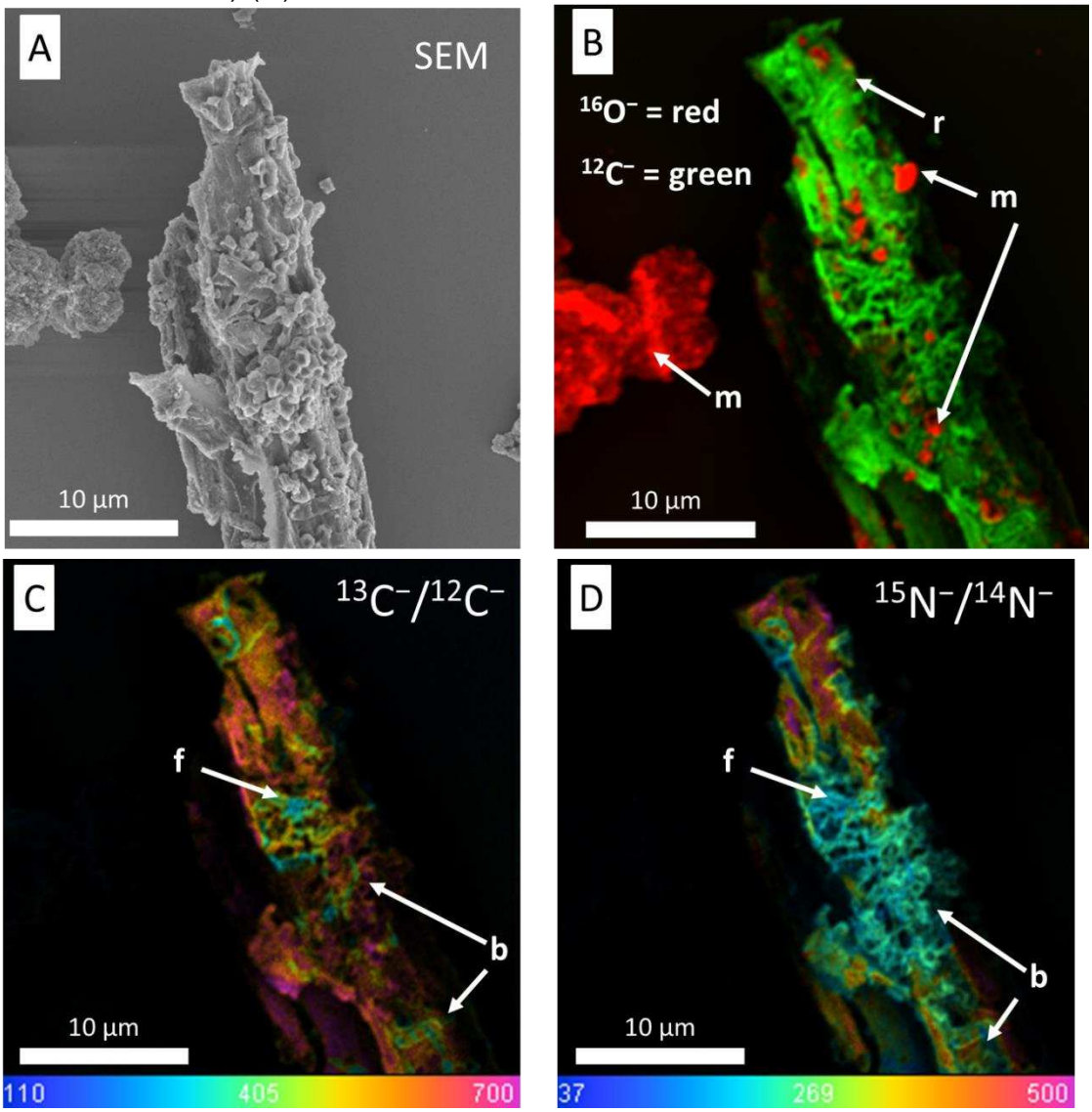

b = bacteria f = filamentous microorganisms, m = mineral r = root litter.
Source: Author.

Figure 11 — Scanning electron microscope (SEM) image of a decomposed root litter fragment at the end of incubation (A); NanoSIMS maps of ^{16}O (red)$^-$ and $^{12}C^-$ (green), representing mineral and organic components, respectively (B); NanoSIMS image of $^{13}C^-/^{12}C^-$ (expressed as Atom% ×1000) (C); NanoSIMS image of $^{15}N^-/^{14}N^-$ (expressed as Atom% ×1000) (D).

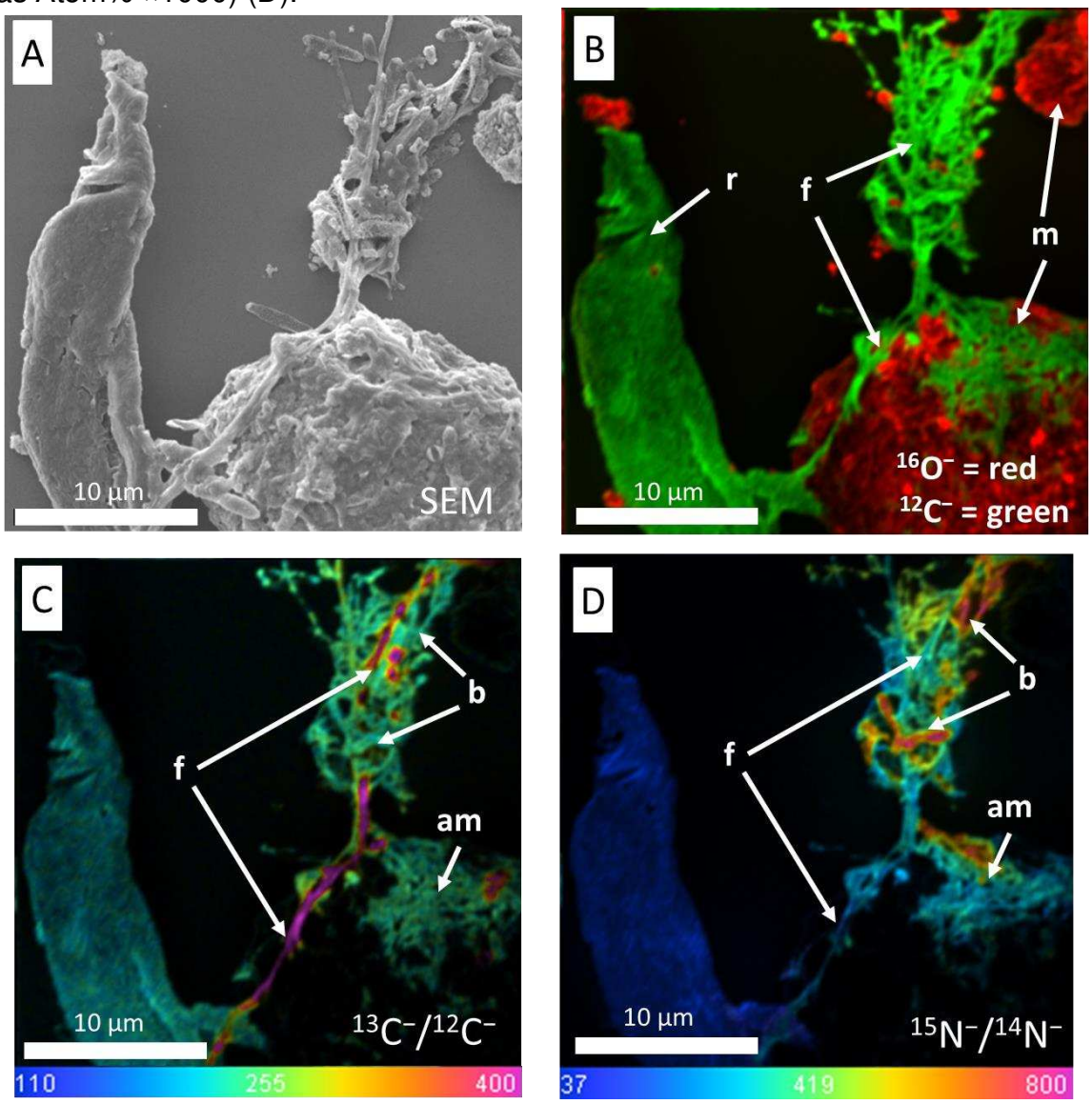

b = bacteria f = filamentous microorganisms, m = mineral r = root litter, am = amorphous organic residue.
Source: Author.

4. Discussion

4.1 Root litter amendment did not affect the fate of rhizo-C

Contrary to our prediction, our results show that the mineralization of rhizo-C was not affected by the presence of root litter. The respiration of rhizo-C tended to reduce the soil ^{13}C enrichment, although this effect was not statistically significant (Figure 3). Notwithstanding, the ^{13}C enrichment of the MAOM fraction after the incubation was higher than the natural abundance of the MAOM (-20.8‰ *vs.* -22.5‰, $P < 0.05$). Furthermore, our results show that more than 90% of the rhizo-C persisted in the soil by the end of the 166-day incubation (43.22 ±10.1 *vs*.38.46 ±9.61 µg ^{13}C cylinder) (Figure 3 - C). This result must be considered carefully due to the high variability that was inherent to our approach. In some replicates, the amount of rhizo-C before the incubation was smaller than the amount at the end of incubation, which may be indicative of a non-homogeneous distribution of the labeled rhizodeposits in the cylinders from the same experimental units. Overall, the amount of rhizo-C that persisted in the soil ranged from 49 to 120%, with a mean of 91 ±11%.

Despite these considerations, some other studies also reported a high persistence of C inputs in the soil. Kindler et al., (2006) incubated labeled bacterial biomass for 224 days and observed that 51% of the added material remained in the soil. Marx et al., (2007) incubated labeled rhizodeposits and observed that after 25 days, 64.2% of the added C was not recovered on active C pools (CO_2, microbial biomass, and dissolved C). The high persistence of the rhizo-C corroborates the theory proposed by Cotrufo et al., (2015), in which non-structural C inputs, such as the rhizodeposits, are preserved in the soil by mineral interactions after been processed and converted into microbial residues.

4.2 Legacy effects did not affect root litter conversion into SOM

Contrary to our hypothesis, the efficiency of root litter C conversion into SOM was not affected by legacy treatments, and only 2.6 and 3.1% of the added root litter C was incorporated into SOM for rhizospheric and non-rhizospheric treatments, respectively (Table 5). About one-third of the added root C was mineralized during the 166 days of incubation (Figure 8). When the efficiency of conversion of root litter into SOM is calculated based on the amount that was mineralized, the efficiency of conversion of SOM reaches 9.68% ±1.15 and 9.59% ±1.12 for rhizospheric and non-rhizospheric treatments, respectively (Table 5). The limited conversion of root litter into

SOM can be attributed to its poor biochemical quality (RASSE; RUMPEL; DIGNAC, 2005), which reduces the microbial C use efficiency for the SOM formation (COTRUFO et al., 2013, 2015). Even though, the conversion efficiency of root litter in our study was smaller than the observed in other experiments (BIRD; KLEBER; TORN, 2008; LAVALLEE et al., 2018). This effect may be resultant from the fact that root litter was added to the top of the soil and not mixed through the volume of soil. The mixing of the root litter can accelerate its mineralization by promoting the contact of the organic substrates with the microorganisms (SOUZA et al., 2016).

The root litter N transfer to the soil from rhizospheric and non-rhizospheric treatments was not distinct (8.7% and 10.2% respectively) and it was three times higher than the conversion of root litter C (Figure 9). The majority of the N incorporated at SOM fractions occurred in the MAOM fraction (75-79%), while oPOM and fPOM retained only 7% and 6% of the N (Table 3). The SSOM retained negligible amounts of root litter N. Despite the release of root litter N, we observed that the total amount of N in the root litter at the end of the incubation was similar to the added N amount. The surplus in root litter N as a result of soil N immobilization, which comprised from 20 to 30% of N present in the remaining root litter (Figure 9). These results suggest that the flux of N in the detritusphere was bidirectional, with the concomitant release of root N to soil and immobilization of soil N by root litter. However, our results reveal that immobilization prevails and was 2.4 times higher than the N mineralization of root litter (0.23 *vs.* 0.09 mg of N). N immobilization was also observed in experiment 1, on which the ^{15}N enrichment in the remaining root litter had increased in comparison with the initial root litter (Table 1). Differently, for the transference of root litter C, we observed that almost one-third of the amount of the incorporated N occurred in the more distant layers of the cylinder (4-25 mm). A higher transference of N through the soil cylinder layers may be related to the higher mobility of N into the soil (NEFF; CHAPIN; VITOUSEK, 2003).

4.3 Rhizodeposits and root litter are incorporated in different SOM fractions

The SOM fractionation results show that root litter and rhizo-C were incorporated into different SOM fractions. At the end of the incubation, root litter remained mostly as particulate SOM (remaining root litter plus fPOM) as rhizo-C were majorly incorporated into MAOM fraction. The allocation of root C inputs into distinct SOM fractions reflects its biochemical composition (LAVALLEE; SOONG; COTRUFO, 2019). Root litter is rich

in structural compounds that require depolymerization before microbial processing (KLEBER et al., 2015; RASSE; RUMPEL; DIGNAC, 2005). In this context, the decomposition of root litter occurs slowly and its incorporation by microorganisms is less efficient (COTRUFO et al., 2013). Rhizodeposits, on the other hand, can be directly processed by microorganisms, as it does not require depolymerization. Rhizodeposit conversion into MAOM follows two distinct pathways: the "*in vivo microbial turnover*" and the "*ex vivo modification pathway*" (LIANG; SCHIMEL; JASTROW, 2017). "*In-vivo pathway*" presumes the assimilation of rhizo-C into microbial metabolism, whose residues will associate with the minerals to form MAOM. The *"ex-vivo pathway"* involves the enzymatic modification of plant-C into compounds that are directly associated with the minerals, passing through the microbial metabolism (LAVALLEE; SOONG; COTRUFO, 2019).

Nevertheless, we observed that a considerable amount of root litter-derived C in the soil was found in the MAOM fraction. Although this amount was much smaller than the particulate fraction, this result shows that root litter also forms the MAOM fraction as it is being decomposed, possibly through the same pathways of rhizo-C (COTRUFO et al., 2015; LIANG; SCHIMEL; JASTROW, 2017). Also, we observed that root litter was also incorporated substantially at the oPOM fraction while negligible amounts of the rhizospheric-derived C were incorporated in this fraction (Figure 8). The incorporation of root litter into oPOM involves the occlusion of root litter fragments into macro and micro aggregates, which provides physical protection of this material against decomposition (VON LÜTZOW et al., 2007).

4.4 Legacy effects changed root-litter mineralization dynamics and soil microbial biomarkers

The dynamics of root litter mineralization were influenced by legacy treatments only in phase 1 (first 46 days) (Figure 6 - B). In this phase, the rhizospheric soil had a higher cumulative root litter-derived respiration in comparison with non-rhizospheric soil in almost all sampling times (Figure 6 - B). The higher mineralization of root litter in rhizospheric soil can be explained by the enhanced microbial activity resultant from the previous rhizodeposition. Before the incubation, rhizospheric soil had 53% more total microbial PLFAs in comparison with non-rhizospheric soil (chapter 1 of this thesis). Moreover, from the tracking of rhizodeposits mineralization (experiment 1), we observed that rhizo-C was more intensely mineralized up to the first 46 days (Figure 2

- A). An enhanced microbial activity proportioned by the presence of easily available organic substrates can accelerate the decomposition of root litter (HICKS PRIES et al., 2018; KUZYAKOV; HILL; JONES, 2007; WANG et al., 2014). In this context, it is possible to affirm that the enhanced microbial activity, provided by the rhizo-C processing, accelerated the mineralization of root litter in rhizospheric treatment in the first 46 days of the incubation.

However, at phase 2, the mineralization of both root litter and rhizo-C had substantially declined and we observed an intensification of the “native” SOM mineralization (Figure 6). The shift in the origin of the C respired may be connected to a change in microbial community composition. Soil microbial community can be roughly divided between r-strategists, which are fast-growing and are specialized in the utilization of easily available substrates, and K strategists, which grow more slowly but have more advantage in the utilization of more recalcitrant substrates (FONTAINE; MARIOTTI; ABBADIE, 2003). In this context, the higher abundance of easily available substrates, both from rhizo-C and root litter, must have favored the r-strategists during phase 1. In contrast, at phase 2, the depletion of easily available C leads the r-strategists to death or dormancy and the K-strategists become dominant, where they preferentially feed on the previous existing SOM (FONTAINE; MARIOTTI; ABBADIE, 2003).

Nevertheless, since we only had evaluated the microbial community structure at the end of the incubation, it is not possible to evaluate changes in the microbial community driven by the transition between the rhizosphere to a detritusphere. By the end of incubation, the PLFAs results showed that rhizospheric treatment had a 12% higher abundance in total PLFA biomarkers in relation to the non-rhizospheric soil (Figure 7 - A). Thus, we observe that the enhanced total PLFA biomarkers that were observed before the incubation was still higher in rhizospheric soil by the end of the incubation. Moreover, we observed that the GP:GN ratio of legacy treatments was differently affected by root litter presence. While the GP:GN ratio of rhizospheric soil was not affected by the presence of root litter, the presence of root litter reduced the GP:GN ratio of non-rhizospheric soil (Figure 7 - C). Gram-positive bacteria are commonly associated with the processing of recalcitrant SOM, while Gram-negative bacteria preferentially use plant-derived SOM, which is generally more labile (FANIN et al., 2019; KRAMER; GLEIXNER, 2006). The non-rhizospheric soil without root treatment was the only treatment that did not receive any source of root C. Thus, the

absence of C inputs must have favored the dominance of microbial communities that can thrive by using the “native” SOM. However, despite the changes in the microbial community revealed by the PLFA analysis, the cumulative root litter-derived respiration by the end of the incubation was not statically different between rhizospheric and non-rhizospheric soils (Figure 3 – D). This result suggests that the processing of “native” SOM during phase 2 overcomes the differences found in the first 46 days of incubation. In conclusion, we can say that the impacts of legacy treatments in the decomposition of root litter were limited to the mineralization dynamics and microbial composition, and not affected the total amount of root litter that was mineralized.

4.5 Root litter-derived C is spatially compartmentalized, while rhizo-C is not

We observed that root litter C incorporation in SOM was constrained only into the small volume of soil (0-4 mm) adjacent to the root litter. Similar results were observed in other incubation studies (GAILLARD et al., 2003, 1999; INGWERSEN et al., 2008; MARSCHNER et al., 2012; POLL et al., 2006). The transportation of C over the volume of soil is driven by diffusive/convective processes in the soil solution or through microorganisms (GAILLARD et al., 1999; POLL et al., 2006). The diffusive/convective processes of litter-derived C are supposed to be smaller in incubation experiments due to the limited amount of water that is added (in comparison with a rain event, for example) (GAILLARD et al., 1999; KAISER; KALBITZ, 2012). Thus, the transportation of root-litter C in our study is more likely to be a result of the growth of microbial structures, such as fungal hypha, which serve as conduits to C transfer in the soil (JOHNSON et al., 2002). We detected intense fungal colonization in the root litter and an enhanced abundance of fungal biomarkers (Figure 7 and Figure B3). Even so, the distribution of root litter-derived C was limited to the 0-4 mm layer, which suggests that the microbial pathway is not effective for the C transportation through longer distances (>4 mm) in the soil volume.

In contrast, rhizodeposit derived C showed less spatial compartmentalization and it was found up to 15-25 mm layer, even after the end of the incubation experiment (Figure 4 – A). These results suggest that the rhizo-C can be transported to a larger extension of soil volume in comparison with root litter. One possible explanation for this effect is that rhizodeposits are mainly formed by soluble compounds which have a higher diffusion in the soil (HÜTSCH; AUGUSTIN; MERBACH, 2002; JONES; NGUYEN; FINLAY, 2009). A larger distribution of rhizo-C can have important

implications for its retention in the soil. Sokol and Bradford, (2019) observed that the extension of the rhizosphere impacts directly the amount of C that is retained in the MAOM, possibly due to an enhanced contact with the mineral surfaces.

In conclusion, we observed that rhizo-C and root litter-derived C showed a contrasting distribution in the layers of the soil cylinders. While root litter C was restricted to a small volume of soil close to the root litter, the rhizo-C showed a wider distribution along with the cylinder layers.

4.6 Root litter C inputs not resulted in priming effects

In our study, the mineralization of "native" SOM was not influenced by legacy treatments, and no significant priming effects were detected (Figure 5) Yet, the cumulative priming effect for rhizospheric and non-rhizospheric treatments was slightly negative on average (-6 ±5% and 3 ±23%, respectively). The direction and magnitude of priming effects are given by the amount and the biochemical quality of the C inputs (BLAGODATSKAYA; KUZYAKOV, 2008; SHAHBAZ et al., 2017). Root litter has a poor biochemical quality and some literature results attest that these substrates induce positive priming effects (SHAHBAZ et al., 2017). Nevertheless, this effect also depends on the amount of C that was added (BLAGODATSKAYA; KUZYAKOV, 2008). In this study, we added 1.8% of the C stock in the whole cylinder and is within the range of most incubation experiments (SHAHBAZ; KUZYAKOV; HEITKAMP, 2017; SOUZA et al., 2018). In our study, the root litter was not mixed with the soil as is commonly done in incubation experiments. This effect resulted in the restriction of the root litter-derived SOM formation was limited to the 0-4 mm soil layer, and if we calculate the amount of C that was added considering only the C stock in 0-4 mm layer, the added root litter C increases from 1.8% to 13% of the total C. The high input of C in a constrained region of soil can affect the direction of the priming effect. When the C input exceeds 200-500% of the microbial biomass C, the priming effect tends to be null or even negative (BLAGODATSKAYA; KUZYAKOV, 2008), which may explain the limited effects of root litter inputs in the decomposition of "native" SOM.

Another factor that must have contributed to this result is that the soil used in this experiment was fertilized. The availability of N and other nutrients can exert an impact on the intensity/direction of priming effects (DIJKSTRA et al., 2013). A deficiency in N, for example, can cause the microorganisms to enhance the SOM mineralization to obtain N (JILLING et al., 2018; VALADARES et al., 2018; YIN et al.,

2018). In our study, the supply of N and other nutrients must have suppressed nitrogen mining, which may also mitigate the impacts of root litter amendments in the decomposition of "native" SOM (DIJKSTRA et al., 2013).

4.7 The detritusphere hotspot at the microscale

The SEM and NanoSIMS images provide direct insight into detritusphere microhabitat and the root litter incorporation into SOM. We identified an abundant number of bacterial and filamentous structures attached to the surface of root litter fragments (Figure 10). This finding demonstrates an important feature of the detritusphere, that is the attachment of the microorganisms in the decomposing root litter and not only in the mineral surfaces (AHMED; HOLMSTRÖM, 2015; NANNIPIERI et al., 2017). The attachment of microbial cells to surfaces is mediated by the production of extracellular polymeric substances (EPS) (COSTA; RAAIJMAKERS; KURAMAE, 2018). In Figure 11 we can identify an amorphous organic structure coating the surface of an aggregate that can be characterized as an EPS. The attachment of microbial-derived structures into minerals is what originates the MAOM fraction, and it is responsible for microbial-derived C retention in the soil (LAVALLEE; SOONG; COTRUFO, 2019). Overall, the ^{13}C and ^{15}N enrichment of the microbial structures was smaller than the enrichment of the adjacent root litter. This observation implies that these microorganisms were not feeding exclusively from the root litter, but also the "native" SOM existing in the soil. Similar results had been observed by Vidal et al., (2018).

4.8 The processing of rhizo-C and root litter are independent of each other

Our study shows that neither rhizo-C and root litter fate is affected by legacy effects. These results suggest that rhizodeposition and root litter decomposition are independent of each other. One possible explanation for this result is that distinct microbial communities are responsible for the processing of each type of root C input. The transition between rhizosphere to detritusphere is characterized by the simultaneous presence of labile (rhizodeposits) and recalcitrant compounds (root litter). Under these circumstances, evidence from the literature shows that microorganisms have a strong degree of specialization according to the chemical recalcitrance of the available C (GOLDFARB et al., 2011; NUCCIO et al., 2019; PATERSON et al., 2008). Goldfarb et al., (2011) evaluated how the bacterial taxa

responded to the biochemistry of C amendments and observed that only 6% of identified taxa increased in relative abundance when labile and recalcitrant C inputs were present. This result suggests the occurrence of niche segregation in the rhizosphere-detritusphere transition (NUCCIO et al., 2019). In this case, the different competing microorganisms can coexist because they occupy a distinct niche, feeding mostly in one type of C source. Besides, the localization effect observed in the two types of root C inputs also contributed to this effect. This is partially supported by our PLFAs results, in which we observed an increase in fungal biomarker abundance only in the presence of root litter (Figure 7). Fungi are more adapted for the processing of more complex compounds such as root litter and are capable to assimilate C directly from the litter layer (GUNINA; KUZYAKOV, 2015; POLL et al., 2006). In contrast, bacteria are more adapted to more simple compounds, although they depend more on the transportation of C (GUNINA; KUZYAKOV, 2015; POLL et al., 2006). Nevertheless, we did not observe alterations in the bacterial community due to legacy treatments. Instead, root litter presence tended to decrease the abundance of bacterial biomarkers, regardless of legacy treatment (Table B5). In this context, the spatial distribution of the root C inputs can contribute to niche segregation by separating the microbial groups that are processing the distinct C inputs.

Furthermore, the absence of competition between microbial communities can explain the negative priming effects results observed in our study. Fontaine et al., (2003) suggest that positive priming effects are resultant from the competition for energy and nutrients between microbial communities that are specialized in the processing of distinct sources of C. Assuming that different microbial communities processed the distinct sources of C independently, their competition for C must have been minimized, which limited the processing of native SOM. It is important to highlight that our soil had a high availability of nutrients because it was fertilized. In this context, it is possible that under more nutrient-limiting conditions, the enhanced competition of distinct microbial groups can lead to higher mineralization of native SOM. (FONTAINE; MARIOTTI; ABBADIE, 2003; VALADARES et al., 2020).

5. Conclusion

Overall, our study shed light on one of the most crucial “hot moments” of soil C biogeochemistry, which is the rhizosphere-detritusphere transition. We observed that neither rhizo-C and root litter fate is affected by legacy effects. This finding suggests

that each of these types of C is processed independently in the rhizosphere-detritusphere transition. In this context, the enhanced efficiency of root C inputs is more related to the intrinsic properties of each type of C than its combined effect. Although we did not evaluate the efficiency of rhizodeposit conversion into SOM, we observed that this type of C input has some characteristics that favor its persistence in the soil. Rhizo-C showed a wider distribution within the soil volume and the greatest majority of rhizo-C was found in the MAOM fraction. Moreover, we detected that the majority of rhizo-C persisted in the soil through the 166-days incubation. This is direct evidence that the interaction of rhizo-C with soil minerals is effective to protect this source of C against microbial decomposition. To our knowledge, this is the first time that this phenomenon has been shown with real plant exudates, and not labeled reactants.

In contrast, the major portion of root litter remains undecomposed as particulate SOM, and only about 10% of what was mineralized is incorporated in the soil. The conversion of root litter was restricted to the first four millimeters from its surroundings. Despite this finding, we observed that root litter is also capable of forming more stable C pools, such as MAOM and oPOM. Nevertheless, the limited distribution of root litter in the soil can hamper the formation of these C sources due to a limitation in the contact with mineral particles. Furthermore, through the NanoSIMS images, we provide direct evidence for the incorporation of root litter into microbial structures at the detritusphere. We observed fungi and bacteria growing attached to the surface of root litter, and the formation of EPS coating on the surface of the mineral particles.

6. References

AHMED, E.; HOLMSTRÖM, S. J. M. Microbe-mineral interactions: The impact of surface attachment on mineral weathering and element selectivity by microorganisms. **Chemical Geology**, [S. l.], v. 403, n. January 2018, p. 13–23, 2015.

ALMEIDA, L. F. J.; HURTARTE, L. C. C.; SOUZA, I. F.; SOARES, E. M. B.; VERGÜTZ, L.; SILVA, I. R. Soil organic matter formation as affected by eucalypt litter biochemistry — Evidence from an incubation study. **Geoderma**, [S. l.], v. 312, 2018.

ANGST, G.; KÖGEL-KNABNER, I.; KIRFEL, K.; HERTEL, D.; MUELLER, C. W. Spatial distribution and chemical composition of soil organic matter fractions in rhizosphere and non-rhizosphere soil under European beech (Fagus sylvatica L.). **Geoderma**, [S. l.], v. 264, n. May, p. 179–187, 2016.

BAUMERT, V. L.; VASILYEVA, N. A.; VLADIMIROV, A. A.; MEIER, I. C.; KÖGEL-KNABNER, I.; MUELLER, C. W. Root exudates induce soil macroaggregation

facilitated by fungi in subsoil. **Frontiers in Environmental Science**, [S. l.], v. 6, n. NOV, 2018.

BIRD, J. A.; KLEBER, M.; TORN, M. S. ^{13}C and ^{15}N stabilization dynamics in soil organic matter fractions during needle and fine root decomposition. **Organic Geochemistry**, [S. l.], v. 39, n. 4, p. 465–477, 2008.

BIRD, J. A.; TORN, M. S. Fine Roots vs. Needles: A Comparison of ^{13}C and ^{15}N Dynamics in a Ponderosa Pine Forest Soil. **Biogeochemistry**, [S. l.], v. 79, n. 3, p. 361–382, 2006.

BLAGODATSKAYA, E.; KUZYAKOV, Yakov. Mechanisms of real and apparent priming effects and their dependence on soil microbial biomass and community structure: critical review. **Biology and Fertility of Soils**, [S. l.], v. 45, p. 115–131, 2008.

BONANOMI, G.; INCERTI, G.; GIANNINO, F.; MINGO, A.; LANZOTTI, V.; MAZZOLENI, S. Litter quality assessed by solid state ^{13}C NMR spectroscopy predicts decay rate better than C/N and Lignin/N ratios. **Soil Biology and Biochemistry**, [S. l.], v. 56, p. 40–48, 2013.

CHENG, W.; PARTON, W. J.; GONZALEZ-MELER, M. A.; PHILLIPS, R.; ASAO, S.; MCNICKLE, G. G.; BRZOSTEK, E.; JASTROW, J. D. Synthesis and modeling perspectives of rhizosphere priming. **New Phytologist**, [S. l.], v. 201, n. 1, p. 31–44, 2014.

COSTA, O. Y. A.; RAAIJMAKERS, J. M.; KURAMAE, E. E. Microbial extracellular polymeric substances: Ecological function and impact on soil aggregation. **Frontiers in Microbiology**, [S. l.], v. 9, n. JUL, p. 1–14, 2018.

COTRUFO, M. F.; SOONG, J. L.; HORTON, A. J.; CAMPBELL, E. E.; HADDIX, M. L.; WALL, D. H.; PARTON, W. J. Formation of soil organic matter via biochemical and physical pathways of litter mass loss. **Nature Geoscience**, [S. l.], v. 8, n. 10, p. 776–779, 2015.

COTRUFO, M. F.; WALLENSTEIN, M. D.; BOOT, C. M.; DENEF, K.; PAUL, E. The Microbial Efficiency-Matrix Stabilization (MEMS) framework integrates plant litter decomposition with soil organic matter stabilization: Do labile plant inputs form stable soil organic matter? **Global Change Biology**, [S. l.], v. 19, n. 4, p. 988–995, 2013.

DIJKSTRA, F. A.; CHENG, W. Interactions between soil and tree roots accelerate long-term soil carbon decomposition. **Ecology Letters**, [S. l.], v. 10, n. 11, p. 1046–1053, 2007.

DIJKSTRA, F. A.; ZHU, B.; CHENG, W. Root effects on soil organic carbon: a double-edged sword. **New Phytologist**, [S. l.], n. C, 2020.

DUNGAIT, J. A. J.; HOPKINS, D. W.; GREGORY, A. S.; WHITMORE, A. P. Soil organic matter turnover is governed by accessibility not recalcitrance. **Global Change Biology**, [S. l.], v. 18, n. 6, p. 1781–1796, 2012.

FANIN, N.; KARDOL, P.; FARRELL, M.; NILSSON, M. C.; GUNDALE, M. J.; WARDLE, D. A. The ratio of Gram-positive to Gram-negative bacterial PLFA markers as an indicator of carbon availability in organic soils. **Soil Biology and Biochemistry**, [S. l.], v. 128, n. June 2018, p. 111–114, 2019.

FONTAINE, S.; MARIOTTI, A.; ABBADIE, L. The priming effect of organic matter: A question of microbial competition? **Soil Biology and Biochemistry**, [S. l.], v. 35, n. 6, p. 837–843, 2003.

FROSTEGÅRD, Å.; TUNLID, A.; BÅÅTH, E. Microbial biomass measured as total lipid phosphate in soils of different organic content. **Journal of Microbiological Methods**, [S. l.], v. 14, n. 3, p. 151–163, 1991.

FROSTEGÅRD, Å; TUNLID, A.; BÅÅTH, E. Use and misuse of PLFA measurements in soils. **Soil Biology and Biochemistry**, [S. l.], v. 43, n. 8, p. 1621–1625, 2011.

GAILLARD, V.; CHENU, C.; RECOUS, S. Carbon mineralisation in soil adjacent to plant residues of contrasting biochemical quality. **Soil Biology and Biochemistry**, [S. l.], v. 35, n. 1, p. 93–99, 2003.

GAILLARD, V.; CHENU, C.; RECOUS, S.; RICHARD, G. Carbon, nitrogen and microbial gradients induced by plant residues decomposing in soil. **European Journal of Soil Science**, [S. l.], v. 50, n. 4, p. 567–578, 1999.

GOLDFARB, K. C.; KARAOZ, U.; HANSON, C. A.; SANTEE, C. A.; BRADFORD, M. A.; TRESEDER, K. K.; WALLENSTEIN, M. D.; BRODIE, E. L. Differential growth responses of soil bacterial taxa to carbon substrates of varying chemical recalcitrance. **Frontiers in Microbiology**, [S. l.], v. 2, n. MAY, p. 1–10, 2011.

GUNINA, A.; KUZYAKOV, Y. Sugars in soil and sweets for microorganisms: Review of origin, content, composition and fate. **Soil Biology and Biochemistry**, [S. l.], v. 90, p. 87–100, 2015.

HAFNER, S.; UNTEREGELSBACHER, S.; SEEBER, E.; LENA, B.; XU, X.; LI, X.; GUGGENBERGER, G.; MIEHE, G.; KUZYAKOV, Y. Effect of grazing on carbon stocks and assimilate partitioning in a Tibetan montane pasture revealed by $^{13}CO_2$ pulse labeling. **Global Change Biology**, [S. l.], v. 18, n. 2, p. 528–538, 2012.

HENNERON, L.; CROS, C.; PICON-COCHARD, C.; RAHIMIAN, V.; FONTAINE, S. Plant economic strategies of grassland species control soil carbon dynamics through rhizodeposition. **Journal of Ecology**, [S. l.], v. 108, n. 2, p. 528–545, 2020.

HICKS PRIES, C. E.; SULMAN, B. N.; WEST, C.; O'NEILL, C.; POPPLETON, E.; PORRAS, R. C.; CASTANHA, C.; ZHU, B.; WIEDEMEIER, D. B.; Torn, M. S. Root litter decomposition slows with soil depth. **Soil Biology and Biochemistry**, [S. l.], v. 125, n. July, p. 103–114, 2018.

HINSINGER, P.; BENGOUGH, A. G.; VETTERLEIN, D.; YOUNG, I. M. Rhizosphere: Biophysics, biogeochemistry and ecological relevance. **Plant and Soil**, [S. l.], v. 321, n. 1–2, p. 117–152, 2009.

HUO, C.; LUO, Y.; CHENG, W. Rhizosphere priming effect: A meta-analysis. **Soil Biology and Biochemistry**, [S. l.], v. 111, p. 78–84, 2017.

HÜTSCH, B. W.; AUGUSTIN, J.; MERBACH, W. Plant rhizodeposition - An important source for carbon turnover in soils. **Journal of Plant Nutrition and Soil Science**, [S. l.], v. 165, n. 4, p. 397–407, 2002.

INGWERSEN, J.; POLL, C.; STRECK, T.; KANDELER, E.. Micro-scale modelling of carbon turnover driven by microbial succession at a biogeochemical interface. **Soil Biology and Biochemistry**, [S. l.], v. 40, n. 4, p. 864–878, 2008.

IUSS WORKING GROUP WRB. **World Reference Base for Soil Resources 2014, Uptade 2015.** International soil classification system for naming soils and creating legends for soil maps**.** World Soil Resources Reports No. 106. FAO, Rome, 2015.

JACKSON, R. B.; LAJTHA, K.; CROW, S. E.; HUGELIUS, G.; KRAMER, M. G.; PIÑEIRO, G. The Ecology of Soil Carbon: Pools, Vulnerabilities, and Biotic and Abiotic Controls. **Annual Review of Ecology, Evolution, and Systematics**, [S. l.], v. 48, n. 1, p. 419-445, 2017.

JILLING, A.; KEILUWEIT, M.; CONTOSTA, A. R.; FREY, S.; SCHIMEL, J.; SCHNECKER, J.; SMITH, R. G.; TIEMANN, L.; GRANDY, A. S. Minerals in the rhizosphere: overlooked mediators of soil nitrogen availability to plants and microbes. **Biogeochemistry**, [S. l.], v. 139, n. 2, p. 103–122, 2018.

JOHNSON, D.; LEAKE, J. R.; OSTLE, N.; INESON, P.; READ, D. J. In situ $^{13}CO_2$ pulse-labelling of upland grassland demonstrates a rapid pathway of carbon flux from arbuscular mycorrhizal mycelia to the soil. **New Phytologist**, [S. l.], v. 153, n. 2, p. 327–334, 2002.

JONES, D. L.; NGUYEN, C.; FINLAY, R. D. Carbon flow in the rhizosphere: Carbon trading at the soil-root interface. **Plant and Soi**l, [S. l.], v. 321, n. 1–2, p. 5–33, 2009.

KAISER, K.; KALBITZ, K. Cycling downwards – dissolved organic matter in soils. **Soil Biology and Biochemistry**, [S. l.], v. 52, p. 29–32, 2012.

KEILUWEIT, M.; BOUGOURE, J. J.; NICO, P. S.; PETT-RIDGE, J.; WEBER, P. K.; KLEBER, M. Mineral protection of soil carbon counteracted by root exudates. **Nature Climate Change**, [S. l.], v. 5, n. 6, p. 588–595, 2015.

KINDLER, R.; MILTNER, A.; RICHNOW, H. H.; KÄSTNER, M. Fate of gram-negative bacterial biomass in soil - Mineralization and contribution to SOM. **Soil Biology and Biochemistry**, [S. l.], v. 38, n. 9, p. 2860–2870, 2006.

KLEBER, M.; EUSTERHUES, K.; KEILUWEIT, M.; MIKUTTA, C.; MIKUTTA, R.; NICO, P. S. Mineral-Organic Associations: Formation, Properties, and Relevance in Soil Environments. **Advances in Agronomy**, [S. l.], v. 130, p. 1–140, 2015.

KÖGEL-KNABNER, I. ^{13}C and ^{15}N NMR spectroscopy as a tool in soil organic matter studies. **Geoderma**, [S. l.], v. 80, n. 3–4, p. 243–270, 1997.

KÖGEL-KNABNER, I. The macromolecular organic composition of plant and microbial residues as inputs to soil organic matter: Fourteen years on. **Soil Biology and Biochemistry**, [S. l.], v. 105, p. A3–A8, 2017.

KRAMER, C.; GLEIXNER, G. Variable use of plant- and soil-derived carbon by microorganisms in agricultural soils. **Soil Biology and Biochemistry**, [S. l.], v. 38, n. 11, p. 3267–3278, 2006.

KUZYAKOV, Y.; CHENG, W. Photosynthesis controls of rhizosphere respiration and organic matter decomposition. **Soil Biology and Biochemistry**, [S. l.], v. 33, n. 14, p. 1915–1925, 2001.

KUZYAKOV, Y.; BLAGODATSKAYA, E. Microbial hotspots and hot moments in soil: Concept & review. **Soil Biology and Biochemistry**, [S. l.], v. 83, n. February, p. 184–199, 2015.

KUZYAKOV, Y.; DOMANSKI, G. Carbon input by plants into the soil. Review. **Journal of Plant Nutrition and Soil Science**, [S. l.], v. 163, n. 4, p. 421–431, 2000.

KUZYAKOV, Y.; HILL, P. W.; JONES, D. L. Root exudate components change litter decomposition in a simulated rhizosphere depending on temperature. **Plant and Soil**, [S. l.], v. 290, n. 1–2, p. 293–305, 2007.

LAVALLEE, J. M.; CONANT, R. T.; PAUL, E. A.; COTRUFO, M. F. Incorporation of shoot versus root-derived ^{13}C and ^{15}N into mineral-associated organic matter fractions: results of a soil slurry incubation with dual-labelled plant material. **Biogeochemistry**, [S. l.], v. 137, n. 3, p. 379–393, 2018.

LAVALLEE, J. M.; SOONG, J. L.; COTRUFO, M. F. Conceptualizing soil organic matter into particulate and mineral-associated forms to address global change in the 21st century. **Global Change Biology**, [S. l.], n. July, p. 1–13, 2019.

LIANG, C.; SCHIMEL, J. P.; JASTROW, J. D. The importance of anabolism in microbial control over soil carbon storage. **Nature Microbiology**, [S. l.], v. 2, n. 8, 2017.

MACHADO, D. N.; NOVAIS, R. F.; SILVA, I. R.; LOUREIRO, M. E.; MILAGRES, J. J.; SOARES, E. M. B. Enriquecimento e alocação de ^{13}C em plantas de eucalipto. **Revista Brasileira de Ciência do Solo**, Viçosa-MG, v. 35, p. 857–866, 2011.

MARSCHNER, P.; MARHAN, S.; KANDELER, E. Microscale distribution and function of soil microorganisms in the interface between rhizosphere and detritusphere. **Soil Biology and Biochemistry**, [S. l.], v. 49, p. 174–183, 2012.

MARX, M.; BUEGGER, F.; GATTINGER, A.; ZSOLNAY, Á.; MUNCH, J. C. Determination of the fate of ^{13}C labelled maize and wheat exudates in an agricultural soil during a short-term incubation. **European Journal of Soil Science**, [S. l.], v. 58, n. 5, p. 1175–1185, 2007.

NANNIPIERI, P.; ASCHER, J.; CECCHERINI, M. T.; LANDI, L.; PIETRAMELLARA, G.; RENELLA, G. Landmark Papers Microbial diversity and soil functions. **European Journal of Soil Science**, [S. l.], v. 68, n. 1, p. 12–26, 2017.

NEFF, J. C.; CHAPIN, F. S.; VITOUSEK, P. M. Breaks in the Cycle: Dissolved Organic Nitrogen in Terrestrial Ecosystems. **Frontiers in Ecology and the Environment**, [S. l.], v. 1, n. 4, p. 205, 2003.

NELSON, P. N.; BALDOCK, J. A. Estimating the molecular composition of a diverse range of natural organic materials from solid-state ^{13}C NMR and elemental analyses. **Biogeochemistry**, [S. l.], v. 72, n. 1, p. 1–34, 2005.

NUCCIO, E. E.; STARR, E.; KARAOZ, U.; BRODIE, E. L.; ZHOU, J.; TRINGE, S. G.; MALMSTROM, R. R.; WOYKE, T.; BANFIELD, J. F.; FIRESTONE, M. K. PETT-RIDGE, J. Niche differentiation is spatially and temporally regulated in the rhizosphere. **The ISME Journal**, [S. l.], v. 14, n. 4, p. 999–1014, 2020.

OLIVER, I. C.; KNOX, O. G. G.; FLAVEL, R. J.; WILSON, B. R. Rhizosphere Legacy: Plant Root Interactions with the Soil and Its Biome. In: GUPTA, V. V. S. R.; SHARMA, A. K. (org.). **Rhizosphere Biology: Interactions Between Microbes and Plant**. Singapore: Springer Nature, 2021. p. 129–153.

PATERSON, E.; OSLER, G.; DAWSON, L. A.; GEBBING, T.; SIM, A.; ORD, B. Labile and recalcitrant plant fractions are utilised by distinct microbial communities in soil: Independent of the presence of roots and mycorrhizal fungi. **Soil Biology and Biochemistry**, [S. l.], v. 40, n. 5, p. 1103–1113, 2008.

POLL, C.; INGWERSEN, J.; STEMMER, M.; GERZABEK, M. H.; KANDELER, E. Mechanisms of solute transport affect small-scale abundance and function of soil microorganisms in the detritusphere. **European Journal of Soil Science**, [S. l.], v. 57, n. 4, p. 583–595, 2006.

R CORE TEAM. R: A language and environment for statistical computing. v. 3.6.0., Vienna: R Foundation for Statistical Computing, 2021.

RASSE, D. P.; RUMPEL, C.; DIGNAC, M. F. Is soil carbon mostly root carbon? Mechanisms for a specific stabilisation. **Plant and Soil**, [S. l.], v. 269, n. 1–2, p. 341–356, 2005.

RUIZ, Hugo Alberto. Incremento da exatidão da análise granulométrica do solo por meio da coleta da suspensão (Silte + Argila). **Revista Brasileira de Ciência do Solo**, Viçosa-MG, v. 29, n. 2, p. 297–300, 2005.

SHAHBAZ, M.; KUZYAKOV, Y.; HEITKAMP, F. Decrease of soil organic matter stabilization with increasing inputs: Mechanisms and controls. **Geoderma**, [S. l.], v. 304, p. 76–82, 2017.

SHAHBAZ, M.; KUZYAKOV, Y.; SANAULLAH, M.; HEITKAMP, F.; ZELENEV, V.; KUMAR, A.; BLAGODATSKAYA, E. Microbial decomposition of soil organic matter is mediated by quality and quantity of crop residues: mechanisms and thresholds. **Biology and Fertility of Soils**, [S. l.], v. 53, n. 3, p. 287–301, 2017.

SOKOL, N. W.; BRADFORD, M. A. Microbial formation of stable soil carbon is more efficient from belowground than aboveground input. **Nature Geoscience**, [S. l.], v. 12, n. 1, p. 46–53, 2019.

SOKOL, N. W.; KUEBBING, S. E.; KARLSEN-AYALA, E.; BRADFORD, M. A. Evidence for the primacy of living root inputs, not root or shoot litter, in forming soil organic carbon. **New Phytologist**, [S. l.], p. 233–246, 2018.

SOKOL, N. W.; SANDERMAN, J.; BRADFORD, M. A. Pathways of mineral-associated soil organic matter formation: integrating the role of plant carbon source, chemistry, and point-of-entry. **Global Change Biology**, [S. l.], n. August, p. 1–13, 2018.

SOUZA, I. F.; BARROS, N. F.; SILVA, I. R.; RENIER, R. F.; SILVA, L. Á.; NOVAIS, R. F. Decomposition of eucalypt harvest residues as affected by management practices, climate and soil properties across southeastern Brazil. **Forest Ecology and Management**, [S. l.], v. 374, p. 186–194, 2016.

SOUZA, I. F.; ALMEIDA, L. F. J.; JESUS, G. L.; PETT-RIDGE, J.; NICO, P. S.; KLEBER, M.; SILVA, I. R. Carbon Sink Strength of Subsurface Horizons in Brazilian Oxisols. **Soil Science Society of America Journal**, [S. l.], v. 82, n. 1, p. 76–86, 2018.

STEWART, C. E.; PAUSTIAN, K.; CONANT, R. T.; PLANTE, A. F.; SIX, J. Soil carbon saturation: Implications for measurable carbon pool dynamics in long-term incubations. **Soil Biology and Biochemistry**, [S. l.], v. 41, n. 2, p. 357–366, 2009.

TEDESCO, M. J.; GIANELLO, C.; BISSANI, C. A.; BOHNEN, H.; VOLKWEISS, S. J. **Análise de solo, plantas e outros materiais**. 2nd ed. Porto Alegre.

VALADARES, R. V.; NEVES, J. C. L.; COSTA, M. D.; SMETHURST, P. J.; PETERNELLI, L. A.; JESUS, G. L.; CANTARUTTI, R. B.; SILVA, I. R. Modeling rhizosphere carbon and nitrogen cycling in Eucalyptus plantation soil. **Biogeosciences**, [S. l.], v. 15, n. 16, p. 4943–4954, 2018.

VALADARES, R. V.; COSTA, M. D.; NEVES, J. C. L.; VIEIRA NETTO, J. A. F.; SILVA, I. R.; MORO, E.; ALVES, M. R.; FERNANDES, L. A. Rhizosphere microbiological processes and eucalypt nutrition: Synthesis and conceptualization. **Science of the Total Environment**, [S. l.], v. 746, p. 141305, 2020.

VIDAL, A.; HIRTE, J.; BENDER, S. F.; MAYER, J.; GATTINGER, A.; HÖSCHEN, C.; SCHÄDLER, S.; IQBAL, T. M.; MUELLER, C. W. Linking 3D Soil Structure and Plant-Microbe-Soil Carbon Transfer in the Rhizosphere. **Frontiers in Environmental Science**, [S. l.], v. 6, n. February, p. 1–14, 2018.

VON LÜTZOW, M.; KÖGEL-KNABNER, I.; EKSCHMITT, K.; FLESSA, H.; GUGGENBERGER, G.; MATZNER, E.; MARSCHNER, B. SOM fractionation methods: Relevance to functional pools and to stabilization mechanisms. **Soil Biology and Biochemistry**, [S. l.], v. 39, n. 9, p. 2183–2207, 2007.

WANG, Q.; WANG, Yanping; WANG, S.; HE, T.; LIU, L.. Fresh carbon and nitrogen inputs alter organic carbon mineralization and microbial community in forest deep soil layers. **Soil Biology and Biochemistry**, [S. l.], v. 72, p. 145–151, 2014.

WURST, S.; OHGUSHI, T. Do plant- and soil-mediated legacy effects impact future biotic interactions? **Functional Ecology**, [S. l.], v. 29, n. 11, p. 1373–1382, 2015.

YEOMANS, J. C.; BREMNER, J. M. A rapid and precise method for routine determination of organic carbon in soil. **Communications in Soil Science and Plant Analysis**, [S. l.], v. 19, n. May 2013, p. 1467–1476, 1988.

YIN, L.; DIJKSTRA, F. A.; WANG, P.; ZHU, B.; CHENG, W. Rhizosphere priming effects on soil carbon and nitrogen dynamics among tree species with and without intraspecific competition. **New Phytologist**, [S. l.], v. 218, n. 3, p. 1036–1048, 2018.

GENERAL CONCLUSIONS

Our work provides several insights into the processes that control the conversion of root C inputs in soil (Figure 1). We demonstrated that rhizodeposits are capable to originate persistent SOM through mineral interactions. To our knowledge, this is the first time that this process was proven using real plant rhizodeposits, and not labeled reactants. Moreover, our results show that the spatial distribution of the root litter and rhizodeposit-derived C showed different patterns. While root litter C conversion in SOM was restricted to the first four millimeters in its surroundings, rhizo-C distribution was much wider, being detected up a few centimeters from the root. Furthermore, from the NanoSIMS results, we provide direct evidence for the incorporation of root litter into microbial structures and the formation of organic coatings in the surfaces of minerals (MAOM formation) at the rhizosphere. Contrary to our hypothesis, neither rhizo-C nor root litter C fate was affected by legacy treatments. This suggests that the decomposition of these two C sources occurred independently in the rhizosphere-detritusphere transition. One possible explanation may be that different microbial communities are responsible for the processing of each type of root C input. Nevertheless, since we only evaluated the microbial communities at the end of the incubation, novel studies are required to prove this theory.

Figure 1 — Simplified illustration of the main findings of the study.

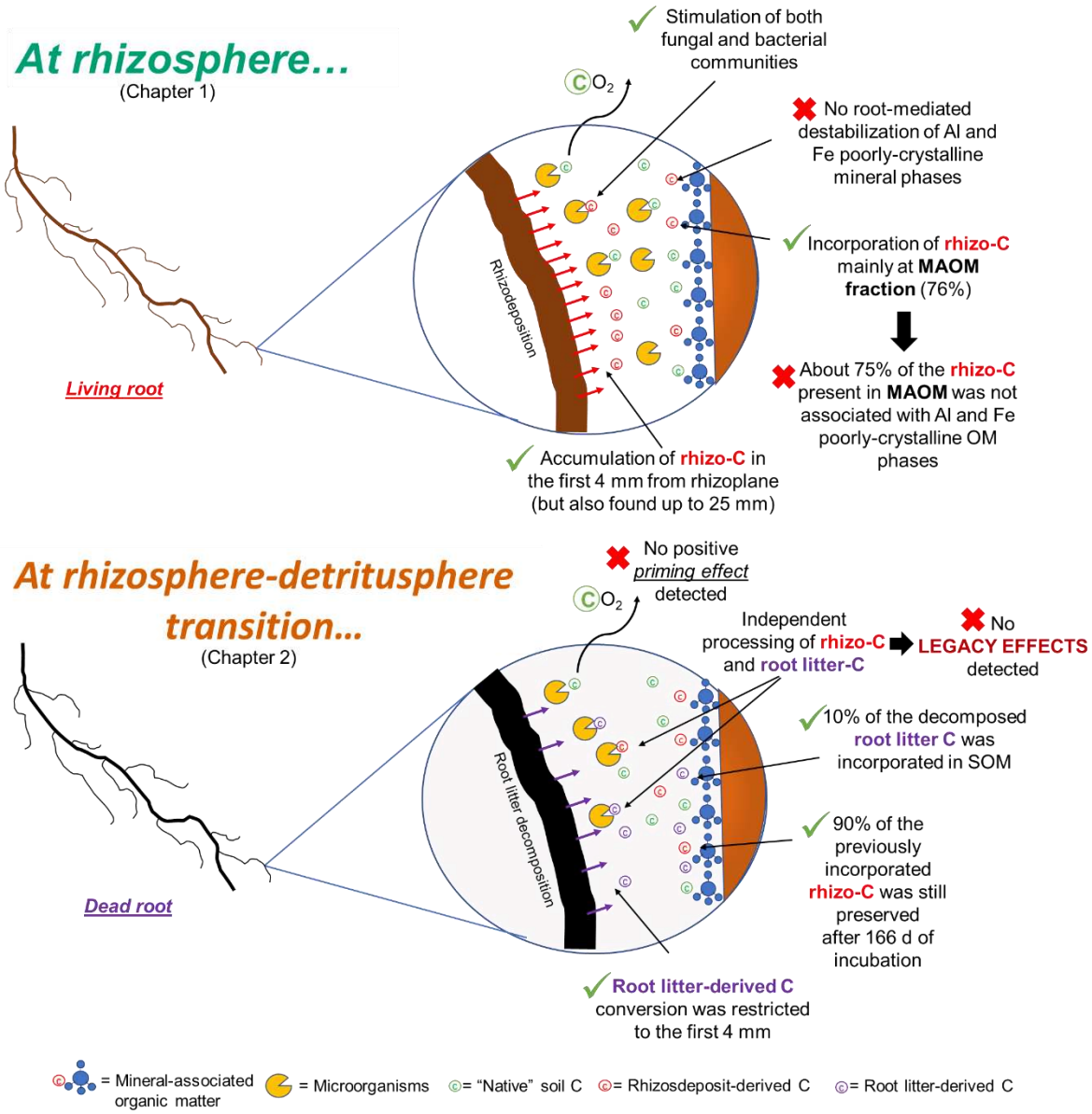

Source: Author.

GENERAL REFERENCES

COTRUFO, M. F.; SOONG, J. L.; HORTON, A. J.; CAMPBELL, E. E.; HADDIX, M. L.; WALL, D. H.; PARTON, W. J. Formation of soil organic matter via biochemical and physical pathways of litter mass loss. **Nature Geoscience**, [S. l.], v. 8, n. 10, p. 776–779, 2015.

COTRUFO, M. F.; WALLENSTEIN, M. D.; BOOT, C. M.; DENEF, K.; PAUL, E. The Microbial Efficiency-Matrix Stabilization (MEMS) framework integrates plant litter decomposition with soil organic matter stabilization: Do labile plant inputs form stable soil organic matter? **Global Change Biology**, [S. l.], v. 19, n. 4, p. 988–995, 2013.

ESHEL, A.; BEECKMAN, T. **Plant Roots: The Hidden Half**. 4. ed. Boca Raton: Taylor and Francis Group, 2014.

HÜTSCH, B. W.; AUGUSTIN, J.; MERBACH, W. Plant rhizodeposition - An important source for carbon turnover in soils. **Journal of Plant Nutrition and Soil Science**, [S. l.], v. 165, n. 4, p. 397–407, 2002.

JACKSON, R. B.; LAJTHA, K.; CROW, S. E.; HUGELIUS, G.; KRAMER, M. G.; PIÑEIRO, G. The Ecology of Soil Carbon: Pools, Vulnerabilities, and Biotic and Abiotic Controls. **Annual Review of Ecology**, Evolution, and Systematics, [S. l.], v. 48, n. 1, p. 419–445, 2017.

JONES, D. L.; NGUYEN, C.; FINLAY, R. D. Carbon flow in the rhizosphere: Carbon trading at the soil-root interface. **Plant and Soil**, [S. l.], v. 321, n. 1–2, p. 5–33, 2009.

KÖGEL-KNABNER, I. The macromolecular organic composition of plant and microbial residues as inputs to soil organic matter. **Soil Biology and Biochemistry**, [S. l.], v. 34, n. 2, p. 139–162, 2002.

KÖGEL-KNABNER, I. The macromolecular organic composition of plant and microbial residues as inputs to soil organic matter: Fourteen years on. **Soil Biology and Biochemistry**, [S. l.], v. 105, p. A3–A8, 2017.

KUZYAKOV, Y.; BLAGODATSKAYA, E. Microbial hotspots and hot moments in soil: Concept & review. **Soil Biology and Biochemistry**, [S. l.], v. 83, n. February, p. 184–199, 2015.

LAVALLEE, J. M.; CONANT, R. T.; PAUL, E. A.; COTRUFO, M. F. Incorporation of shoot versus root-derived ^{13}C and ^{15}N into mineral-associated organic matter fractions: results of a soil slurry incubation with dual-labelled plant material. **Biogeochemistry,** [S. l.], v. 137, n. 3, p. 379–393, 2018.

OLIVER, I. C.; KNOX, O. G. G.; FLAVEL, R. J.; WILSON, B. R. Rhizosphere Legacy: Plant Root Interactions with the Soil and Its Biome. In: GUPTA, V. V. S. R.; SHARMA, A. K. (org.). **Rhizosphere Biology: Interactions Between Microbes and Plant**. Singapore: Springer Nature, 2021. p. 129–153.

POWLSON, D.; XU, J.; BROOKES, P. Through the Eye of the Needle — The Story of the Soil Microbial Biomass. In: TATE, Kevin (org.). **Microbial Biomass A Paradigm Shift in Terrestrial Biogeochemistry**. New Jersey-USA: World Scientific, 2017. p. 1–40.

RASSE, D. P.; RUMPEL, C.; DIGNAC, M. F. Is soil carbon mostly root carbon? Mechanisms for a specific stabilisation**. Plant and Soil**, [S. l.], v. 269, n. 1–2, p. 341–356, 2005.

SOKOL, N. W.; KUEBBING, S. E.; KARLSEN-AYALA, E.; BRADFORD, M. A. Evidence for the primacy of living root inputs, not root or shoot litter, in forming soil organic carbon. **New Phytologist**, [S. l.], p. 233–246, 2018.

WAISEL, Y.; ESHEL, A.; KAFKAFI, U. **Plant roots: the hidden half**. [S. l.], p. 948, 1991.

WURST, S.; OHGUSHI, T. Do plant- and soil-mediated legacy effects impact future biotic interactions? **Functional Ecology**, [S. l.], v. 29, n. 11, p. 1373–1382, 2015.m1

APPENDIX A – CHAPTER 1

Table A1 — Physical and chemical attributes of soil.

pH[1]	C[2]	N[3]	$\delta^{13}C$[4]	P[5]	K[5]	Ca^{2+}[6]	Mg^{2+}[6]	Al^{3+}[6]	CEC[7]
	------%-------		‰	mg dm^{-3}		----------	$mmol_c$ dm^{-3}	----------	
4.0	3.22	0.19	-23	1.0	12	1.7	0.5	10.8	111.5

[1] pH determined in H_2O, 1:2.5 soil:water solution; [2]Yeomans and Bremner, (1988); [3] Tedesco et al. (1985) and [4] Determined using an elemental isotope ratio mass spectrometer; [5] P and K determined with Mehlich-1 extractor; [6] Ca^{2+}, Mg^{2+}, and Al^{3+}determined in KCl 1 mol L^{-1}, [7] Cation exchange capacity.

Sand[1]	Silt[1]	Clay[1]	S[2]	B[3]	Cu [4]	Mn[4]	Fe[4]	Zn[4]
------ g g^{-1} ------			---------- mg dm^{-3}	----------				
0.25	0.09	0.66	0.6	0.26	0.33	4.8	65.8	1.06

[1]Determined following Ruiz (2005); [2]S determined by Monocalcium Phosphate in acetic acid, [3] B extracted with hot water, [4] Cu, Mn, Fe, and Zn determined with Mehlich^{-1} extractor.
Source: Author.

Table A2 — Sources and nutrients applied to soil prior to the beginning of the experiment

Source of nutrient	N	P	K	S	Cu	Zn	B	Fe	Mn	Mo
	---------- mg kg^{-1} soil----------									
$NH_4H_2PO_4$	100.0	221.4	-	-	-	-	-	-	-	-
KH_2PO_4	-	93.4	99.3	-	-	-	-	-	-	-
K_2SO_4	-	-	50.4	20.7	-	-	-	-	-	-
Na_2SO_4	-	-	-	16.7	-	-	-	-	-	-
$CuSO_4.5H_2O$	-	-	-	0.8	1.6	-	-	-	-	-
$ZnSO_4.7H_2O$	-	-	-	1.9	-	4.0	-	-	-	-
H_3BO_3	-	-	-	-	-	-	0.8	-	-	-
$FeCl_3.6H_2O$	-	-	-	-	-	-	-	1.5	-	-
$MnCl_2.4H_2O$	-	-	-	-	-	-	-	-	3.7	-
$NaMoO_4.2H_2O$	-	-	-	-	-	-	-	-	-	0.2
Total nutrient (mg kg^{-1} soil)	100.0	314.8	149.7	40.0	1.6	4.0	0.8	1.5	3.7	0.2

*Ca and Mg were supplied as CaO and MgO (4:1 ratio) at the rate of 1.5 g kg^{-1} of soil.
Source: Author.

Figure A1 — Root isolator cylinder capped with a nylon membrane of pore-size of 5 µm and sealed with a rubber cap at the bottom (A); Root isolator cylinder filled with Rhodic ferralsol (B); Positioning of the root isolator cylinders in the mesocosm (C); Planting of the eucalypt seedling in the center of the root isolator cylinders (D).
Source: Author.

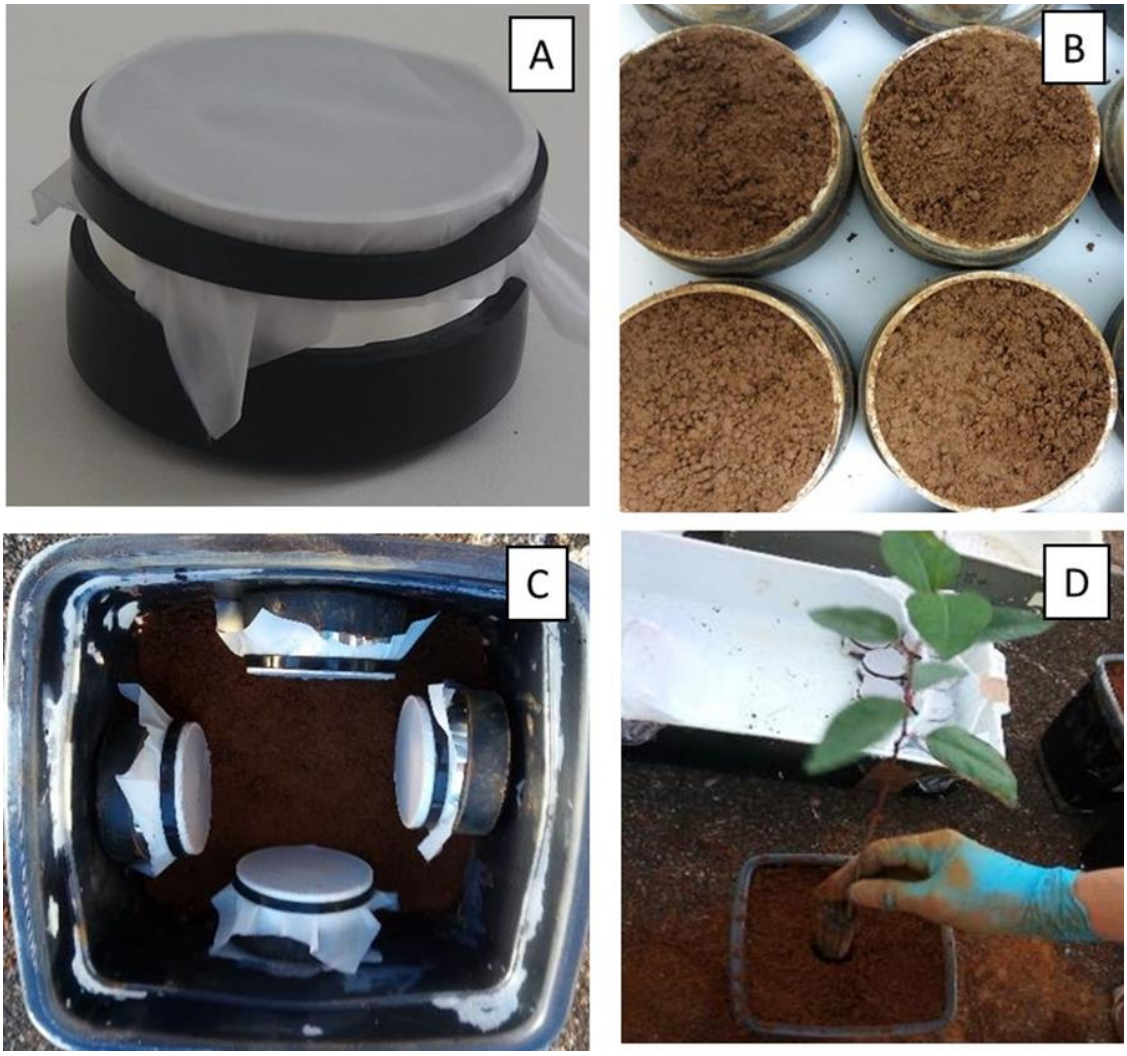

Figure A2 — Mesocosms inside the labeling chamber 37 days after the seedling planting (A); Mesocosms inside the labeling chamber 63 days after the seedling planting (B); Injection of acid solution in a petri dish containing $Na_2{}^{13}CO_3$ (C).
Source: Author.

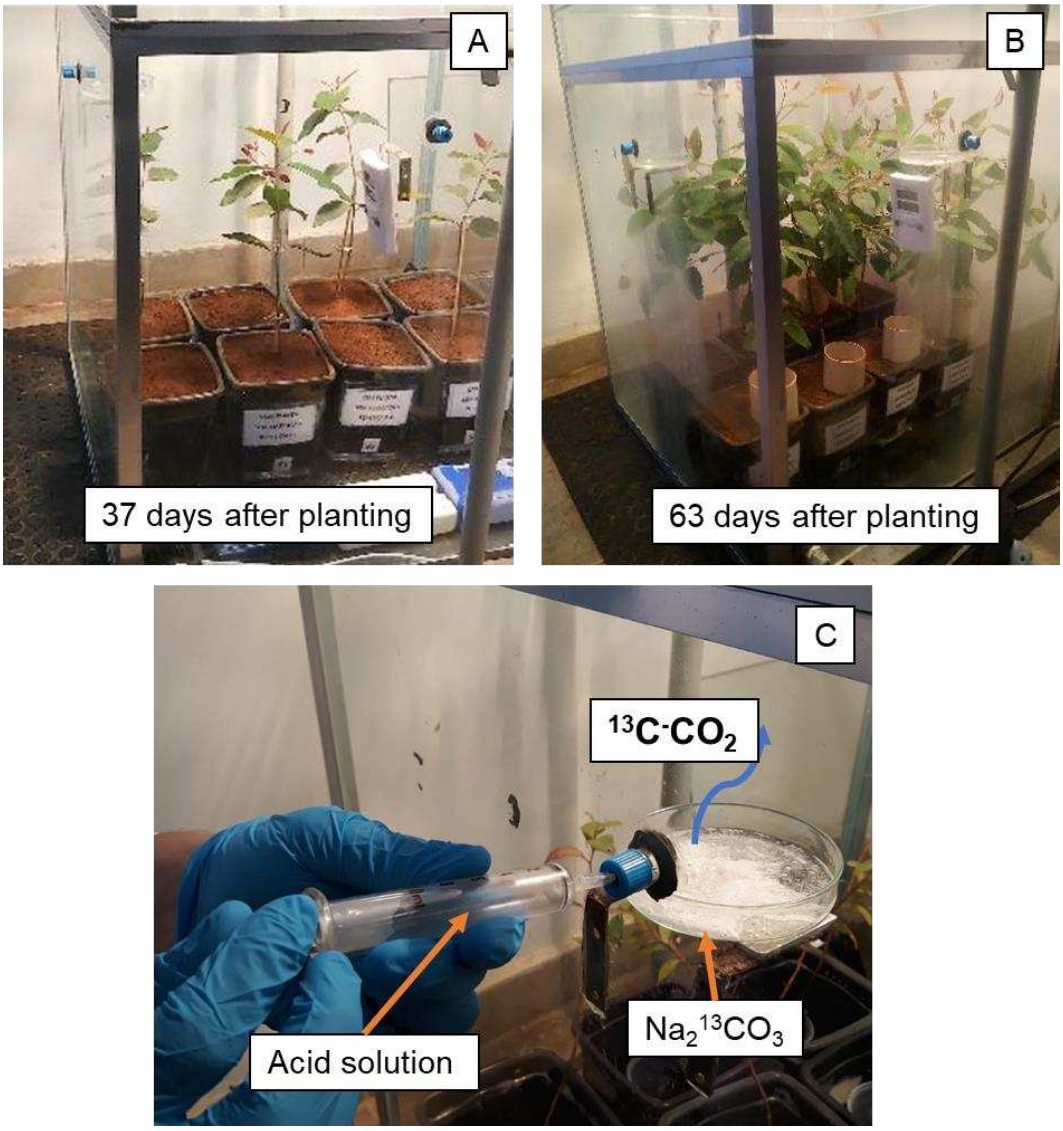

Figure A3 — Mesocosm after the seedling shoot harvest (A); Removal of the root isolator cylinders (B); Details of root growth in the vicinity of the nylon mesh of root isolator cylinders (C and D).

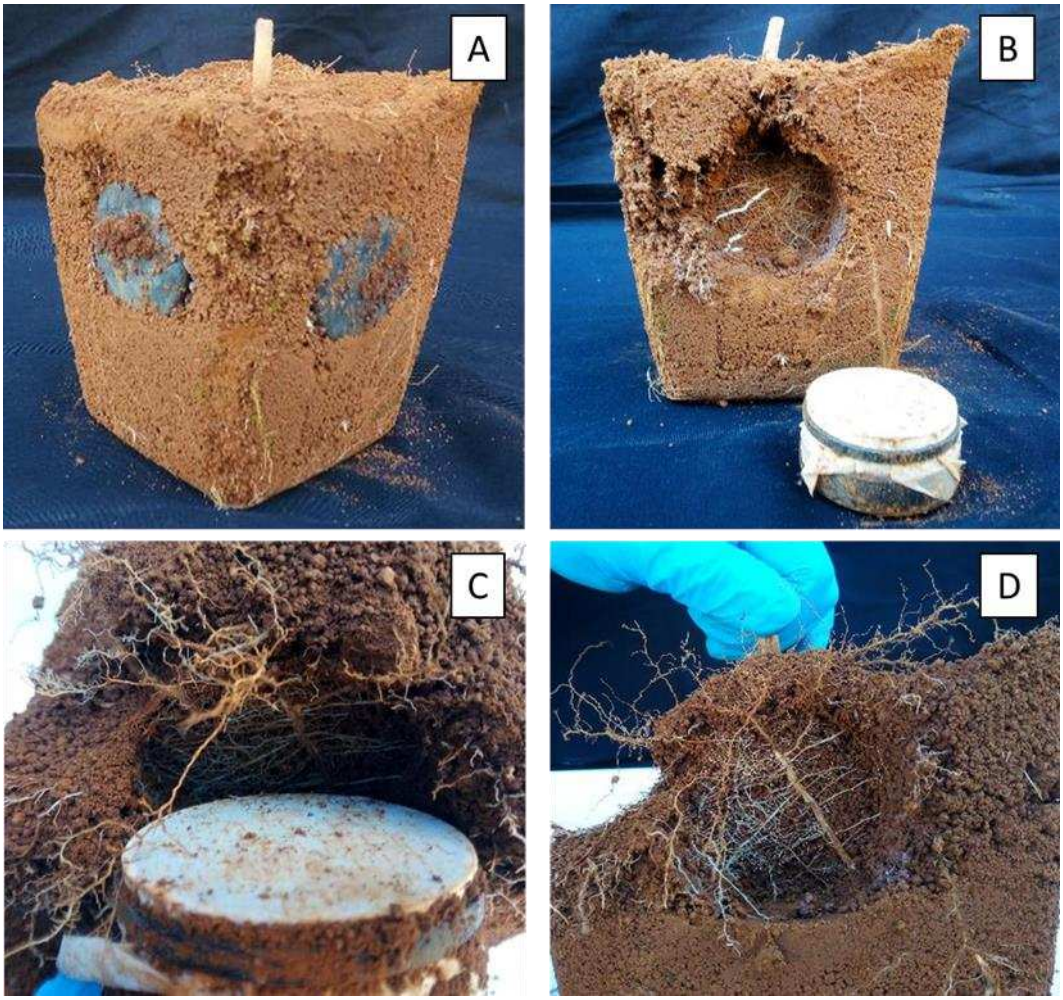

Source: Author.

Table A3 — Fluctuation range of CO_2 and temperature in each pulse event for labeled and unlabeled samples.

Event	Day	Days after planting	Cumulative C input ($^{13}Na_2CO_3$) (g)	Nº of Pulses day^{-1}	CO_2 fluctuation range (ppm)	Temperature Range (°C)
			Labeled			
1	6/5/2019	16	0.12	1	632 - 1061	19.3 - 23.9
2	6/13/2019	24	0.24	1	446 - 1148	19.6 - 24.1
3	6/20/2019	31	0.36	1	124 - 1023	17.4 - 23.3
4	6/26/2019	37	0.48	1	121 - 1075	17.3 - 22.3
5	6/28/2019	39	0.65	2	222 - 1155	18.4 - 22.4
6	7/4/2019	45	0.89	2	213 - 1137	18.0 - 22.4
7	7/5/2019	47	1.13	2	134 - 1061	18.9 - 24.3
8	7/10/2019	51	1.37	2	236 - 1006	17.5 - 23.9
9	7/17/2019	58	1.61	2	118 - 892	17.8 - 22.3
10	7/22/2019	63	1.85	2	152 - 1012	18.8 - 25.4
			Unlabeled			
1	6/4/2019	15	0.12*	1	627 - 1229	19.1 - 23.8
2	6/11/2019	22	0.23*	1	521 - 1335	19.5 - 23.6
3	6/18/2019	29	0.35*	1	176 - 1102	18.7 - 23.6
4	6/25/2019	36	0.47*	1	178 - 1086	20.7 - 22.3
5	6/27/2019	38	0.65*	2	138 - 1021	17.1 - 21.9
6	7/3/2019	44	0.88*	2	172 - 849	18.0 - 23.2
7	7/6/2019	46	1.12*	2	183 - 1051	17.8 - 23.1
8	7/9/2019	50	1.35*	2	292 - 904	17.5 - 23.7
9	7/16/2019	57	1.59*	2	146 - 958	18.0 - 22.1
10	7/21/2019	62	1.82*	2	208 - 882	18.7 - 25.2

*For the unlabeled experimental units, we added the equivalent of non-isotopically enriched $Na_2CO_3.10H_2O$.
Source: Author.

Table A4 — Shoot and root biomass of eucalypt plants used in labeled and unlabeled treatments

Treatment	Total (g)	Shoot (g)	Root (g)	Root:shoot ratio
Labeled	21.09 ±2.1 **a**	17.65 ±2.2 **a**	3.44 ±0.2 **a**	20% ±2.8 **a**
Unlabeled	20.22 ±2.7 **a**	16.40 ±2.2 **a**	3.82 ±0.5 **a**	23% ±1.2 **a**

Standard deviations from the mean are given in brackets. Different case letters indicate significant differences between labeled and unlabeled treatments ($p < 0.05$).
Source: Author.

Table A5 — $\delta^{13}C$ and ^{13}C Atm% of unlabeled reference treatments with rhizodeposition and control along with the distances to the root.

	Treatment	Distance to root			
		0-4 mm	4-8 mm	8-15 mm	15-25 mm
$\delta^{13}C$	With rhizodeposition	-23.05 **a**	-23.32 **a**	-23.31 **a**	-23.21 **a**
	Control	-23.16 **a**	-23.24 **a**	-23.46 **b**	-23.15 **a**
^{13}C Atm%	With rhizodeposition	1.0804 **a**	1.0801 **a**	1.0801 **a**	1.0803 **a**
	Control	1.0803 **a**	1.0802 **a**	1.0799 **a**	1.0803 **a**

Different letters indicate significant differences between the treatments with and without plant ($p < 0.05$).
Source: Author.

Table A6 — Molar ratios of C:Fe, C:Al and C:Al+Fe for the OM complexes and SRO phase extraction.

Extraction	Ratio	With rhizodeposition	Control
OM complexes extraction	C:Fe ratio	2.21 ±0.09 **a**	2.12 ±0.22 **a**
	C:Al ratio	0.67 ±0.01 **a**	0.69 ±0.02 **a**
	C:Al+Fe ratio	0.89 ±0.03 **a**	0.86 ±0.08 **a**
SRO phases extraction	C:Fe ratio	11.95 ±2.31 **a**	11.08 ±1.78 **a**
	C:Al ratio	0.39 ±0.06 **a**	0.34 ±0.06 **a**
	C:Al+Fe ratio	0.38 ±0.06 **a**	0.33 ±0.06 **a**

Source: Author.

Table A7 — $\delta^{13}C$ values (‰), amount of rhizosphere-derived C (rhizo-C, µg of ^{13}C g^{-1} of soil), and the relative distribution of Rhizo-C (rhizo-C) in the SOM fractions and organo-mineral (OM) complexes and short-range order (SRO) phases.

SOM fraction		$\delta^{13}C$ (‰)	Rhizo-C (µg of ^{13}C g^{-1} of soil)	Relative distribution[2] (%)
fPOM		**-28.15 ±026**	**0.028± 0.03**	**1.4% ±3**
oPOM		**-27.84 ±0.08**	**0.023 ±0.01**	**2.8% ±1**
SSOM		**-24.59 ±0.11**	**0.000 ±0.01**	**0.0% ±0**
MAOM	OM	-	0.041 ±0.03	6.4% ±5
	SRO	-	0.145 ±0.06	12.5% ±5
	Residual	-	0.581 ±0.12	57.8% ±4
	Subtotal	**-19.99 ±0.46**	**0.77 ±0.14**	**76.2% ±3**
Bulk soil		**-20.40 ±0.53**	**1.01 ±0.20**	**100%**

Means ± SE (n = 4) are presented.
[1]$\delta^{13}C$ values of OM complexes and SRO were not measured directly, but the rhizo-C were calculated by the difference between the ^{13}C abundance after and before the extraction.
[2]The relative distribution was calculated according to the bulk soil (unfractionated soil).
Source: Author.

APPENDIX B – CHAPTER 2

Table B1 — Physical and chemical attributes of soil

pH[1]	C[2]	N[3]	$\delta^{13}C$[4]	P[5]	K[5]	Ca^{2+}[6]	Mg^{2+}[6]	Al^{3+}[6]	CEC[7]
	------%-------		‰	mg dm^{-3}		---------- $mmol_c$ dm^{-3}----------			
4.0	3.22	0.19	-23	1.0	12	1.7	0.5	10.8	111.5

[1] pH determined in H_2O, 1:2.5 soil:water solution; [2]Yeomans and Bremner, (1988); [3] Tedesco et al. (1985) and [4] Determined using an elemental isotope ratio mass spectrometer; [5] P and K determined with Mehlich-1 extractor; [6] Ca^{2+}, Mg^{2+}, and Al^{3+}determined in KCl 1 mol L^{-1}, [7] Cation exchange capacity.

Sand[1]	Silt[1]	Clay[1]	S[2]	B[3]	Cu[4]	Mn[4]	Fe[4]	Zn[4]
------ g g^{-1} ------				---------- mg dm^{-3}----------				
0.25	0.09	0.66	0.6	0.26	0.33	4.8	65.8	1.06

[1]Determined following Ruiz (2005); [2]S determined by Monocalcium Phosphate in acetic acid, [3] B extracted with hot water, [4] Cu, Mn, Fe, and Zn determined with Mehlich-1 extractor.
Source: Author.

Figure B1 — Aluminum cylinder and plastic cap separately (A); Plastic cover attached to the bottom of the aluminum cylinder (B); Cylinder filled with soil (C); 0.5 µm pore-sized nylon membrane covering the cylinder (D).

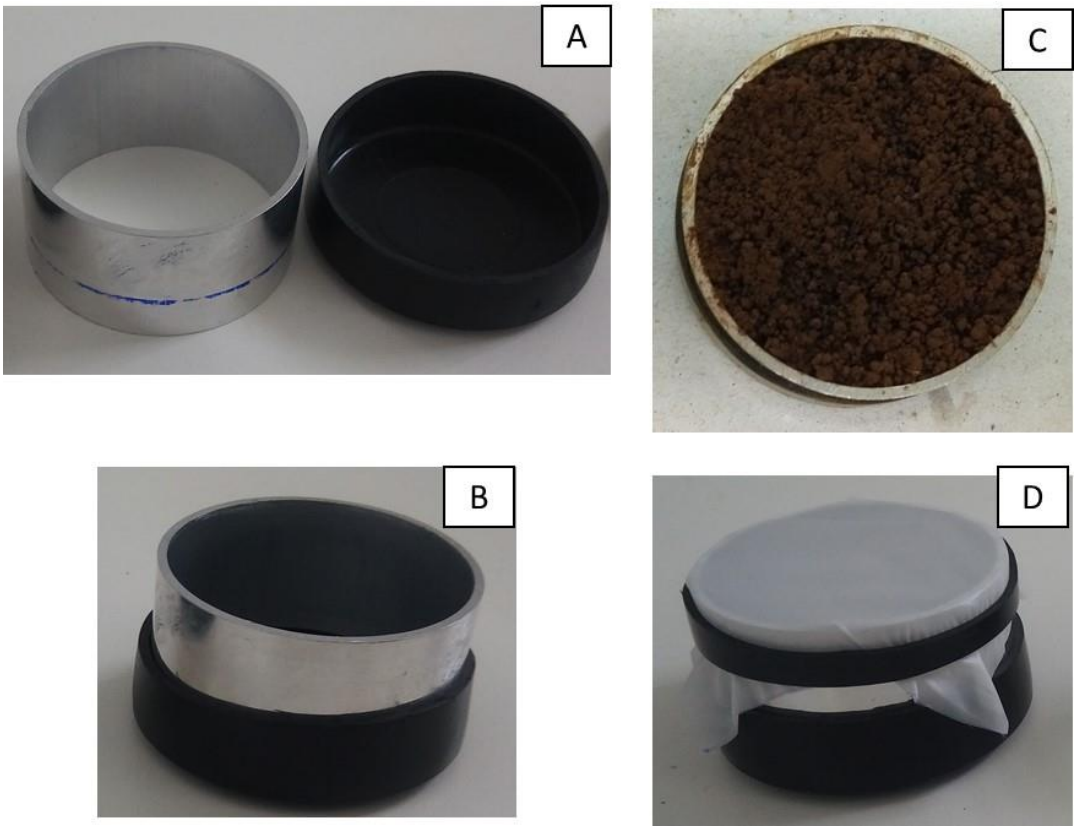

Source: Author.

Figure B2 — Soil cylinder inside the glass jar during the incubation (A); Remaining root litter at the end of incubation (B); Detail of the cylinder slicing device and the measurement of the layer with a pachymeter (C); Slicing of the soil cylinder with a razor (D).

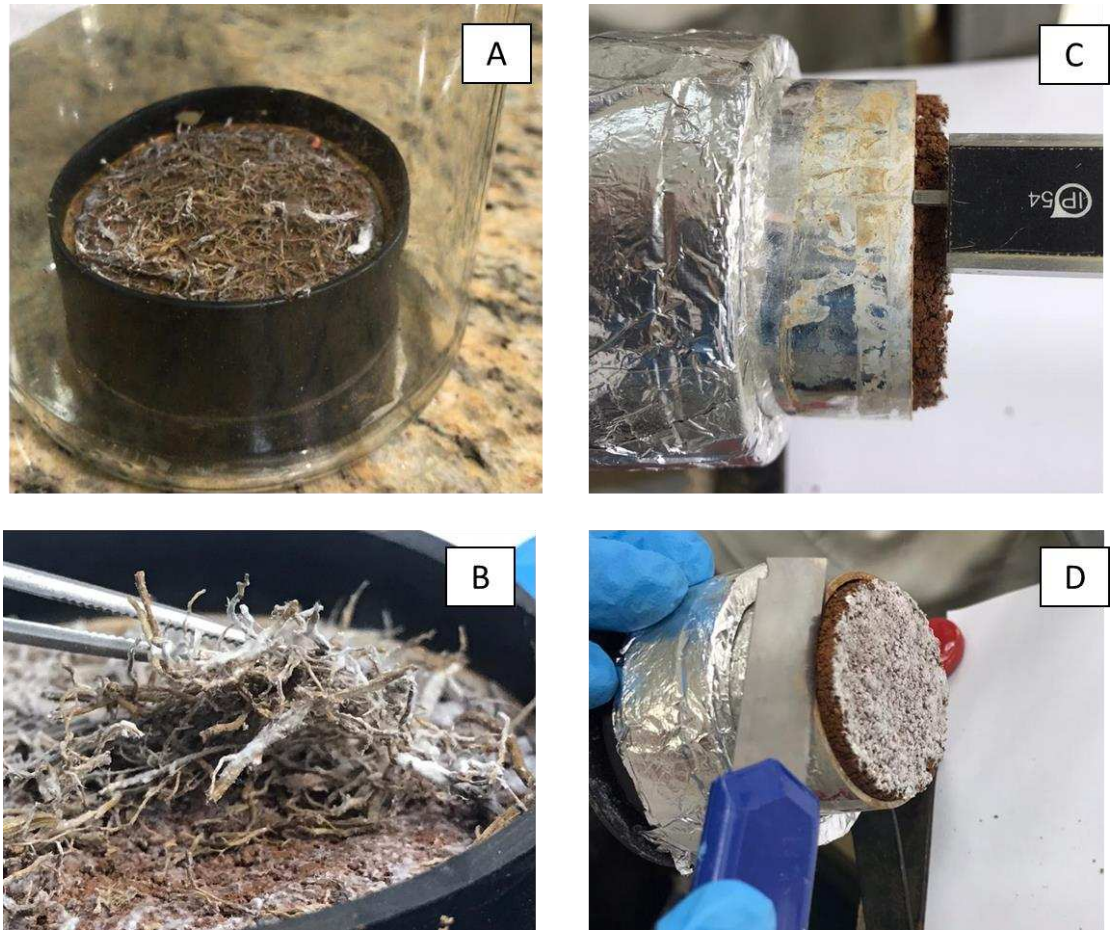

Source: Author.

Figure B3 — Treatment with root litter before the incubation (A); Treatment without root litter before the incubation (B); Treatment with root litter at the end of the incubation (C); Treatment without root litter at the end of the incubation (D).

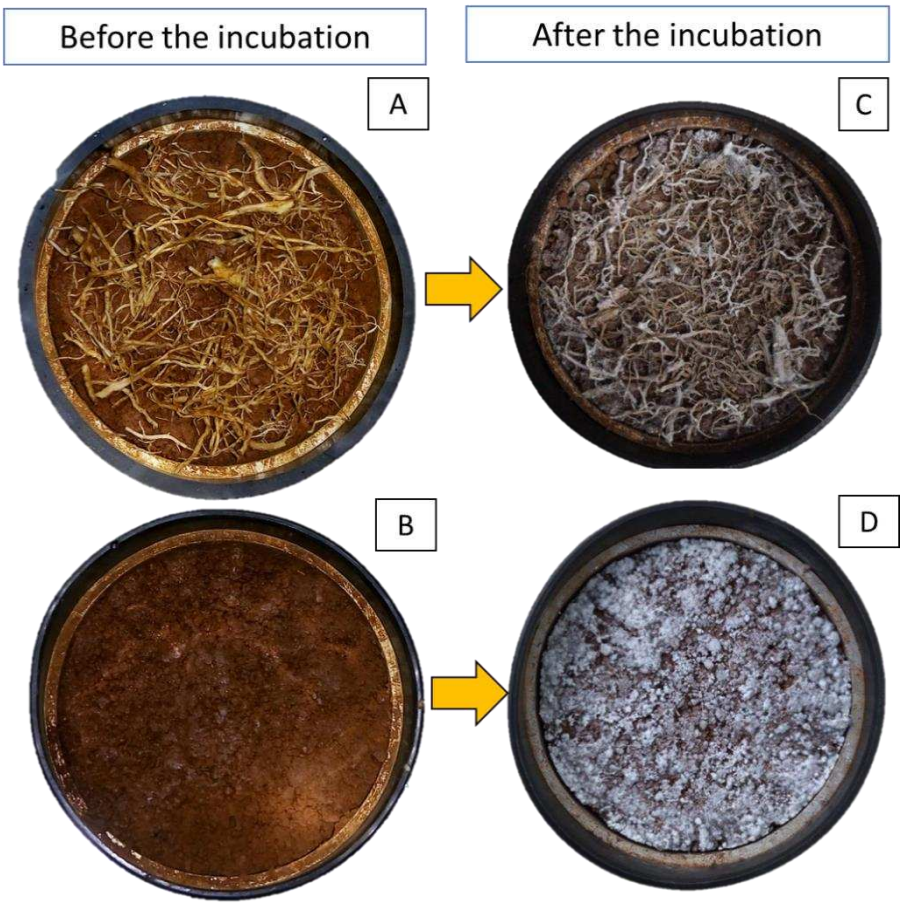

Source: Author.

Table B2 — Number of Samplings, the interval of time between the consecutive samplings (days), and cumulative incubation time (days).

Sampling	Time interval (days)	Cumulative incubation time (days)
1	0.5	0.5
2	1	1
3	1	2
4	1	3
5	4	7
6	4	11
7	3	14
8	4	18
9	3	21
10	4	25
11	3	28
12	4	32
13	7	39
14	7	46
15	10	56
16	7	63
17	7	70
18	7	77
19	7	84
20	7	91
21	7	98
22	7	105
23	14	119
24	14	133
25	14	147
26	14	161

Source: Author.

Figure B4 — Soil organic carbon (C) for legacy (rhizospheric vs. non-rhizospheric) and root litter (with and without) treatments as a function of the distance to the detritusphere for experiments 1 (A) and 2 (B). Soil nitrogen (N) for legacy (rhizospheric vs. non-rhizospheric) and root litter (with and without) treatments as a function of the distance to the detritusphere for experiments 1 (C) and 2 (D). Different letters indicate significant differences between the legacy and root litter treatments. Means ± SE (n = 4) from all treatments is compared within depths by Kruskal-Wallis test followed by a pairwise Mann–Whitney U-tests at 0.05 of significance.

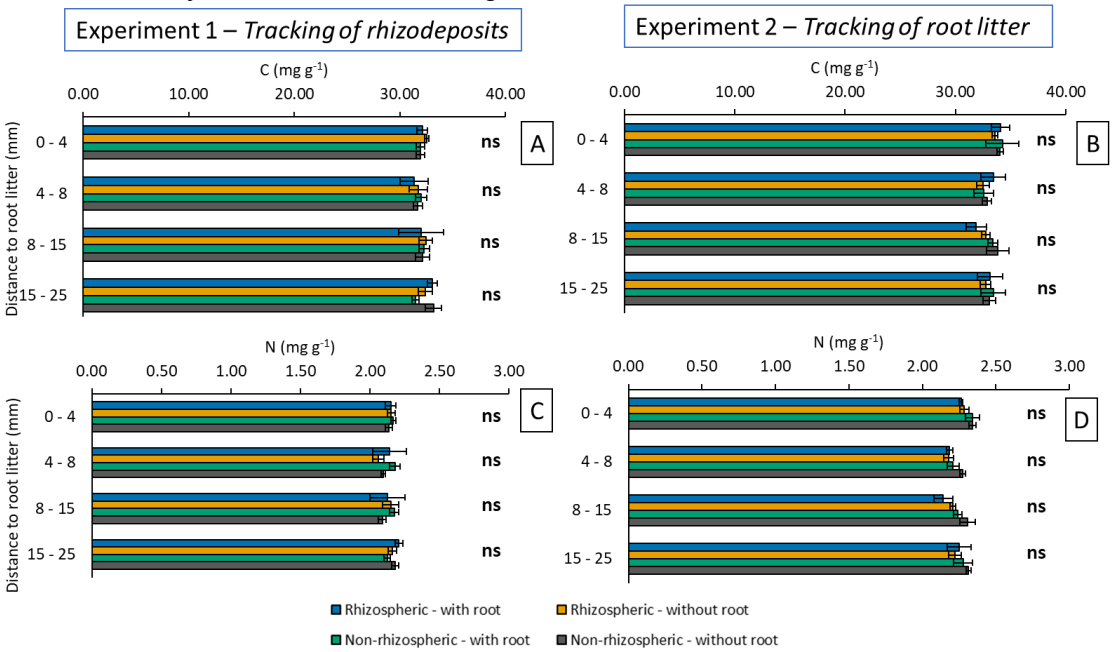

Source: Author.

Table B3 — Carbon (C) and nitrogen (N) contents of SOM fractions for legacy (rhizospheric vs. non-rhizospheric) and root litter (with and without) treatments for the 0-4 mm layer of experiment 1.

Layers	Rhizospheric		Non-rhizospheric	
	With root	Without root	With root	Without root
	C (mg g^{-1})			
fPOM	1.21 ±0.24 **A**	0.98 ±0.31 **A**	1.60 ±0.32 **A**	1.79 ±0.30 **A**
oPOM	4.70 ±0.07 **A**	4.39 ±0.13 **A**	3.71 ±0.04 **A**	3.73 ±0.22 **A**
SSOM	0.75 ±0.89 **A**	0.79 ±0.84 **A**	0.43 ±0.52 **A**	0.34 ±1.02 **A**
MAOM	27.55 ±0.21 **A**	26.34 ±0.41 **B**	27.55 ±0.21 **A**	26.49 ±0.36 **A**
	N (mg g^{-1})			
fPOM	0.05 ±0.01 **A**	0.04 ±0.01 **A**	0.06 ±0.01 **A**	0.08 ±0.02 **A**
oPOM	0.20 ±0.00 **A**	0.20 ±0.01 **A**	0.17 ±0.00 **A**	0.17 ±0.01 **A**
SSOM	0.04 ±0.04 **A**	0.04 ±0.04 **A**	0.02 ±0.03 **A**	0.02 ±0.05 **A**
MAOM	2.01 ±0.01 **A**	1.97 ±0.03 **A**	1.95 ±0.02 **A**	1.99 ±0.03 **A**

Different letters indicate significant differences between the legacy and root litter treatments. Means ± SE (n = 4) from all treatments is compared within depths by the Kruskal-Wallis test followed by pairwise Mann–Whitney U-tests at 0.05 of significance.
Source: Author.

Table B4 — Carbon (C) and nitrogen (N) contents of SOM fractions for legacy (rhizospheric vs. non-rhizospheric) and root litter (with and without) treatments for the 0-4 mm layer of experiment 2.

Layers	Rhizospheric		Non-rhizospheric	
	With root	Without root	With root	Without root
	C (mg g^{-1})			
fPOM	1.76 ±0.27 **A**	1.73 ±0.29 **A**	1.80 ±0.23 **A**	1.98 ±0.21 **A**
oPOM	3.64 ±0.86 **A**	5.09 ±0.80 **A**	4.46 ±0.64 **A**	5.41 ±0.58 **A**
SSOM	0.59 ±0.08 **A**	0.91 ±0.11 **A**	0.44 ±0.05 **A**	1.07 ±0.16 **A**
MAOM	27.08 ±0.18 **A**	27.46 ±0.35 **A**	26.79 ±0.46 **A**	27.49 ±0.33 **A**
	N (mg g^{-1})			
fPOM	0.07 ±0.01 **A**	0.07 ±0.02 **A**	0.08 ±0.01 **A**	0.09 ±0.01 **A**
oPOM	0.16 ±0.04 **A**	0.22 ±0.03 **A**	0.21 ±0.04 **A**	0.23 ±0.04 **A**
SSOM	0.04 ±0.00 **A**	0.05 ±0.01 **A**	0.03 ±0.01 **A**	0.06 ±0.01 **A**
MAOM	2.01 ±0.03 **A**	2.03 ±0.05 **A**	1.96 ±0.01 **A**	2.02 ±0.04 **A**

Different letters indicate significant differences between the legacy and root litter treatments. Means ± SE (n = 4) from all treatments is compared within depths by the Kruskal-Wallis test followed by pairwise Mann–Whitney U-tests at 0.05 of significance.
Source: Author.

Table B5 — Total Phospholipid fatty acid (PLFA), bacterial and fungi biomarkers, fungal: bacterial ratio (F:B), and gram-positive: gram-negative ratio (GP:GN) for the Legacy effect treatments (Rhizospheric and Non-rhizospheric soil) with and without root litter input for both experiments analyzed together.

	Legacy effect	Root litter	
		With	Without
Total PLFA (µmol g^{-1} C)	Rhizospheric	2.14 ±0.15 **aA**	2.42 ±0.14 **aA**
	Non-rhizospheric	1.97 ±0.13 **aA**	2.09 ±0.21 **aA**
Bacteria (µmol g^{-1} C)	Rhizospheric	1.00 ±0.06 **aA**	1.12 ±0.09 **aA**
	Non-rhizospheric	0.88 ±0.07 **aA**	1.01 ±0.11 **aA**
Fungi (µmol g^{-1} C)	Rhizospheric	0.08 ±0.01 **aA**	0.08 ±0.01 **aA**
	Non-rhizospheric	0.08 ±0.01 **aA**	0.07 ±0.01 **aA**
F:B ratio	Rhizospheric	0.08 ±0.01 **aA**	0.08 ±0.01 **aA**
	Non-rhizospheric	0.09 ±0.01 **aA**	0.08 ±0.01 **aA**
GP:GN ratio	Rhizospheric	7.84 ±0.88 **aA**	6.96 ±0.78 **bA**
	Non-rhizospheric	6.62 ±0.43 **aA**	8.18 ±0.53 **aA**

Lowercase letters indicate significant differences between the Legacy Effects treatments. Uppercase letters indicate significant differences between root litter within the same Legacy effect treatment. Means ± SE (n = 8) from both experiments is compared between treatments by t-test at 0.05 of significance.
Source: Author.

Figure B5 — Partitioning of soil C-CO_2 respiration (%) in root litter-derived and SOM-derived respiration for rhizospheric (A) and non-rhizospheric soils (B) of experiment 2. Means (n = 4) are presented.

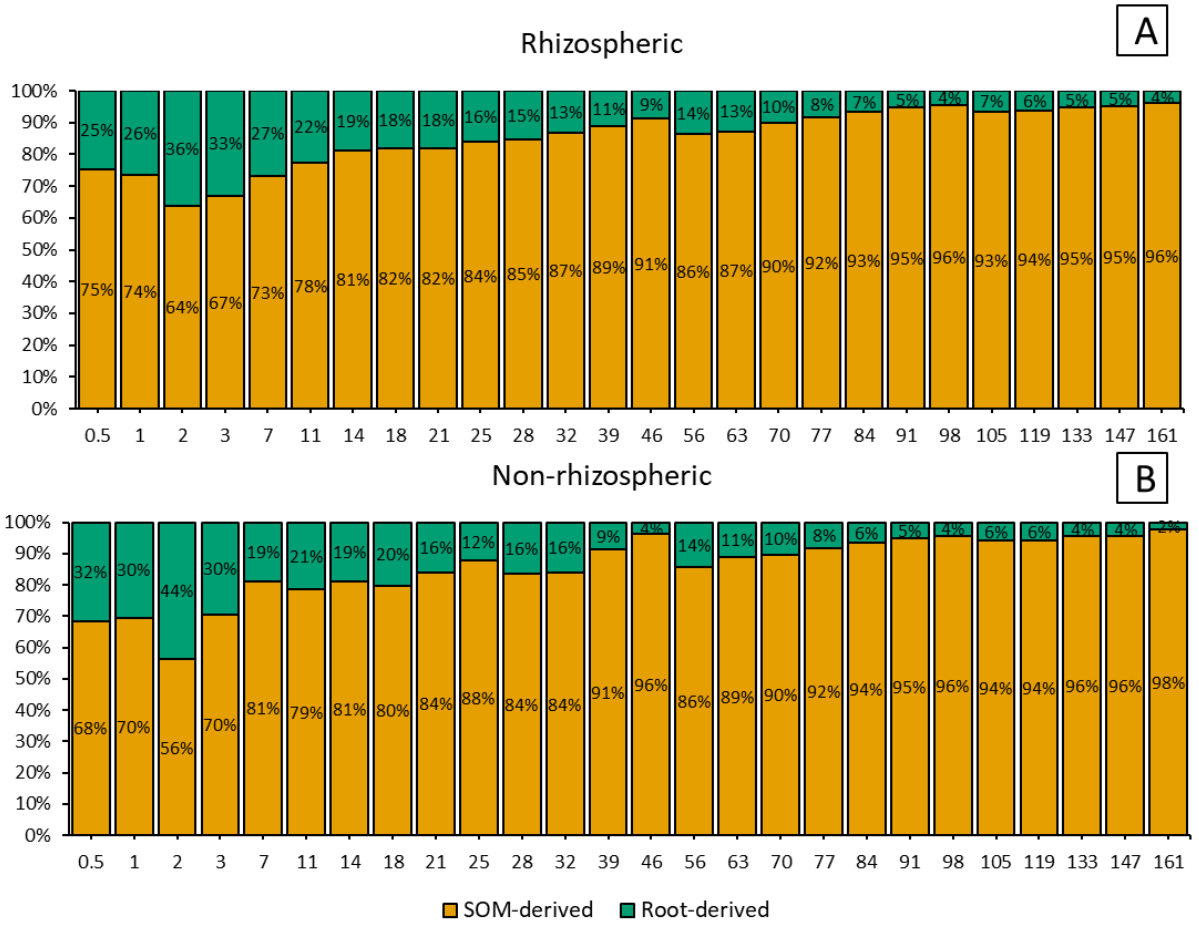

Source: Author.

Table B6 — Total Phospholipid fatty acid (PLFA), bacterial and fungi biomarkers, fungal: bacterial ratio (F:B), and gram-positive: gram-negative ratio (GP:GN) for the Legacy effect treatments (Rhizospheric and Non-rhizospheric soil) with and without root litter input for experiment 1.

	Legacy effect	Root litter	
		With	Without
Total PLFA (µmol g^{-1} C)	Rhizospheric	2.44 ±0.15 **aA**	2.50 ±0.17 **aA**
	Non-rhizospheric	2.17 ±0.12 **aA**	2.31 ±0.09 **aA**
Bacteria (µmol g^{-1} C)	Rhizospheric	1.14 ±0.05 **aA**	1.19 ±0.07 **aA**
	Non-rhizospheric	0.97 ±0.11 **aA**	1.13 ±0.05 **aA**
Fungi (µmol g^{-1} C)	Rhizospheric	0.09 ±0.01 **aA**	0.09 ±0.01 **aA**
	Non-rhizospheric	0.09 ±0.01 **aA**	0.07 ±0.01 **aA**
F:B ratio	Rhizospheric	0.09 ±0.01 **aA**	0.09 ±0.01 **aA**
	Non-rhizospheric	0.09 ±0.01 **aA**	0.09 ±0.00 **aA**
GP:GN ratio	Rhizospheric	7.16 ±0.64 **aA**	6.84 ±0.59 **bA**
	Non-rhizospheric	6.20 ±0.81 **aA**	8.53 ±0.49 **aA**

Lowercase letters indicate significant differences between the Legacy Effects treatments. Uppercase letters indicate significant differences between root litter within the same Legacy effect treatment. Means ± SE (n = 4) from both experiments is compared between treatments by t-test at 0.05 of significance.
Source: Author.

Table B7 — Total Phospholipid fatty acid (PLFA), bacterial and fungi biomarkers, fungal: bacterial ratio (F:B), and gram-positive: gram-negative ratio (GP:GN) for the Legacy effect treatments (Rhizospheric and Non-rhizospheric soil) with and without root litter input for experiment 2.

	Legacy effect	Root litter	
		With	Without
Total PLFA (µmol g^{-1} C)	Rhizospheric	1.85 ±0.15 **aA**	2.34 ±0.24 **aA**
	Non-rhizospheric	1.76 ±0.20 **aA**	1.87 ±0.41 **aA**
Bacteria (µmol g^{-1} C)	Rhizospheric	0.86 ±0.05 **aA**	1.05 ±0.16 **aA**
	Non-rhizospheric	0.79 ±0.09 **aA**	0.89 ±0.22 **aA**
Fungi (µmol g^{-1} C)	Rhizospheric	0.08 ±0.01 **aA**	0.07 ±0.01 **aA**
	Non-rhizospheric	0.07 ±0.01 **aA**	0.06 ±0.00 **aA**
F:B ratio	Rhizospheric	0.08 ±0.01 **aA**	0.07 ±0.01 **aA**
	Non-rhizospheric	0.07 ±0.01 **aA**	0.06 ±0.01 **aA**
GP:GN ratio	Rhizospheric	8.51 ±1.71 **aA**	7.07 ±1.58 **aA**
	Non-rhizospheric	7.04 ±0.26 **aA**	7. 83 ±1.00 **aA**

Lowercase letters indicate significant differences between the Legacy Effects treatments. Uppercase letters indicate significant differences between root litter within the same Legacy effect treatment. Means ± SE (n = 4) from both experiments is compared between treatments by t-test at 0.05 of significance.
Source: Author.